

Simultaneous measurement of ν_μ charged-current single π^+ production in CH, C, H₂O, Fe, and Pb targets in MINERvA

A. Bercelee,¹ K.A. Kroma-Wiley,^{2,1} S. Akhter,³ Z. Ahmad Dar,^{4,3} F. Akbar,³ V. Ansari,³ M. V. Ascencio,^{5,*} M. Sajjad Athar,³ L. Bellantoni,⁶ M. Betancourt,⁶ A. Bodek,¹ J. L. Bonilla,⁷ A. Bravar,⁸ H. Budd,¹ G. Caceres,^{9,†} T. Cai,¹ G.A. Díaz,¹ H. da Motta,⁹ S.A. Dytman,¹⁰ J. Felix,⁷ L. Fields,¹¹ A. Filkins,⁴ R. Fine,^{1,‡} A.M. Gago,⁵ H. Gallagher,¹² P.K.Gaur,³ A. Ghosh,^{13,9} S.M. Gilligan,¹⁴ R. Gran,¹⁵ E.Granados,⁷ D.A. Harris,^{16,6} D. Jena,⁶ S. Jena,¹⁷ J. Kleykamp,^{1,§} A. Klustová,¹⁸ M. Kordosky,⁴ D. Last,² T. Le,^{12,19} A. Lozano,⁹ X.-G. Lu,^{20,21} I. Mahbub,¹⁵ E. Maher,²² S. Manly,¹ W.A. Mann,¹² C. Mauger,² K.S. McFarland,¹ B. Messerly,^{10,¶} J. Miller,¹³ O. Moreno,^{4,7} J.G. Morfín,⁶ D. Naples,¹⁰ J.K. Nelson,⁴ C. Nguyen,²³ A. Olivier,¹ V. Paolone,¹⁰ G.N. Perdue,^{6,1} K.-J. Plows,²¹ M.A. Ramírez,^{2,7} R.D. Ransome,¹⁹ H. Ray,²³ D. Ruterbories,¹ H. Schellman,¹⁴ C.J. Solano Salinas,²⁴ H. Su,¹⁰ M. Sultana,¹ V.S. Syrotenko,¹² B. Utt,¹⁵ E. Valencia,^{4,7} N.H. Vaughan,¹⁴ A.V. Waldron,¹⁸ B. Yaeggy,^{13,**} and L. Zazueta⁴

(The MINERvA Collaboration)

¹*Department of Physics and Astronomy, University of Rochester, Rochester, New York 14627 USA*

²*Department of Physics and Astronomy, University of Pennsylvania, Philadelphia, PA 19104*

³*AMU Campus, Aligarh, Uttar Pradesh 202001, India*

⁴*Department of Physics, William & Mary, Williamsburg, Virginia 23187, USA*

⁵*Sección Física, Departamento de Ciencias, Pontificia Universidad Católica del Perú, Apartado 1761, Lima, Perú*

⁶*Fermi National Accelerator Laboratory, Batavia, Illinois 60510, USA*

⁷*Campus León y Campus Guanajuato, Universidad de Guanajuato, Lascurain de Retana No. 5, Colonia Centro, Guanajuato 36000, Guanajuato México.*

⁸*University of Geneva, 1211 Geneva 4, Switzerland*

⁹*Centro Brasileiro de Pesquisas Físicas, Rua Dr. Xavier Sigaud*

150, Urca, Rio de Janeiro, Rio de Janeiro, 22290-180, Brazil

¹⁰Department of Physics and Astronomy, University
of Pittsburgh, Pittsburgh, Pennsylvania 15260, USA

¹¹Department of Physics, University of Notre Dame, Notre Dame, Indiana 46556, USA

¹²Physics Department, Tufts University, Medford, Massachusetts 02155, USA

¹³Departamento de Física, Universidad Técnica Federico Santa
María, Avenida España 1680 Casilla 110-V, Valparaíso, Chile

¹⁴Department of Physics, Oregon State University, Corvallis, Oregon 97331, USA

¹⁵Department of Physics, University of Minnesota – Duluth, Duluth, Minnesota 55812, USA

¹⁶York University, Department of Physics and
Astronomy, Toronto, Ontario, M3J 1P3 Canada

¹⁷Department of Physical Sciences, IISER Mohali, Knowledge
City, SAS Nagar, Mohali - 140306, Punjab, India

¹⁸The Blackett Laboratory, Imperial College London, London SW7 2BW, United Kingdom

¹⁹Rutgers, The State University of New Jersey, Piscataway, New Jersey 08854, USA

²⁰Coventry CV4 7AL, UK

²¹Oxford University, Department of Physics, Oxford, OX1 3PJ United Kingdom

²²Massachusetts College of Liberal Arts, 375 Church Street, North Adams, MA 01247

²³University of Florida, Department of Physics, Gainesville, FL 32611

²⁴Facultad de Ciencias, Universidad Nacional de Ingeniería, Apartado 31139, Lima, Perú

(Dated: June 6, 2023)

Abstract

Neutrino-induced charged-current single π^+ production in the $\Delta(1232)$ resonance region is of considerable interest to accelerator-based neutrino oscillation experiments. In this work, high statistics differential cross sections are reported for the semi-exclusive reaction $\nu_\mu A \rightarrow \mu^- \pi^+ +$ nucleon(s) on scintillator, carbon, water, iron, and lead targets recorded by MINERvA using a wide-band ν_μ beam with $\langle E_\nu \rangle \approx 6$ GeV. Suppression of the cross section at low Q^2 and enhancement of low T_π are observed in both light and heavy nuclear targets compared to phenomenological models used in current neutrino interaction generators. The cross-sections per nucleon for iron and lead compared to CH across the kinematic variables probed are 0.8 and 0.5 respectively, a scaling which is also not predicted by current generators.

* Now at Iowa State University, Ames, IA 50011, USA

† now at Department of Physics and Astronomy, University of California at Davis, Davis, CA 95616, USA

‡ Now at Los Alamos National Laboratory, Los Alamos, New Mexico 87545, USA

§ now at Department of Physics and Astronomy, University of Mississippi, Oxford, MS 38677

¶ Now at University of Minnesota, Minneapolis, Minnesota 55455, USA

** Now at Department of Physics, University of Cincinnati, Cincinnati, Ohio 45221, USA

Charged pion production is an important process for accelerator-based oscillation experiments. For low energy experiments, T2K [1], T2HK [2], and SBN [3], this process is both a significant background to quasielastic scattering and is used as a signal reaction when the pion is identified. For higher energy experiments, NOvA [4] and DUNE [5], the process is a large fraction of the signal. Neutrino oscillation experiments rely on an accurate model of pion production to evaluate neutrino energy for events with charged pions. Although NOvA, T2K, and T2HK utilize relatively low- A nuclear media such as hydrocarbons or water, SBN and DUNE experiments rely on argon ($A = 40$) targets. In order for these experiments to make use of the wealth of neutrino interaction data obtained with light nuclei, a knowledge of neutrino cross-section scaling as a function of target A is required. This work tests scaling behavior by simultaneously measuring the differential cross sections of $\nu_\mu + A \rightarrow \mu^- + \pi^+ + \text{nucleons}$ as the target nucleon number is changed from carbon ($A=12$) to lead ($A= 208$). We also present cross section ratios to scintillator, where many systematic uncertainties cancel, allowing a precise measurement of the nuclear dependence.

Previous measurements of charged-current pion production [6–11] have found disagreements between data and models at both low Q^2 (the negative of the square of the four momentum transfer from the lepton) and in pion kinetic energy. Simulations of this process must model both the primary neutrino-nucleon interaction and a variety of nuclear effects, including interactions of produced hadrons within the nucleus. This convolution of primary production and nuclear modification makes it difficult to isolate the model features responsible for the disagreements. Measurements on multiple nuclei can help separate nuclear effects from other aspects of the interaction.

Signal reactions for this measurement are ν_μ charged-current interactions which produce a single negatively charged muon and a single positively charged pion. Any number of baryons may be in the final state; however, no other mesons may be produced. To match MINERvA’s acceptance, the muon is restricted in momentum (p_μ) and angle with respect to the neutrino beam (θ_μ), such that $1.5 < p_\mu < 20$ GeV/ c and $\theta_\mu < 13^\circ$. Pion kinetic energy (T_π) is restricted to $35 < T_\pi < 350$ MeV.

To enhance reactions involving a Δ baryon resonance, a selection is made on the invariant hadronic mass of the final state. We define $W_{\text{exp}} = M^2 + 2ME_{\text{had}} - Q^2$, where $E_{\text{had}} = E_\nu - E_\mu$, M is the average of the proton and neutron masses. W_{exp} is the invariant mass of the hadronic final state under the assumption that the target nucleon is at rest. W_{exp} is required to be

less than $1.4 \text{ GeV}/c^2$.

This analysis provides measurements in eight kinematic variables: the magnitude of the muon momentum and its longitudinal and transverse components (p_μ , $p_{\mu,||}$, and $p_{\mu,T}$), the angle of the muon (θ_μ), the kinetic energy and angle of the charged pion with respect to the neutrino beam (T_π and θ_π), Q^2 , and W_{exp} as defined by the kinematics of the final state particles.

These measurements use event samples collected at the MINERvA detector using the medium energy NuMI beam at Fermilab [12]. To create the neutrino beam, 120 GeV protons impact a graphite target and produce pions and kaons. Two magnetic horns focus these charged particles into a pipe where they decay into primarily muon neutrinos. A GEANT4 simulation of the NuMI beamline [13] predicts the neutrino flux using constraints from hadron production data. Previous MINERvA measurements of neutrino elastic scattering on atomic electrons, $\nu e^- \rightarrow \nu e^-$, constrain the normalization of the neutrino flux, reducing the uncertainty of the flux between 2 and 20 GeV from 7.8% to 3.9% [14, 15]. Another MINERvA measurement of inverse muon decay, $\nu_\mu e^- \rightarrow \mu^- \nu_e$, constrains the flux at higher neutrino energies [16]. These data represent an exposure of 10.6×10^{20} protons on target, half of which were taken with the water target filled.

The MINERvA detector consists of a central polystyrene-based scintillator tracker with an upstream nuclear target region and downstream electromagnetic and hadronic calorimeters. The nuclear target region contains five planes of passive material comprised of carbon, water, iron, and lead targets. The scintillator tracking planes are 95% CH by weight. The passive targets are interspersed between regions of active tracking volumes. The finely segmented tracking volumes of the MINERvA detector consist of hexagonal planes of nested triangular scintillator strips with a pitch of 1.7 cm, allowing for spatial reconstruction with a resolution of 3 mm [12]. The MINOS Near Detector, located 2 m downstream of the MINERvA detector measures charge and momentum of exiting muons [17].

The simulation of the MINERvA detector utilizes GEANT4 version 4.9.4p2 [18] with the QGSP_BERT physics list [19–21] to model the detector response. Calibrations using through-going muons provide the absolute energy scale [12]. Measurements on a scaled down version of the MINERvA detector in a charged particle test beam set the hadronic energy response [22]. Overlaying data onto simulated events captures the effects of overlapping activity due to additional beam interactions.

A modified version of the GENIE v2.12.6 event generator, denoted “MnvTune v4.3.1”, supplies the neutrino interaction simulation [23]. For inelastic events with the invariant hadronic mass $W < 1.7 \text{ GeV}/c^2$, resonance pion production assumes the Rein-Seghal model [24] with an axial mass of $M_A^{RES} = 1.12 \text{ GeV}/c^2$ [25]. Deep inelastic scattering relies on the Bodek-Yang model [26] tuned to agree with external measurements of pion production and total cross sections. Coherent pion production is simulated with the Rein-Seghal [27, 28] model with corrections for muon mass. The nuclear medium is modeled as a relativistic Fermi gas (with Fermi momentum $p_F \sim 250 \text{ MeV}/c$) [29] with an added Bodek-Ritchie high momentum tail [30, 31]. Simulation of hadron final state interactions within the nucleus are predicted by the INTRANUKE-hA package [23].

The GENIE simulation has been tuned to better reproduce MINERvA data and provide more accurate signal and background models. Modifications to the quasielastic process are described in Ref. [32, 33]. Pion production through baryon resonances is modified to match the D_2 bubble chamber data as in Ref. [34]. Coherent pion production is reweighted in both the energy of the pion E_π and θ_π to agree with a recent measurement of coherent pion production [35]. The normalization of coherent pion production is increased by 43.7% to account for coherent interactions on hydrogen, known as diffractive pion production, based on the Kopeliovic model [36]. The changes above comprise “MnvTune v4.2.1”.

However, signal events in the scintillator disagree with the prediction of this model. The model for all targets except hydrogen was corrected by matching the simulated cross section versus Q^2 to the data. This results in improved estimates of efficiencies and backgrounds. The correction decreases the single pion production for $Q^2 < 0.1 \text{ GeV}^2/c^2$ with a slow logarithmic increase for higher Q^2 . Details of this tune are given in the supplemental material. This modification, combined with those of MnvTune v4.2.1, forms MnvTune v4.3.1.

Selected events are required to have at least two tracked particles that start in the correct target. One track must be identified as a negatively charged muon by the MINOS Near Detector. One remaining track must be identified as a non-interacting charged pion by matching a Michel electron to the endpoint of the track and having longitudinal energy deposition (dE/dx) consistent with a non-interacting pion. All remaining tracks must not have dE/dx consistent with a pion. The charged pion tracking efficiency decreases at lower momentum and at angles perpendicular to the detector axis. The efficiency to reconstruct the Michel electron from the μ^+ was predicted from the simulation and validated in the

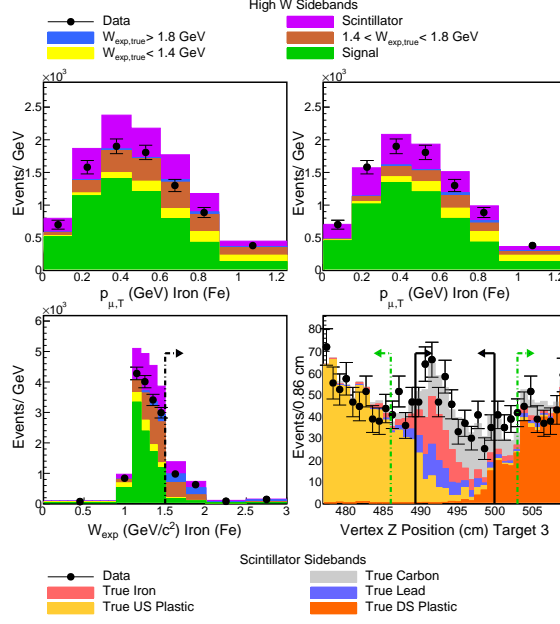


FIG. 1. $p_{\mu,T}$ distributions in iron for the signal regions before (top left) and after (top right) the simulation has been constrained with background estimates from data, the high W sideband in W_{exp} in iron (bottom left) and the scintillator sidebands in vertex z of target 3 (bottom left). The background in the bottom plots have not been constrained. The solid (dashed) arrows in the lower right plot delineate the signal (sideband) regions. Events labeled $W_{exp,true} < 1.4 GeV$ are those that pass the signal $W_{exp,true}$ selection but fail other elements of the signal definition.

scintillator tracker using stopping muons produced in the rock upstream of the detector [37]. The $W_{exp} < 1.4 GeV/c^2$ requirement strongly reduces the number of multipion events. Both W_{exp} and Q^2 are computed using the visible calorimetric energy in the detector to estimate E_{had} [37]. After all cuts there are 33,231 events in the tracker, and 1403 (1033) events in the iron (lead), and 295 (291) events in the carbon (water).

The two primary backgrounds are pion production events with $W_{exp} > 1.4 GeV/c^2$ and pion production events that appear to originate from the passive nuclear targets but are actually produced in the adjacent scintillator. First, simulated events with reconstructed $W_{exp} > 1.4 GeV/c^2$ in the scintillator target are weighted to match data using two scale factors, one for events with true W_{exp} between 1.4 and 1.8 GeV/c^2 and one for events with W_{exp} above 1.8 GeV/c^2 . True W_{exp} is computed in the same manner as reconstructed W_{exp} but uses true simulated values. To improve the background prediction from events in scintillator adjacent to the passive target, pions with low T_π or $\theta_\pi > 90^\circ$ also receive additional

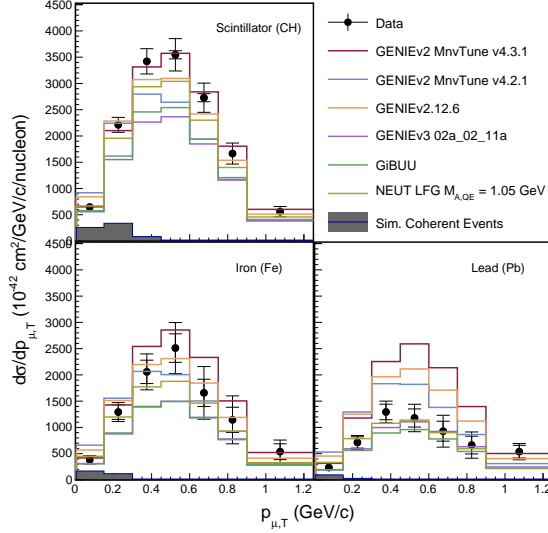


FIG. 2. Differential cross section $\frac{d\sigma}{dp_{\mu,T}}$ measured on scintillator, iron, and lead (solid points) compared to GENIE, GIBUU and NEUT generators, all of which are discrepant with one if not all nuclei.

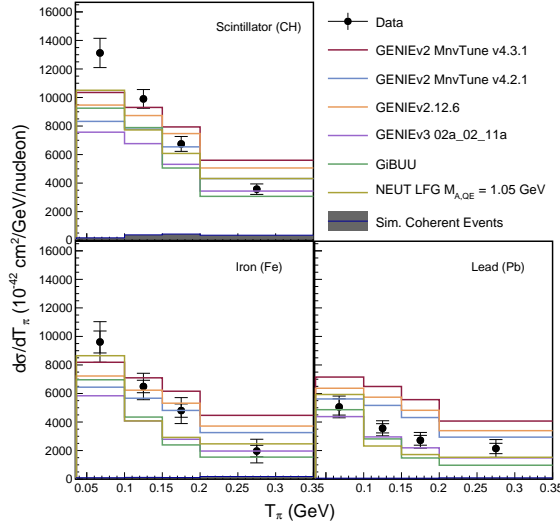


FIG. 3. Differential cross section $\frac{d\sigma}{dT_{\pi}}$ in scintillator, iron, and lead (solid points) compared to GENIE, GIBUU and NEUT generators, all of which are discrepant.

weights to improve agreement with the scintillator target data. Next, simulated events in each target are weighted to correct the prediction of adjacent scintillator backgrounds using events observed in data near the passive targets. Finally, a weight is applied for events with high reconstructed W_{exp} , in the same manner as above, for each target material. Fig. 1

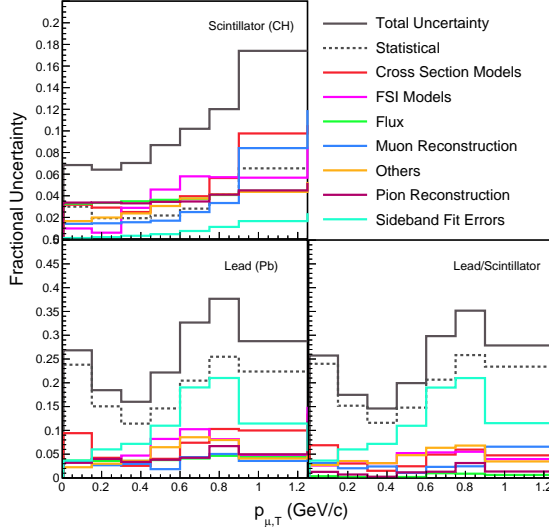


FIG. 4. Systematic uncertainties on the differential cross section $\frac{d\sigma}{dp_{\mu,T}}$ in lead and scintillator and uncertainties of the ratio of $\left(\frac{d\sigma_{Pb}}{dp_{\mu,T}}\right) / \left(\frac{d\sigma_{CH}}{dp_{\mu,T}}\right)$.

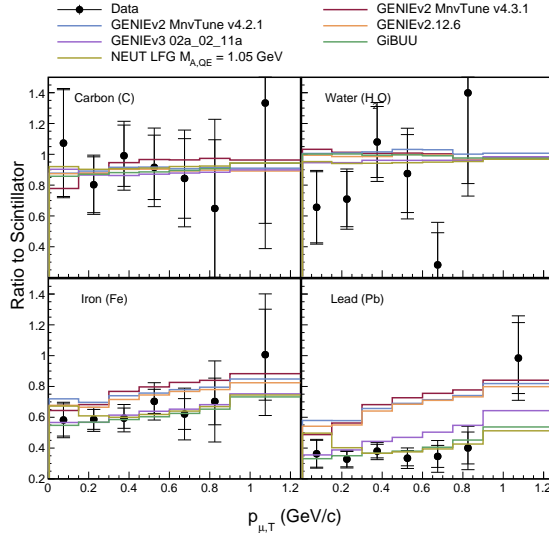


FIG. 5. Cross section ratios $\left(\frac{d\sigma_A}{dp_{\mu,T}}\right) / \left(\frac{d\sigma_{CH}}{dp_{\mu,T}}\right)$ for carbon, water, iron, and lead (solid points), as compared to GENIE, NEUT, and GIBUU.

shows a sample of data used in the background constraints, before and after constraints. The full set of weights are given in the supplemental material.

Kinematic smearing due to the detector in the background-subtracted distributions is removed with iterative D'Agostini unfolding [38, 39] as implemented in the RooUnfold [40] framework. The number of iterations was chosen by studying the fidelity of unfolding ran-

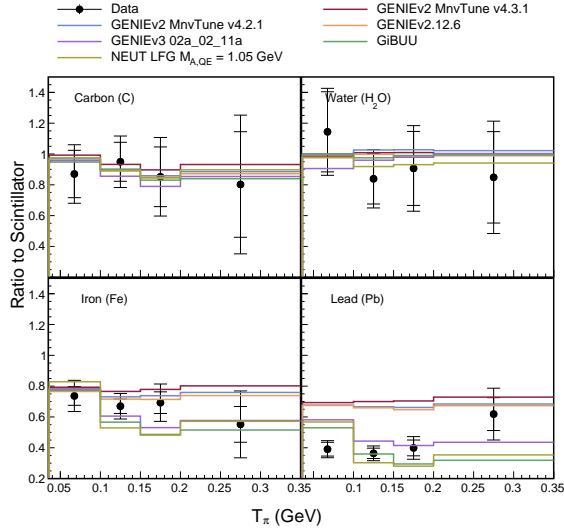


FIG. 6. Cross section ratios $(\frac{d\sigma_A}{dT_{\pi^+}})/(\frac{d\sigma_{CH}}{dT_{\pi^+}})$ for carbon, water, iron, and lead (solid points) compared to predictions from GENIE, NEUT, and GIBUU. The predictions from GIBUU and NEUT agree better with the measurements than those from GENIE.

domly thrown pseudodata samples generated from alternate physics models. The event distributions are corrected for selection efficiency and acceptance, which is 4.5% (1%) on average in the tracker (passive targets). Efficiencies are available in the supplement. The differential cross sections are obtained by normalizing the resulting event rates by the integrated neutrino flux and number of target nucleons.

One complication of forming ratios of cross sections between the passive targets and the tracker is that the fluxes have small differences due to the distributions of mass relative to the beam axis, as shown in the supplemental material. This is corrected by measuring the cross section on scintillator in several regions of the detector, each integrated over a slightly different neutrino energy distribution. Linear combinations of these regional cross sections are used to form a cross section integrated over a flux that matches the relevant target. These cross sections are used to form the ratio of target-to-tracker cross-section ratios [37, 41].

Figure 2 shows the differential cross section $\frac{d\sigma}{dp_{\mu,T}}$ on materials with highest statistics (iron, lead, and scintillator). Lower statistics measurements on water and carbon are available in the supplement. The statistical uncertainty dominates in all measurements, except in the scintillator. An example of the uncertainties on the cross sections are

shown in Fig. 4; uncertainties in the cross section models which enter via efficiency and unfolding are the largest, but are lower than the statistical uncertainties in all targets but the scintillator. Statistical uncertainties in the sideband constraints are also significant for the passive targets. Systematic uncertainties are smaller in the cross section ratios, which benefit from partial cancellation of the flux, cross section model, and reconstruction uncertainties.

Ratios of cross sections to that in scintillator are shown for $\frac{d\sigma}{dp_{\mu,T}}$ and $\frac{d\sigma}{dT_{\pi}}$ in Figs. 5 and 6. The cross-section ratios of carbon or water to scintillator can be characterized by a scale factor of unity, while ratios between iron or lead to scintillator are constant at 0.8 and 0.5 respectively, with no large modifications to distribution shapes for either $p_{\mu,T}$ or T_{π} . Cross sections and cross section ratios to scintillator in other kinematic variables are tabulated and shown in the supplemental material. Ratios in the other variables also exhibit this scaling behavior.

None of the six generator models investigated capture the evolution of absolute cross section. The generators NEUT[42] and GIBUU[43] do correctly predict the cross section ratios between Fe and Pb and scintillator, as shown in Figs. 5 and 6, while the GENIE predictions do not agree. The GENIE models use pion- and nucleon-nucleus scattering data to implement single-step absorption and other scattering processes (INTRANUKE-hA) [23], whereas NEUT, NuWRO and GIBUU employ different microscopic transport algorithms to simulate pion and nucleon intranuclear scattering.

As previously noted, the scintillator cross section showed a large discrepancy with the MINERvA-tuned GENIE model, which is corrected with a weight as a function of Q^2 . In Fig. 2, the differential cross section as a function of the related observable $p_{\mu,T}$ ($Q^2 \approx p_{\mu,T}^2 \left[1 + \mathcal{O}\left(\frac{E_{\text{had}}}{E_{\mu}}\right)\right]$) shows poor agreement both with untuned GENIE models (GENIEv2.12.6) and with tuned models without this weighting function (GENIEv2 MnvTune v4.2.1). The shape of the data is in better agreement with the weighted model (GENIEv2 MnvTune v4.3.1) in all targets, even though the weight is derived using only the scintillator measurement. The absolute normalization of the cross section is not well described by MnvTune v4.3.1 in Iron or Lead.

Similarly, the ratios of $d\sigma/dp_{\mu,T}$ between the targets and scintillator are consistent with being independent of $p_{\mu,T}$. A feature of both the GENIE v3 and GiBUU models is that they predict the large suppression lead relative to other targets. However, as seen in Fig. 6,

these models also predict a larger ratio at low T_π in the heavy targets, a feature which is not seen in the data.

In summary, these data on single pion production on a wide variety of nuclei provide a new way to test nuclear models through their nuclear dependence. We observe a large modification to the predicted Q^2 distribution of single π^+ events that it can be consistently seen in all nuclei. These results give guidance in how the wealth of data on scintillator targets can be applied to models for oxygen and argon for future neutrino experiments.

ACKNOWLEDGMENTS

This document was prepared by members of the MINERvA Collaboration using the resources of the Fermi National Accelerator Laboratory (Fermilab), a U.S. Department of Energy, Office of Science, HEP User Facility. Fermilab is managed by Fermi Research Alliance, LLC (FRA), acting under Contract No. DE-AC02-07CH11359. These resources included support for the MINERvA construction project, and support for construction also was granted by the United States National Science Foundation under Award No. PHY-0619727 and by the University of Rochester. Support for participating scientists was provided by NSF and DOE (USA); by CAPES and CNPq (Brazil); by CoNaCyT (Mexico); by ANID PIA / APOYO AFB180002, CONICYT PIA ACT1413, and Fondecyt 3170845 and 11130133 (Chile); by CONCYTEC (Consejo Nacional de Ciencia, Tecnología e Innovación Tecnológica), DGI-PUCP (Dirección de Gestión de la Investigación - Pontificia Universidad Católica del Perú), and VRI-UNI (Vice-Rectorate for Research of National University of Engineering) (Peru); NCN Opus Grant No. 2016/21/B/ST2/01092 (Poland); by Science and Technology Facilities Council (UK); by EU Horizon 2020 Marie Skłodowska-Curie Action; by a Cottrell Postdoctoral Fellowship from the Research Corporation for Scientific Advancement; by an Imperial College London President's PhD Scholarship. We thank the MINOS Collaboration for use of its near detector data. Finally, we thank the staff of Fermilab for support of the beam line, the detector, and computing infrastructure.

[1] K. Abe *et al.* (T2K), Nucl. Instrum. Meth. A **659**, 106 (2011).

- [2] K. Abe *et al.* (Hyper-Kamiokande), “Hyper-Kamiokande Design Report,” (2018), (unpublished), arXiv:1805.04163 [physics.ins-det].
- [3] M. Antonello *et al.* (MicroBooNE, LAr1-ND, ICARUS-WA104), “A Proposal for a Three Detector Short-Baseline Neutrino Oscillation Program in the Fermilab Booster Neutrino Beam,” (2015), (unpublished), arXiv:1503.01520 [physics.ins-det].
- [4] D. S. Ayres *et al.* (NOvA), “NOvA: Proposal to Build a 30 Kiloton Off-Axis Detector to Study $\nu_\mu \rightarrow \nu_e$ Oscillations in the NuMI Beamline,” (2004), (unpublished), arXiv:hep-ex/0503053.
- [5] R. Acciarri *et al.* (DUNE), “Long-Baseline Neutrino Facility (LBNF) and Deep Underground Neutrino Experiment (DUNE): Conceptual Design Report, Volume 2: The Physics Program for DUNE at LBNF,” (2015), (unpublished), arXiv:1512.06148 [physics.ins-det].
- [6] A. A. Aguilar-Arevalo *et al.* (MiniBooNE), Phys. Rev. D **83**, 052007 (2011).
- [7] P. Adamson *et al.* (MINOS), Phys. Rev. D **91**, 012005 (2015).
- [8] B. Eberly *et al.* (MINERvA), Phys. Rev. D **92**, 092008 (2015).
- [9] T. Le *et al.* (MINERvA), Phys. Lett. B **749**, 130 (2015).
- [10] C. L. McGivern *et al.* (MINERvA), Phys. Rev. D **94**, 052005 (2016).
- [11] O. Altinok *et al.* (MINERvA), Phys. Rev. D **96**, 072003 (2017).
- [12] L. Aliaga *et al.* (MINERvA), Nucl. Instrum. Meth. A **743**, 130 (2014).
- [13] L. Aliaga *et al.* (MINERvA), Phys. Rev. D **94**, 092005 (2016), [Addendum: Phys. Rev. D **95**, 039903 (2017)].
- [14] E. Valencia *et al.* (MINERvA), Phys. Rev. D **100**, 092001 (2019).
- [15] L. Zazueta *et al.* (MINERvA), “Improved constraint on the MINERvA medium energy neutrino flux using $\bar{\nu}e^- \rightarrow \bar{\nu}e^-$ data,” (2022), (unpublished), arXiv:2209.05540 [hep-ex].
- [16] D. Ruterbories *et al.* (MINERvA), Phys. Rev. D **104**, 092010 (2021).
- [17] D. G. Michael *et al.* (MINOS), Nucl. Instrum. Meth. A **596**, 190 (2008).
- [18] S. Agostinelli *et al.* (GEANT4), Nucl. Instrum. Meth. **A506**, 250 (2003).
- [19] M. P. Guthrie, R. G. Alsmiller, and H. W. Bertini, Nucl. Instrum. Meth. **66**, 29–36 (1968).
- [20] H. W. Bertini and M. P. Guthrie, Nucl. Phys. A **169**, 670–672 (1971).
- [21] A. B. Kaidalov, Phys. Lett. **116B**, 459–463 (1982).
- [22] L. Aliaga *et al.* (MINERvA), Nucl. Instrum. Meth. A **789**, 28 (2015).
- [23] C. Andreopoulos *et al.* (GENIE), Nucl. Instrum. Meth. **A614**, 87 (2010).
- [24] D. Rein and L. M. Sehgal, Annals Phys. **133**, 79 (1981).

- [25] K. S. Kuzmin, V. V. Lyubushkin, and V. A. Naumov, *Acta Phys. Polon. B* **37**, 2337 (2006), arXiv:hep-ph/0606184.
- [26] A. Bodek, I. Park, and U.-K. Yang, *Nucl. Phys. Proc. Suppl.* **139**, 113 (2005).
- [27] D. Rein and L. M. Sehgal, *Nucl. Phys. B* **223**, 29 (1983).
- [28] D. Rein and L. Sehgal, *Phys. Lett. B* **657**, 207 (2007), arXiv:hep-ph/0606185 [hep-ph].
- [29] E. J. Moniz, I. Sick, R. R. Whitney, J. R. Ficencic, R. D. Kephart, *et al.*, *Phys. Rev. Lett.* **26**, 445 (1971).
- [30] A. Bodek and J. L. Ritchie, *Phys. Rev. D* **23**, 1070 (1981).
- [31] J. Bodek, A. and Ritchie, *Phys. Rev. D* **24**, 1400 (1981).
- [32] M. Carneiro *et al.* (MINERvA), *Phys. Rev. Lett.* **124**, 121801 (2020).
- [33] P. A. Rodrigues *et al.* (MINERvA), *Phys. Rev. Lett.* **116**, 071802 (2016).
- [34] P. Rodrigues, C. Wilkinson, and K. McFarland, *Eur. Phys. J. C* **76**, 474 (2016).
- [35] M. A. Ramirez *et al.* (MINERvA), ““ ν_μ -Induced CC Coherent π^+ Production from C, CH, Fe and Pb nuclei in the MINERvA Detector” (manuscript in preparation),” (2022), “ ν_μ -Induced CC Coherent π^+ Production from C, CH, Fe and Pb nuclei in the MINERvA Detector” (manuscript in preparation).
- [36] B. Z. Kopeliovich, I. Schmidt, and M. Siddikov, *Phys. Rev. D* **85**, 073003 (2012).
- [37] A. Bercellie (MINERvA), *Muon Neutrino Charged Current Single Pion Production on Various Targets in the MINERvA Detector*, Ph.D. thesis, Rochester U. (2022).
- [38] G. D’Agostini, *Nucl. Instrum. Meth. A* **362**, 487 (1995).
- [39] G. D’Agostini, in *Alliance Workshop on Unfolding and Data Correction* (2010) arXiv:1010.0632 [physics.data-an].
- [40] T. Adye, in *PHYSTAT 2011* (CERN, Geneva, 2011) pp. 313–318, arXiv:1105.1160 [physics.data-an].
- [41] J. Kleykamp, *A-scaling of CCQE-like cross sections at MINERvA*, Ph.D. thesis, Rochester U., Rochester U. (2021).
- [42] Y. Hayato, *Acta Phys. Polon. B* **40**, 2477 (2009).
- [43] K. Gallmeister, U. Mosel, and J. Weil, *Phys. Rev. C* **94**, 035502 (2016), arXiv:1605.09391 [nucl-th].
- [44] P. Adamson *et al.* (MINOS), *Phys. Rev. D* **91**, 012005 (2015), arXiv:1410.8613 [hep-ex].
- [45] P. Stowell *et al.* (MINERvA), *Phys. Rev. D* **100**, 072005 (2019), arXiv:1903.01558 [hep-ex].

I. SUPPLEMENTAL MATERIAL

A. Flux Differences between Targets and Tracker before Reweighting of Tracker

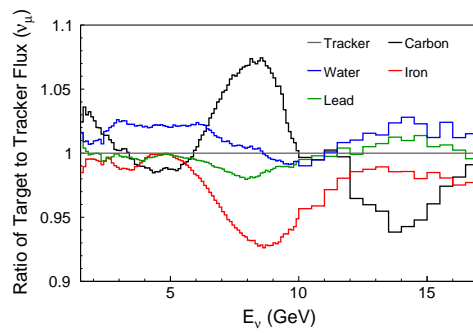


FIG. Supp.1. Ratio of neutrino fluxes in carbon, water, iron, and lead to scintillator as a function of energy before reweighting of the scintillator sample denominator.

B. Single π^+ Q^2 tune function

The disagreement between the initial tuned GENIE model described above and the scintillator data was addressed by applying a weighting function, $w(Q^2)$ to all non-coherent single pion production on nuclei other than hydrogen. Coherent pion production and production on hydrogen are excluded from the correction because they are independently constrained by the results of Ref. [35] and Ref. [34], respectively. The predicted coherent and hydrogen cross section on scintillator in the data was subtracted from the measurement in the data, and compared to the same quantity in the simulation, and the ratio was fit to find $w(Q^2)$.

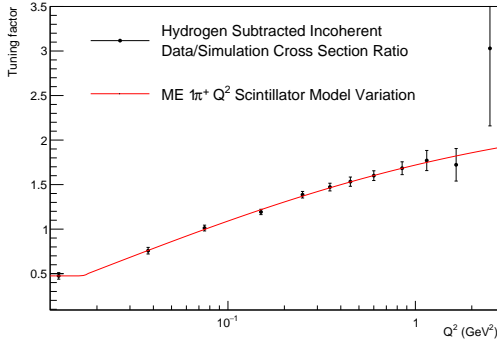
This fit has the form shown in equation 1, where Erf is the Gaussian error function, and the fitted parameters are given in Tab. Supp.I. Figure Supp.2 shows the cross section ratio as well as the fit.

These suppression at low Q^2 relative to high Q^2 is a feature that has been observed in different data sets, including MINOS on iron [44] and in other MINERvA pion measurements on scintillator [8, 10, 11, 45]. Models have some differences in prediction, although generally do not predict this large suppression. The high Q^2 shape evolution of different versions and tunes of GENIE goes from GENIEv2 MnvTune v4.2.1 (steepest), to untuned GENIE v2.12.6 to GENIE v3 02a_02_11a to GENIEv2 MnvTune v4.3.1 (flattest) via changes to the axial form factor and, in the case of GENIE v3, also the vector form factor and FSI processes. Like the tunes of Refs. 45 and 44, the MnvTune v4.3.1 adds the *ad hoc* additional shape at low Q^2 evident in these data.

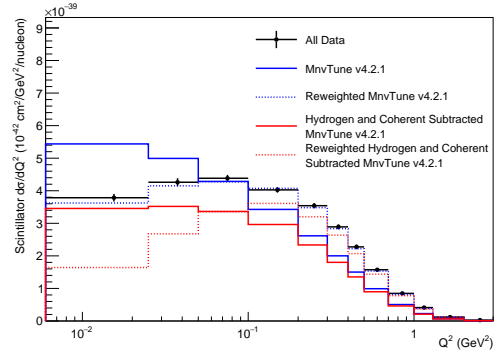
$$w(Q^2) = a + b \times \text{Max} \left[0, \text{Erf} \left[x_3 \ln \left(\frac{Q^2}{x_1} \right) \right] \right] \quad (1)$$

Parameter	Fitted Value
a	0.475 ± 0.037
b	1.837 ± 0.537
x_1	0.017 ± 0.003
x_3	0.171 ± 0.069
χ^2/ndf	1.58/11

TABLE Supp.I. Fitted parameters of the Q^2 model variation



(a)



(b)

FIG. Supp.2. (a) Hydrogen Subtracted Incoherent Data/Simulation Cross Section Ratio and the Q^2 weighting function (FHC nu-e constraint). (b) Unweighted and Reweighted Total and Hydrogen Subtracted Incoherent Simulated Cross Section Compared to Data Cross Section.

C. Sideband scale factors

Target	$1.4 < W_{\text{exp,true}} < 1.8 \text{ GeV}/c^2$	$1.8 < W_{\text{exp,true}} \text{ GeV}/c^2$	χ^2/ndf
Carbon	0.58 ± 0.44	1.71 ± 0.71	0.147/4
Water	1.53 ± 0.30	0.00 ± 0.90	18.956/4
Iron	0.48 ± 0.25	1.05 ± 0.29	1.705/4
Lead	0.09 ± 0.16	1.06 ± 0.20	0.324/4
Scintillator	0.58 ± 0.02	0.80 ± 0.02	3.192/4

TABLE Supp.II. W_{exp} sideband scales found from the fit in the high $W > 1.4 \text{ GeV}$ sideband for all targets.

Target	Upstream Scale	Upstream χ^2/ndf	Downstream Scale	Downstream χ^2/ndf
Target 1	0.69 ± 0.13	1.45/6	0.93 ± 0.07	2.76/6
Target 2	0.99 ± 0.05	3.90/7	0.88 ± 0.07	12.00/6
Target 3	0.92 ± 0.04	6.93/10	0.88 ± 0.06	4.03/7
Target 4	0.92 ± 0.06	4.18/5	0.83 ± 0.05	13.70/7
Target 5	0.92 ± 0.05	9.89/7	0.86 ± 0.05	11.89/7

TABLE Supp.III. Upstream and downstream scintillator target sideband scales for all nuclear targets

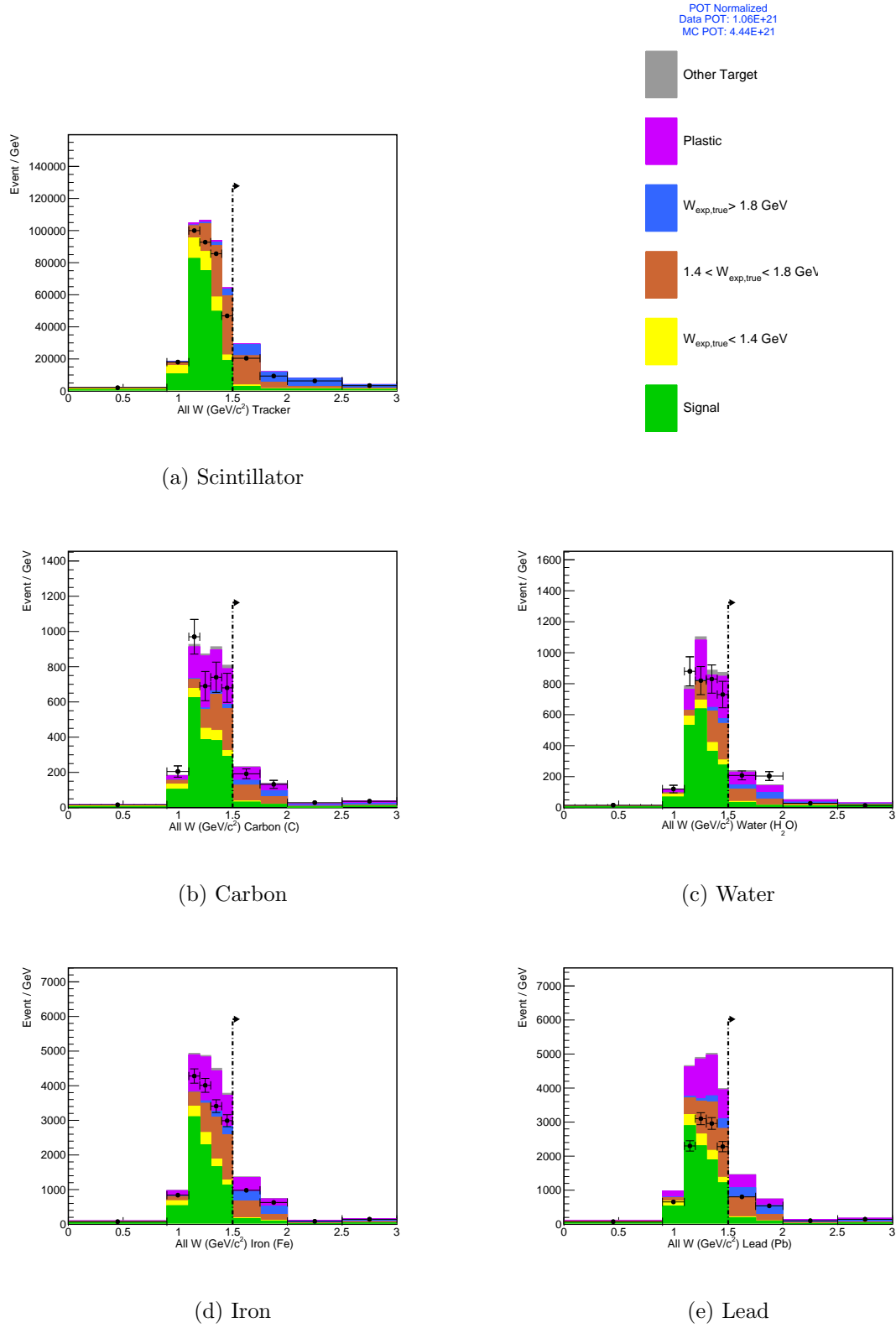


FIG. Supp.3. W_{exp} distribution of selected events before constraining the simulation using background estimates from data. The dashed arrow delineates the high W_{exp} sideband region.

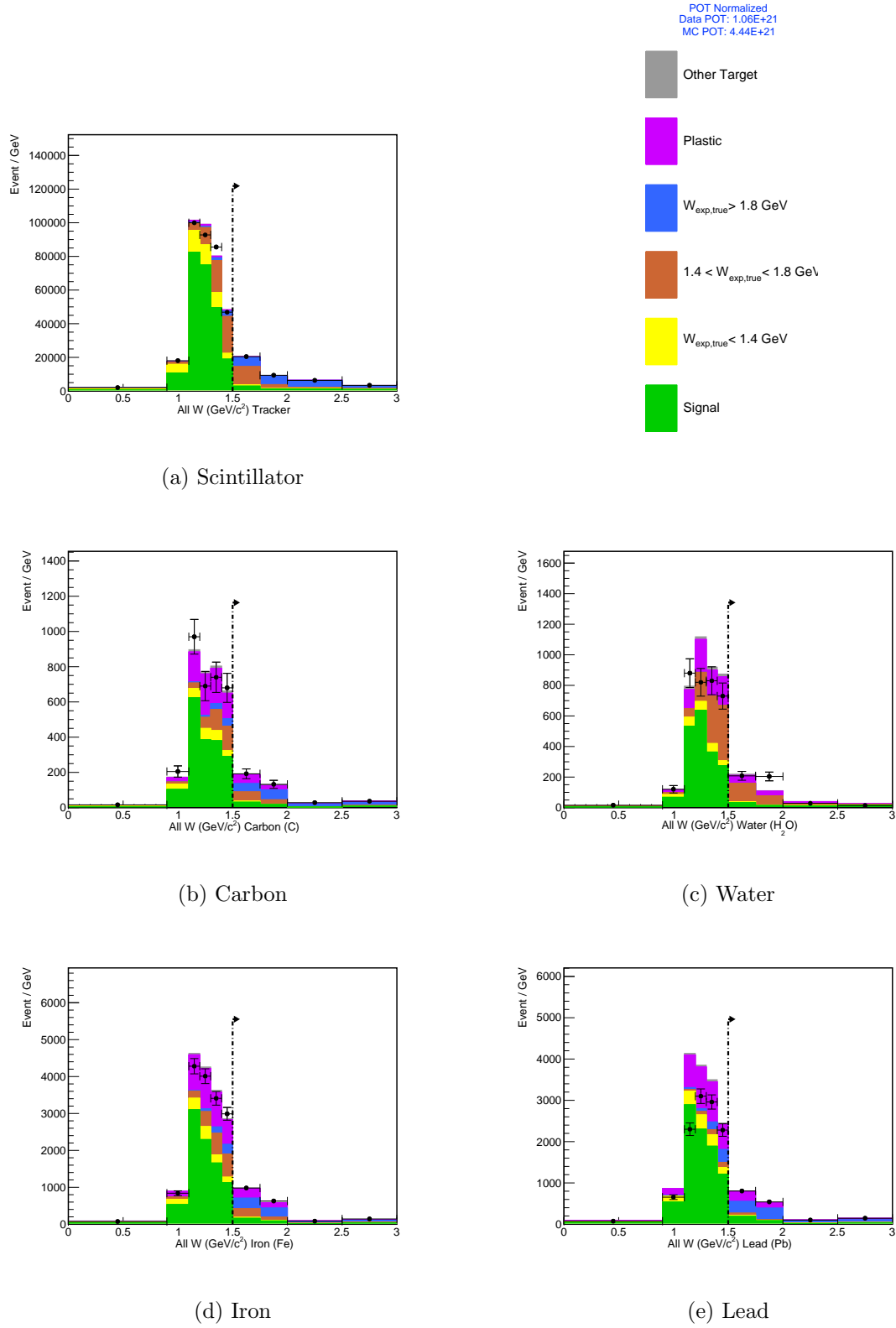


FIG. Supp.4. W_{exp} distribution of selected events after constraining the simulation using background estimates from data. The dashed arrow delineates the high W_{exp} sideband region.

D. Coherent Pion Production Weights

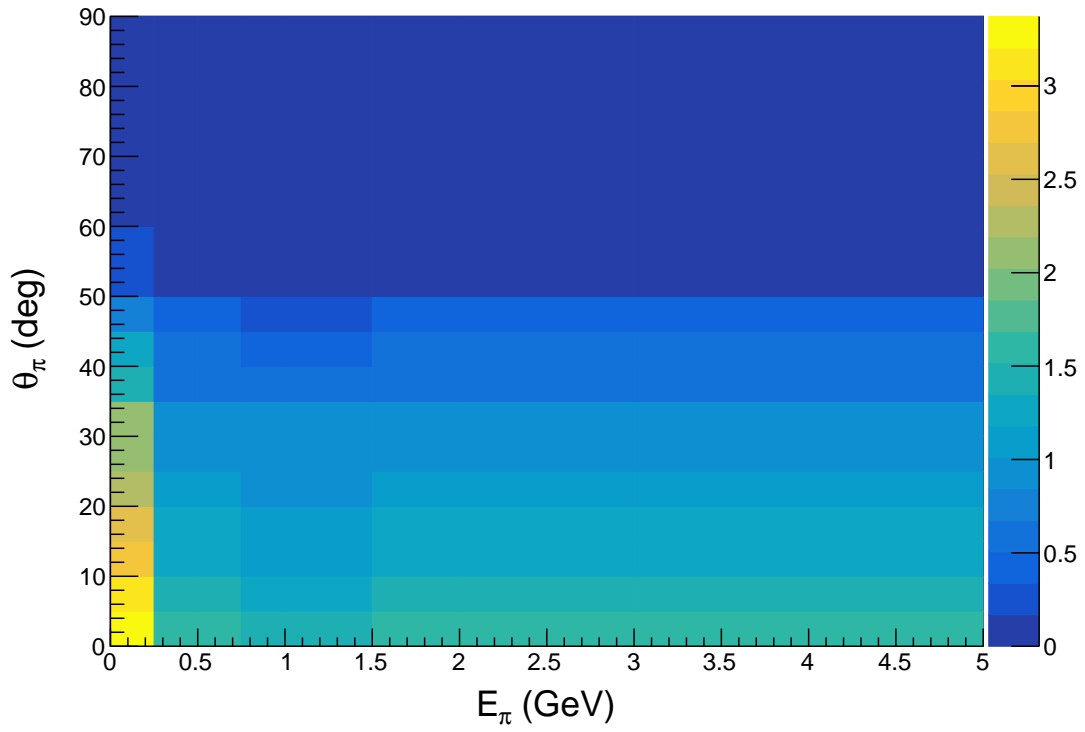
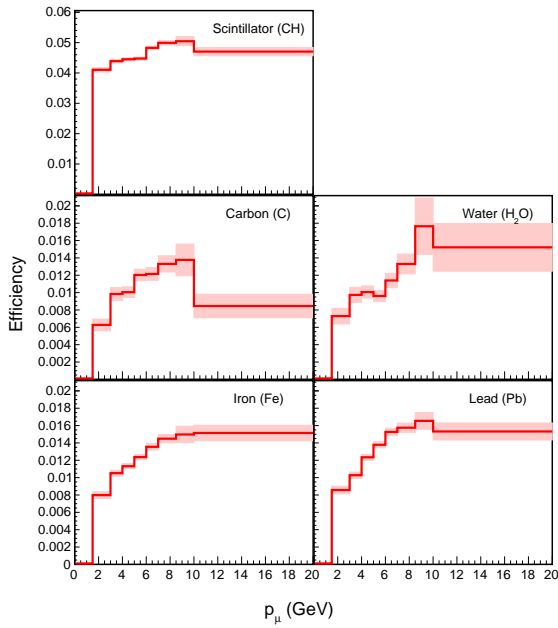


FIG. Supp.5. Plot of weights applied to coherent pion production events, given the kinematics of the coherent π^+ , derived from ME MINERvA data [35]

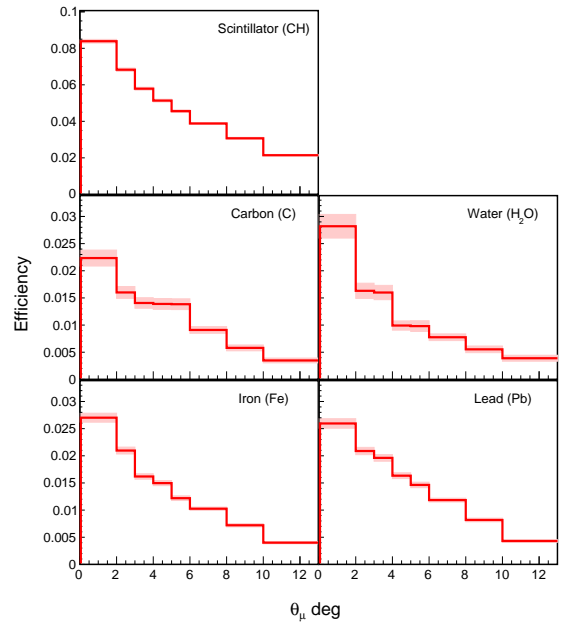
E_π (GeV)	0.0-0.25	0.25-0.5	0.5-0.75	0.75-1.0	1.0-1.5	1.5-2.0	2.0-3.0	3.0-5.0
θ_π (deg)								
0-5	3.372	1.593	1.593	1.369	1.360	1.593	1.593	1.593
5-10	3.083	1.456	1.456	1.251	1.243	1.456	1.456	1.456
10-15	2.742	1.296	1.296	1.113	1.106	1.296	1.296	1.296
15-20	2.577	1.218	1.218	1.046	1.039	1.218	1.218	1.218
20-25	2.345	1.108	1.108	0.952	0.945	1.108	1.108	1.108
25-30	2.116	1.000	1.000	0.859	0.853	1.000	1.000	1.000
30-35	2.116	1.000	1.000	0.859	0.853	1.000	1.000	1.000
35-40	1.422	0.672	0.672	0.577	0.573	0.672	0.672	0.672
40-45	1.238	0.585	0.585	0.503	0.499	0.585	0.585	0.585
45-50	0.713	0.337	0.337	0.289	0.288	0.337	0.337	0.337
50-60	0.263	0.124	0.124	0.107	0.106	0.124	0.124	0.124
60-70	0.049	0.023	0.023	0.020	0.020	0.023	0.023	0.023
70-80	0.049	0.023	0.023	0.020	0.020	0.023	0.023	0.023
80-90	0.049	0.023	0.023	0.020	0.020	0.023	0.023	0.023

TABLE Supp.IV. Tabulation of weights applied to coherent pion production events, given the kinematics of the coherent π^+ , derived from ME MINERvA data [35]

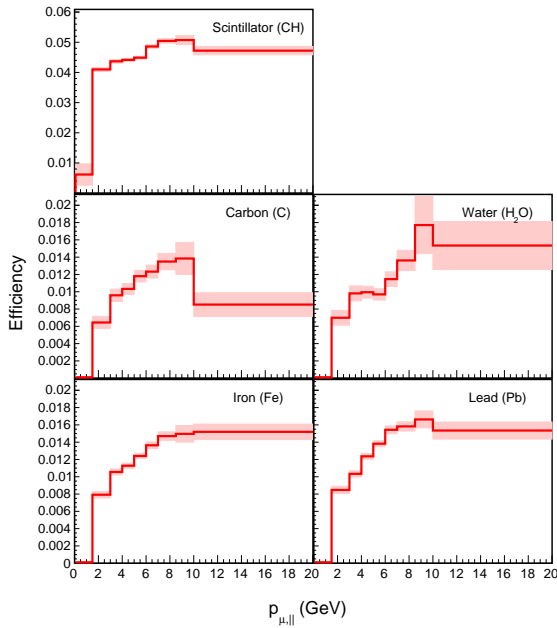
E. Efficiencies



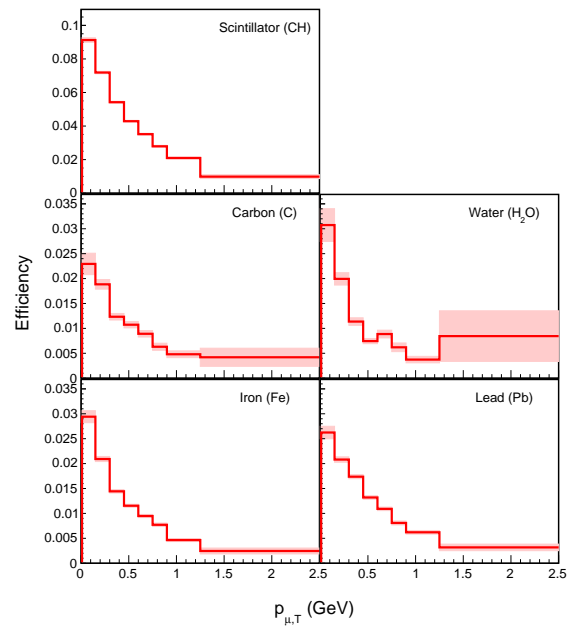
(a) Efficiency versus muon momentum



(b) Efficiency versus muon angle

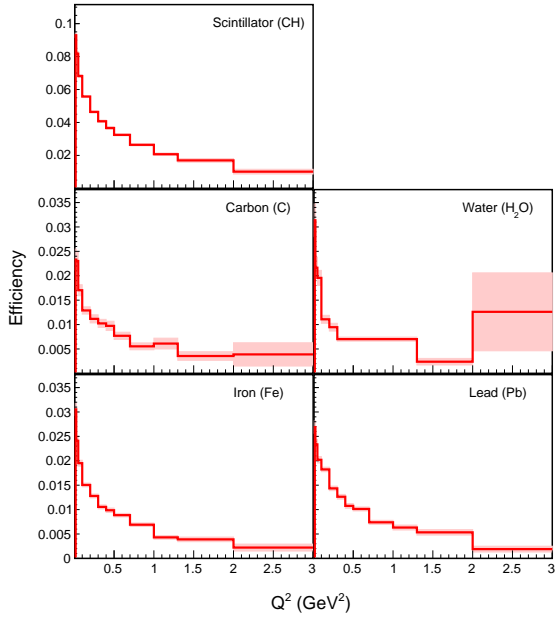


(c) Efficiency versus longitudinal muon momentum

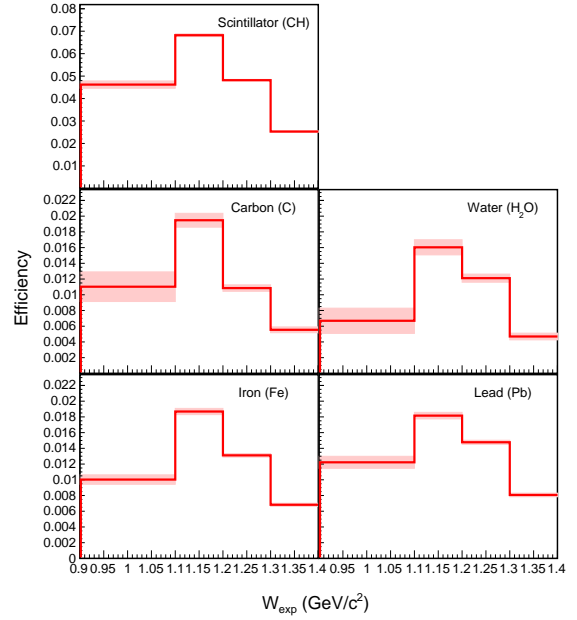


(d) Efficiency versus transverse muon momentum

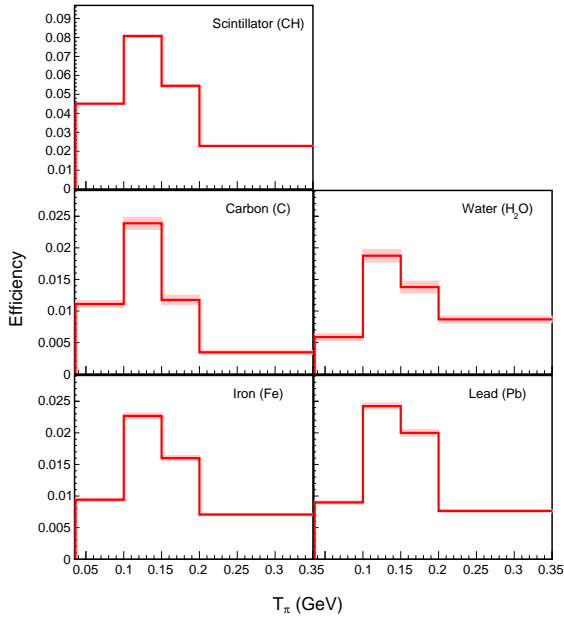
FIG. Supp.6. Efficiencies for scintillator (top left), carbon (middle left), water (middle right), iron (bottom left) and lead (bottom right). The shaded error bands show total uncertainties, including systematics and simulated statistics.



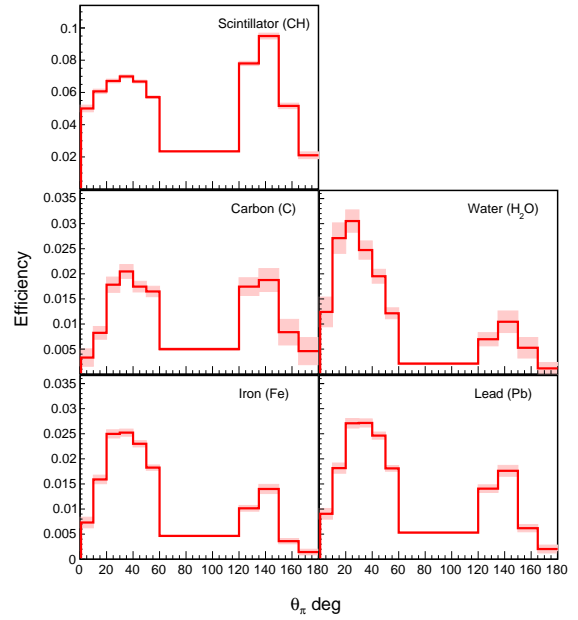
(a) Efficiency versus Q^2



(b) Efficiency versus W



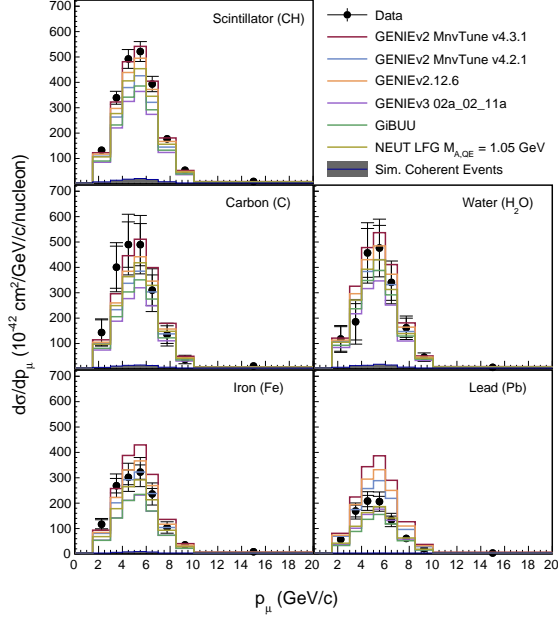
(c) Efficiency versus pion kinetic energy



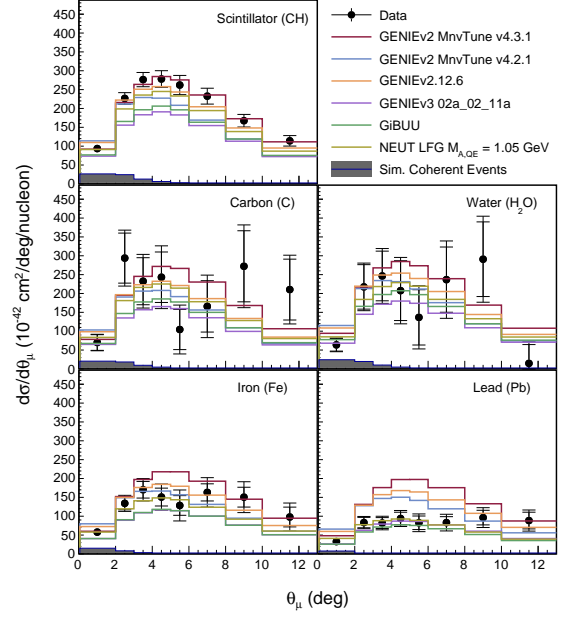
(d) Efficiency versus pion angle

FIG. Supp.7. Efficiencies for scintillator (top left), carbon (middle left), water (middle right), iron (bottom left) and lead (bottom right). The shaded error bands show total uncertainties, including systematics and simulated statistics.

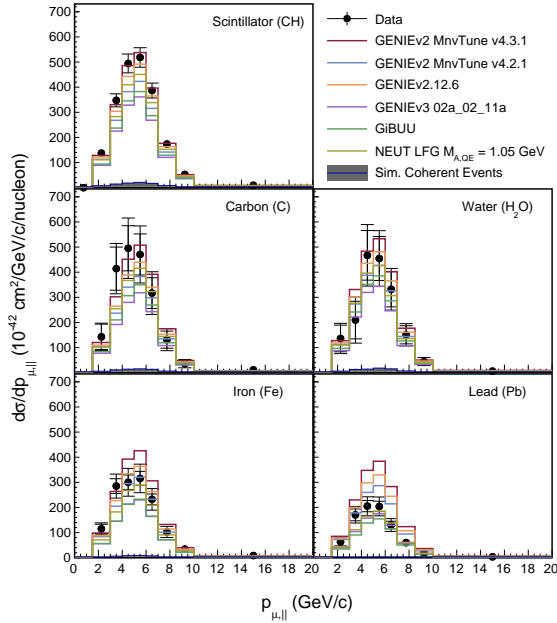
F. Absolute Cross Section Plots



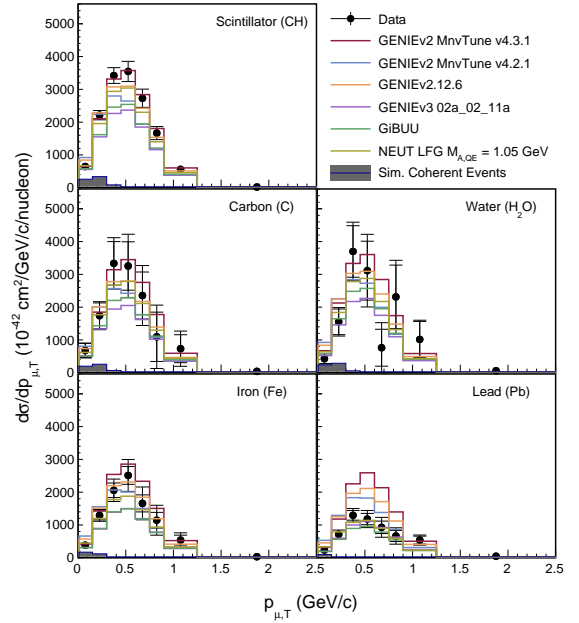
(a) Differential cross section $\frac{d\sigma}{dp_\mu}$ for scintillator, carbon, water, iron, and lead.



(b) Differential cross section $\frac{d\sigma}{d\theta_\mu}$ for scintillator, carbon, water, iron, and lead.

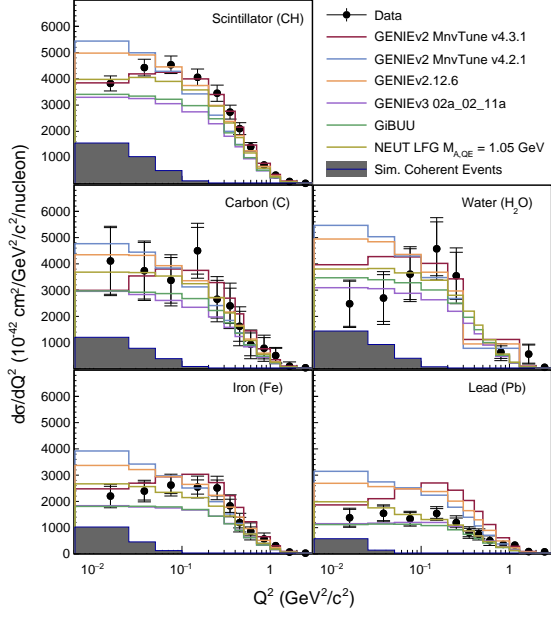


(c) Differential cross section $\frac{d\sigma}{dp_{\mu,||}}$ for scintillator, carbon, water, iron, and lead.

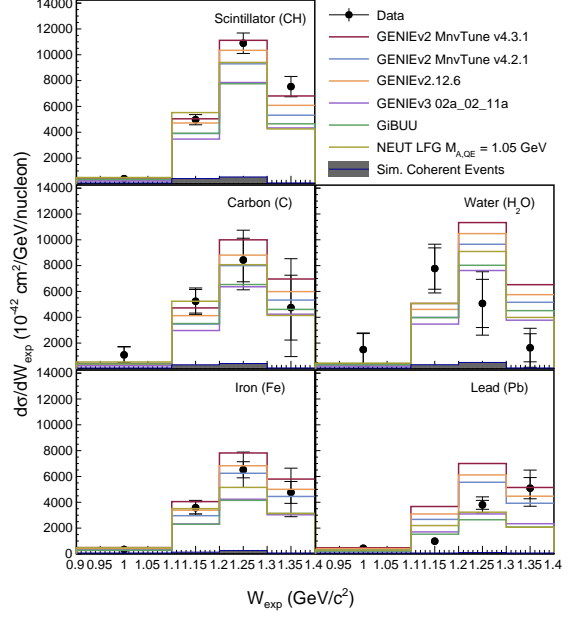


(d) Differential cross section $\frac{d\sigma}{dp_{\mu,T}}$ for scintillator, carbon, water, iron, and lead.

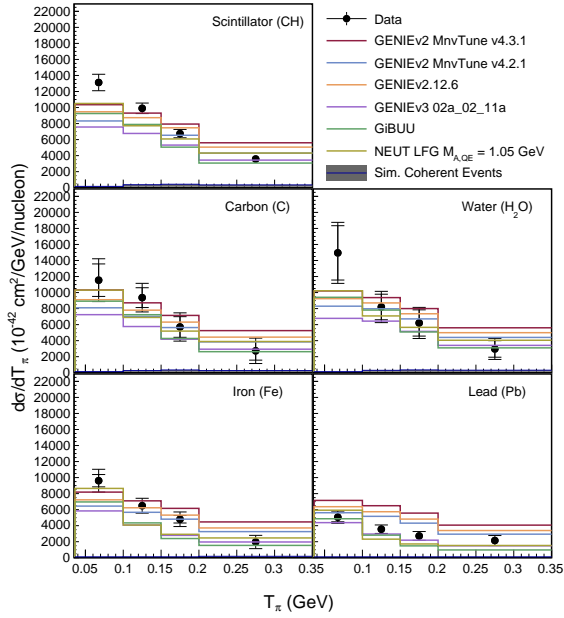
FIG. Supp.8. Differential cross sections versus muon variables.



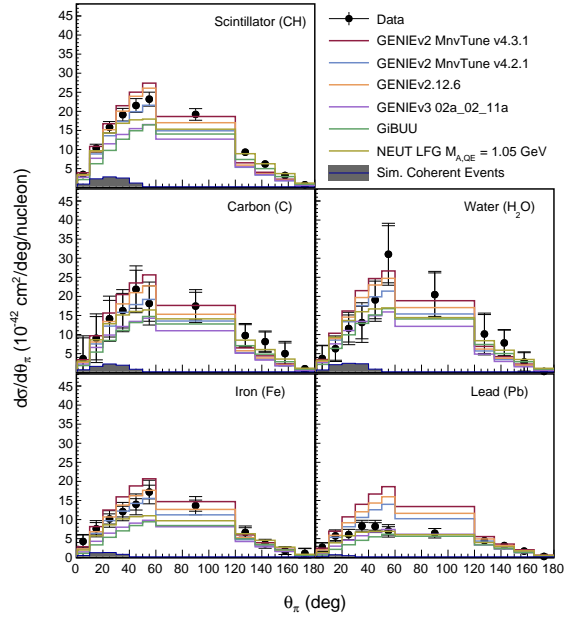
(a) Differential cross section $\frac{d\sigma}{dQ^2}$ for scintillator, carbon, water, iron, and lead.



(b) Differential cross section $\frac{d\sigma}{dW_{exp}}$ for scintillator, carbon, water, iron, and lead.



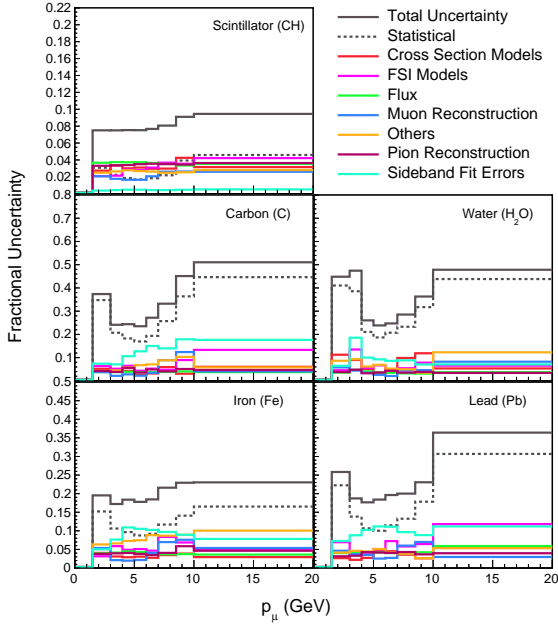
(c) Differential cross section $\frac{d\sigma}{dT_\pi}$ for scintillator, carbon, water, iron, and lead.



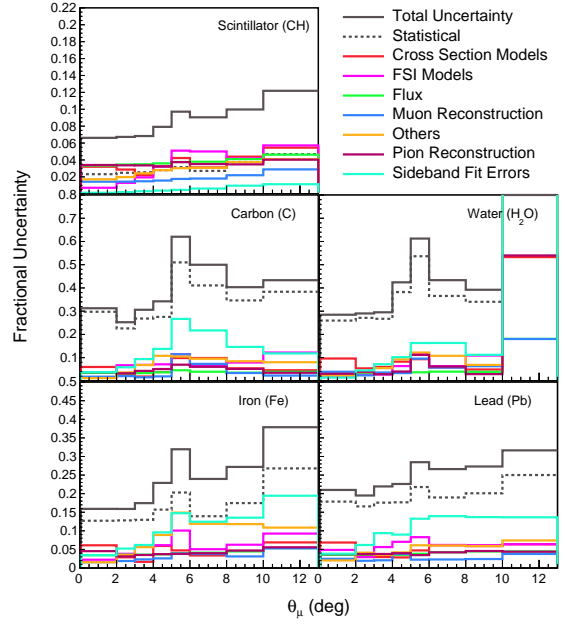
(d) Differential cross section $\frac{d\sigma}{d\theta_\pi}$ for scintillator, carbon, water, iron, and lead.

FIG. Supp.9. Differential cross sections versus other variables.

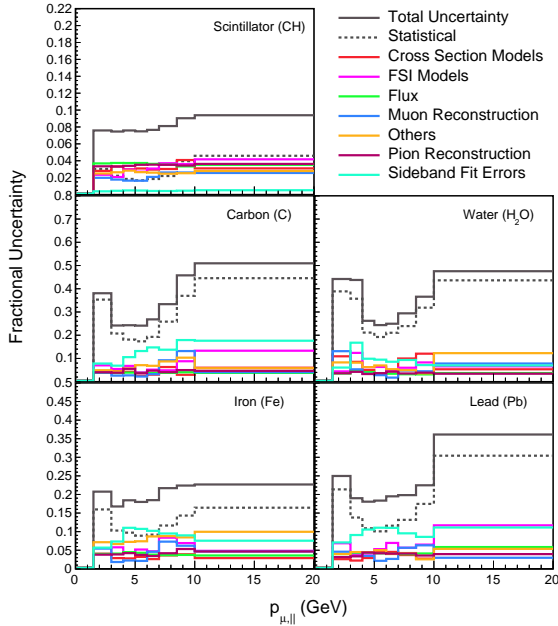
G. Absolute Cross Section Error Summaries



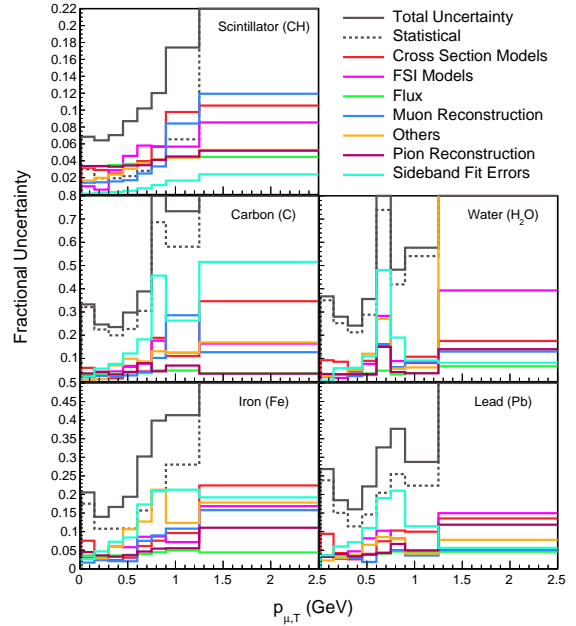
(a) Fractional uncertainties of $\frac{d\sigma}{dp_\mu}$.



(b) Fractional uncertainties of $\frac{d\sigma}{d\theta_\mu}$.

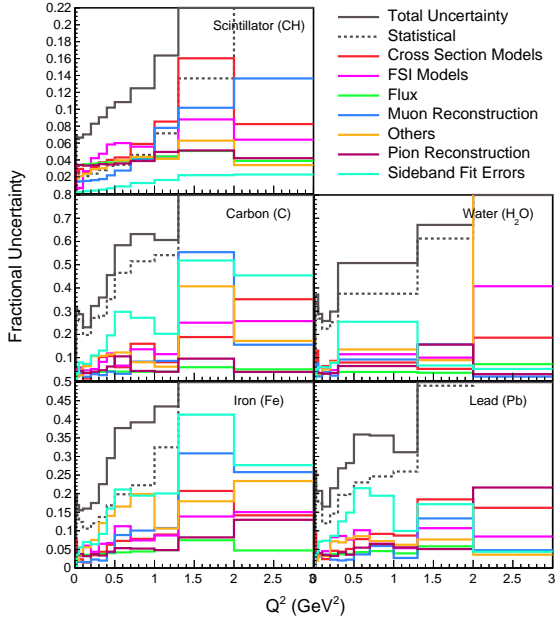


(c) Fractional uncertainties of $\frac{d\sigma}{dp_{\mu,||}}$.

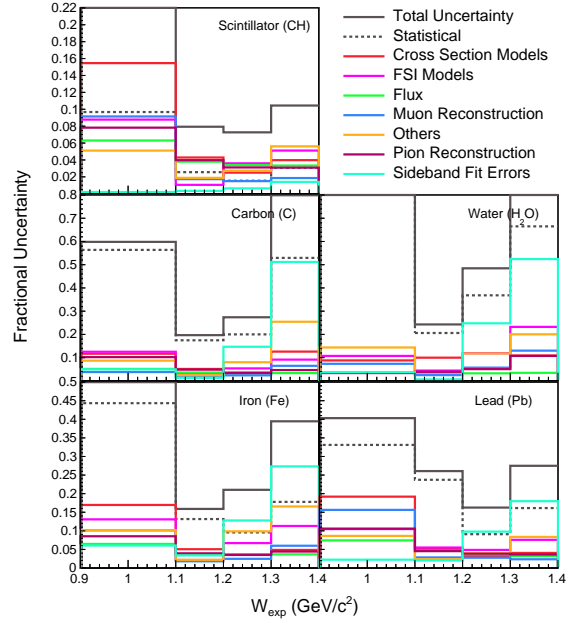


(d) Fractional uncertainties of $\frac{d\sigma}{dp_{\mu,T}}$.

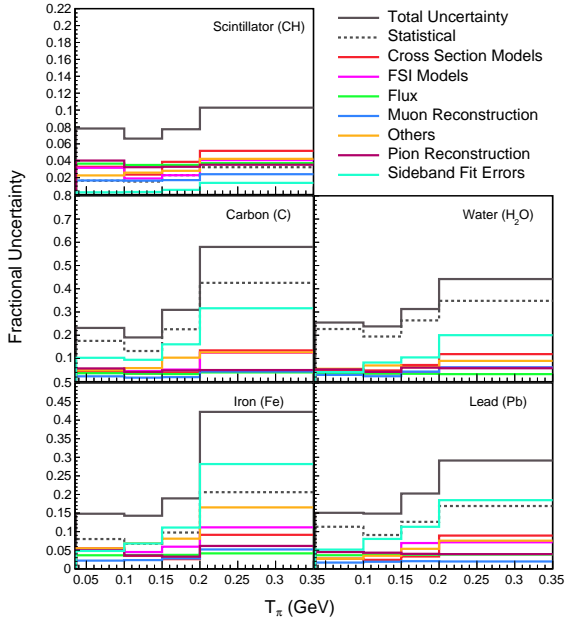
FIG. Supp.10. Systematic uncertainties of differential cross sections for scintillator (top left), carbon (middle left), water (middle right), iron (bottom left) and lead (bottom right)



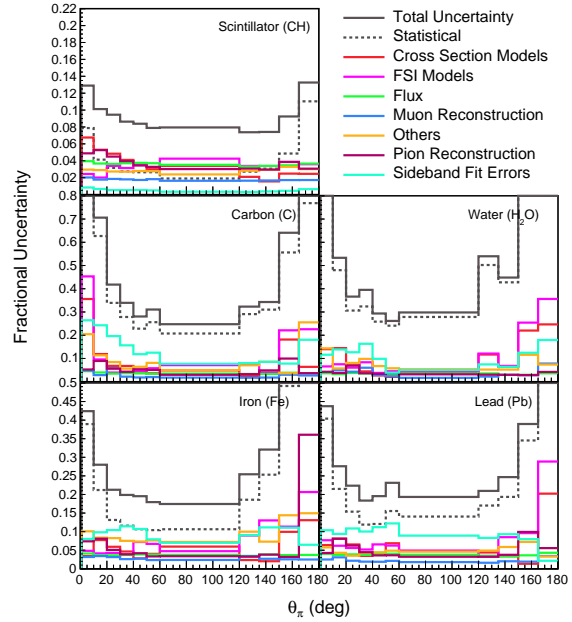
(a) Fractional uncertainties of $\frac{d\sigma}{dQ^2}$.



(b) Fractional uncertainties $\frac{d\sigma}{dW_{exp}}$.



(c) Fractional uncertainties $\frac{d\sigma}{dT_\pi}$.

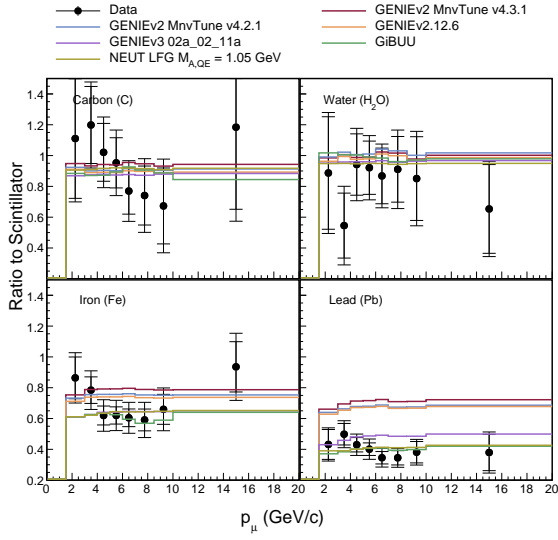


(d) Fractional uncertainties $\frac{d\sigma}{d\theta_\pi}$.

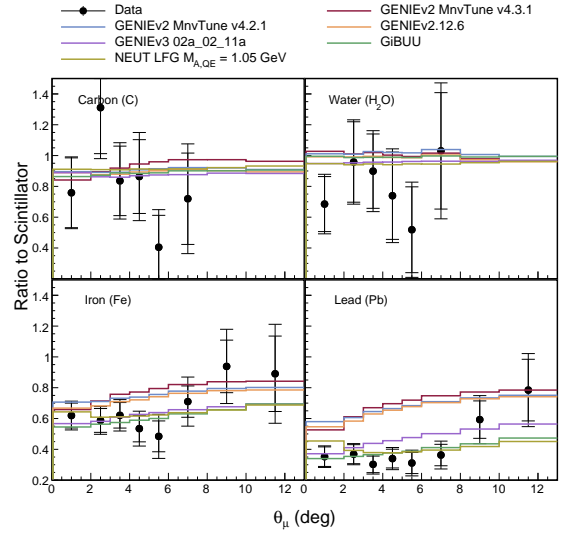
FIG. Supp.11. Systematic uncertainties of differential cross sections for scintillator (top left), carbon (middle left), water (middle right), iron (bottom left) and lead (bottom right)

H. Cross Section Ratio Plots

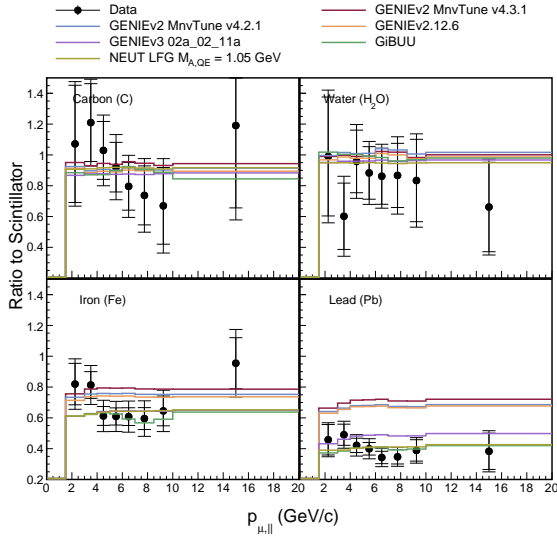
One of the striking features in these comparisons is that there are large difference in the ratios between the GENIEv2 and GENIEv3 models for the iron and lead targets. These are primarily from different the FSI effects in the generators. The increased pion scattering and absorption rates in heavy nuclei in GENIEv3 appear to better describe our data.



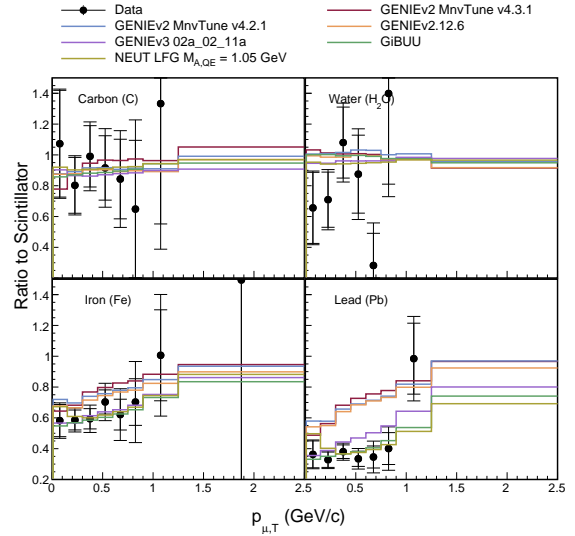
(a) Cross section ratios $\left(\frac{d\sigma_A}{dp_\mu}\right) / \left(\frac{d\sigma_{CH}}{dp_\mu}\right)$ for carbon, water, iron, and lead.



(b) Cross section ratios $\left(\frac{d\sigma_A}{d\theta_\mu}\right) / \left(\frac{d\sigma_{CH}}{d\theta_\mu}\right)$ for carbon, water, iron, and lead.

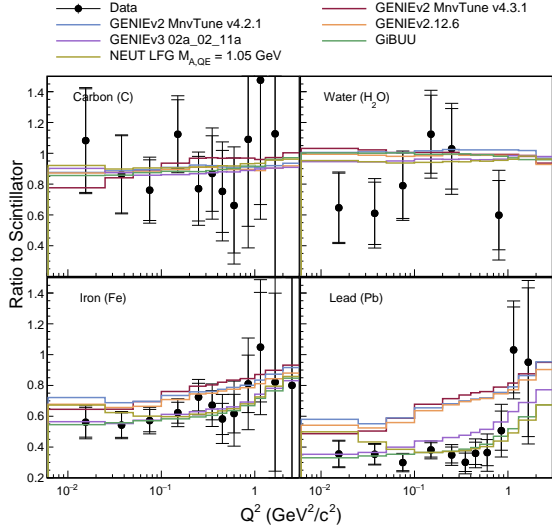


(c) Cross section ratios $\left(\frac{d\sigma_A}{dp_{\mu,||}}\right) / \left(\frac{d\sigma_{CH}}{dp_{\mu,||}}\right)$ for carbon, water, iron, and lead.

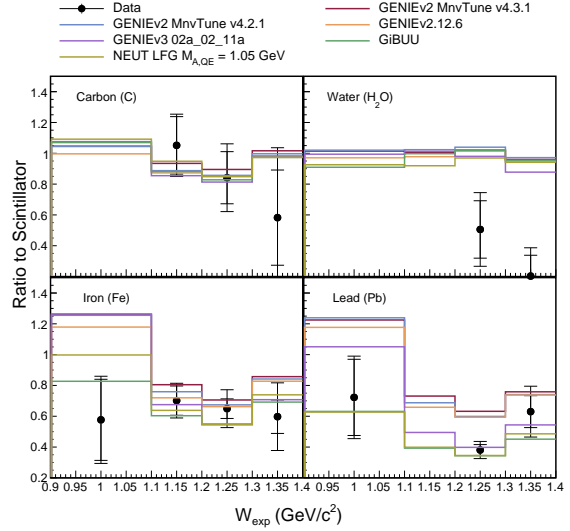


(d) Cross section ratios $\left(\frac{d\sigma_A}{dp_{\mu,T}}\right) / \left(\frac{d\sigma_{CH}}{dp_{\mu,T}}\right)$ for carbon, water, iron, and lead.

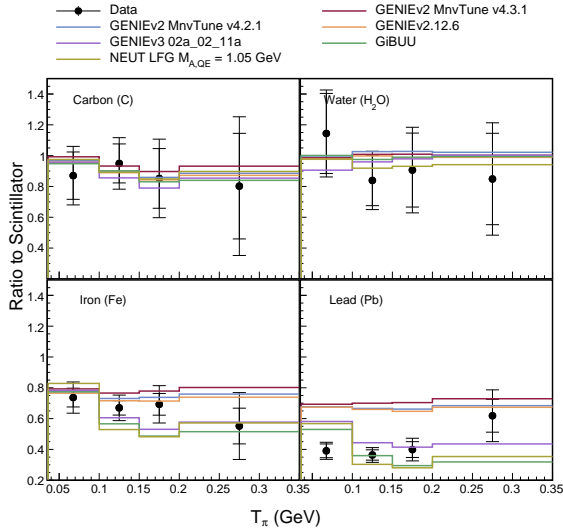
FIG. Supp.12. Cross section ratios versus muon variables.



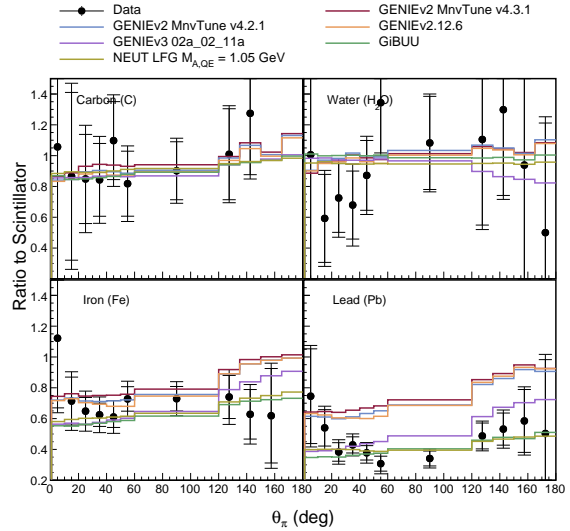
(a) Cross section ratios $\left(\frac{d\sigma_A}{dQ^2}\right) / \left(\frac{d\sigma_{CH}}{dQ^2}\right)$ for carbon, water, iron, and lead.



(b) Cross section ratios $\left(\frac{d\sigma_A}{dW_{exp}}\right) / \left(\frac{d\sigma_{CH}}{dW_{exp}}\right)$ for carbon, water, iron, and lead.



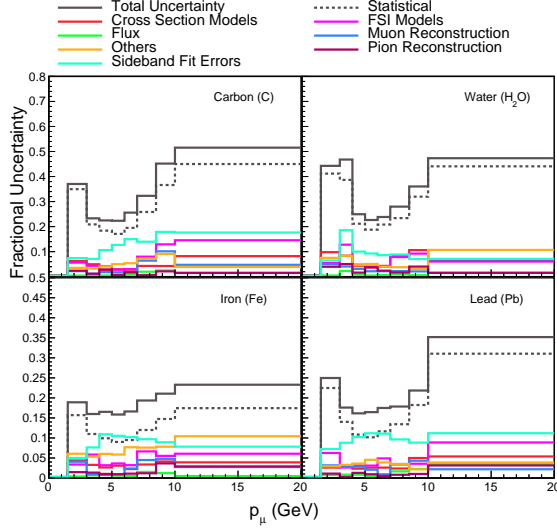
(c) Cross section ratios $\left(\frac{d\sigma_A}{dT_\pi}\right) / \left(\frac{d\sigma_{CH}}{dT_\pi}\right)$ for carbon, water, iron, and lead.



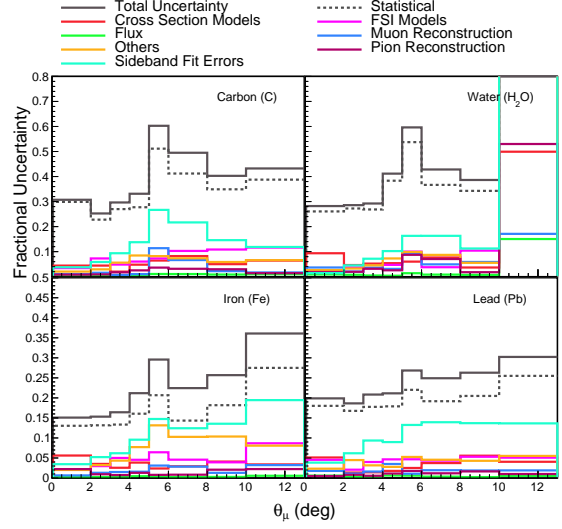
(d) Cross section ratios $\left(\frac{d\sigma_A}{d\theta_\pi}\right) / \left(\frac{d\sigma_{CH}}{d\theta_\pi}\right)$ for carbon, water, iron, and lead.

FIG. Supp.13. Cross section ratios versus other variables.

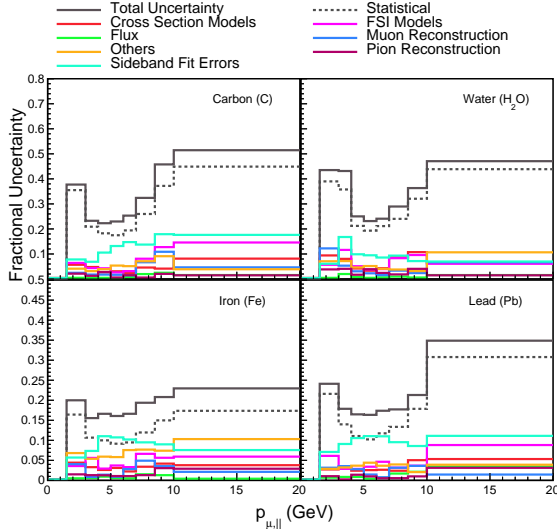
I. Cross Section Ratio Error Summaries



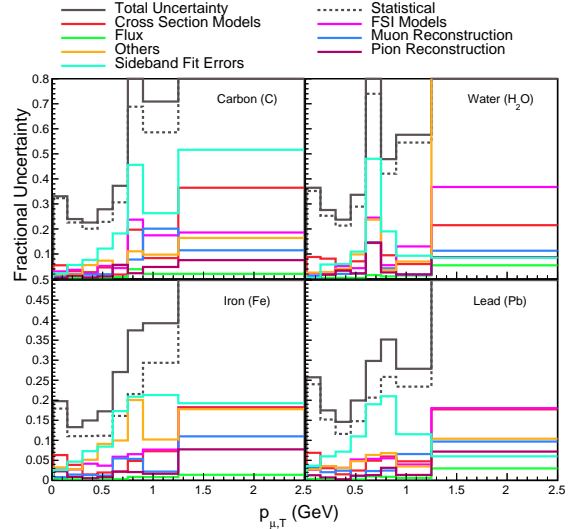
(a) Fractional uncertainties $\left(\frac{d\sigma_A}{dp_\mu}\right) / \left(\frac{d\sigma_{CH}}{dp_\mu}\right)$.



(b) Fractional uncertainties $\left(\frac{d\sigma_A}{d\theta_\mu}\right) / \left(\frac{d\sigma_{CH}}{d\theta_\mu}\right)$.

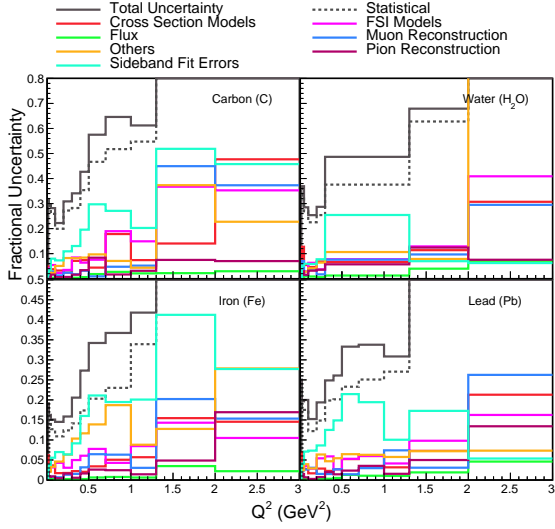


(c) Fractional uncertainties $\left(\frac{d\sigma_A}{dp_{\mu,||}}\right) / \left(\frac{d\sigma_{CH}}{dp_{\mu,||}}\right)$.

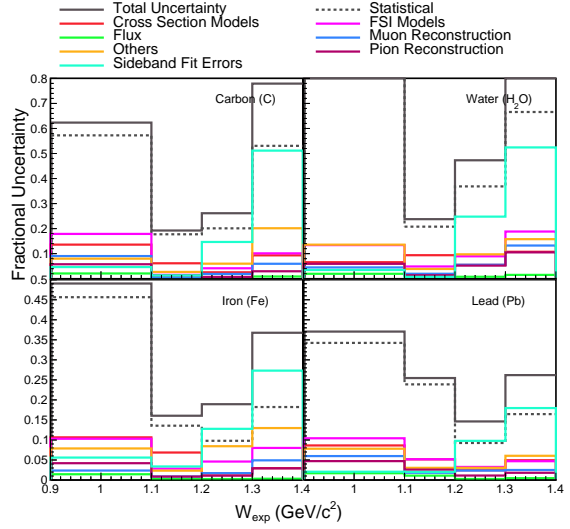


(d) Fractional uncertainties $\left(\frac{d\sigma_A}{dp_{\mu,T}}\right) / \left(\frac{d\sigma_{CH}}{dp_{\mu,T}}\right)$.

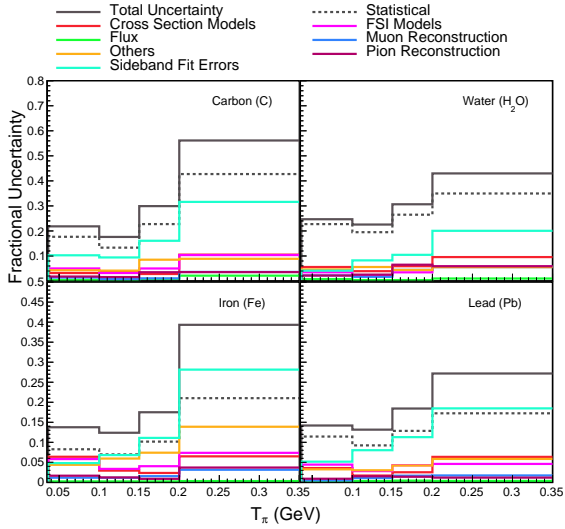
FIG. Supp.14. Systematic uncertainties of cross section ratios for carbon/scintillator (top left), water/scintillator (top right), iron/scintillator (bottom left) and lead/scintillator (bottom right)



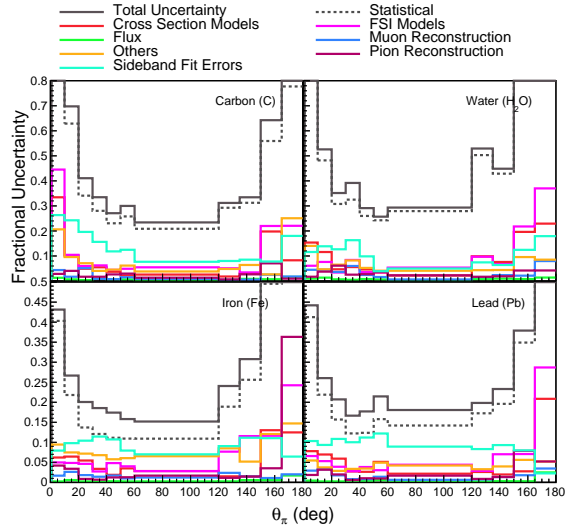
(a) Fractional uncertainties $\left(\frac{d\sigma_A}{dQ^2}\right) / \left(\frac{d\sigma_{CH}}{dQ^2}\right)$.



(b) Fractional uncertainties $\left(\frac{d\sigma_A}{dW_{exp}}\right) / \left(\frac{d\sigma_{CH}}{dW_{exp}}\right)$.



(c) Fractional uncertainties $\left(\frac{d\sigma_A}{dT_\pi}\right) / \left(\frac{d\sigma_{CH}}{dT_\pi}\right)$.



(d) Fractional uncertainties $\left(\frac{d\sigma_A}{d\theta_\pi}\right) / \left(\frac{d\sigma_{CH}}{d\theta_\pi}\right)$.

FIG. Supp.15. Systematic uncertainties of cross section ratios for carbon/scintillator (top left), water/scintillator (top right), iron/scintillator (bottom left) and lead/scintillator (bottom right)

J. Cross Section Tables

TABLE Supp.V. Measured cross section as function of p_μ on scintillator, in units of 10^{-42} $\text{cm}^2/\text{GeV}/c/\text{nucleon}$, and the absolute and fractional cross section uncertainties

Bin edges (GeV/c)	σ	Abs. Unc.	Frac. Stat. Unc.	Frac. Sys. Unc.	Frac. Flux Unc.
1.5-3.0	132.41	9.94	0.031	0.068	0.037
3.0-4.0	339.29	25.45	0.022	0.072	0.037
4.0-5.0	492.23	37.09	0.019	0.073	0.037
5.0-6.0	521.41	39.22	0.017	0.073	0.037
6.0-7.0	393.48	30.19	0.018	0.074	0.036
7.0-8.5	177.43	14.31	0.022	0.078	0.035
8.5-10.0	53.66	4.89	0.039	0.082	0.033
10.0-20.0	9.51	0.90	0.046	0.083	0.035

TABLE Supp.VI. Statistical covariance matrix of measured cross section as function of p_μ on scintillator, in units of 10^{-84} $(\text{cm}^2/\text{GeV}/c/\text{nucleon})^2$

Bin edges (GeV/c)	1.5-3.0	3.0-4.0	4.0-5.0	5.0-6.0	6.0-7.0	7.0-8.5	8.5-10.0	10.0-20.0
1.5-3.0	16.658	4.105	0.935	0.338	0.170	0.049	0.020	0.002
3.0-4.0	4.105	57.479	12.979	3.077	0.916	0.225	0.043	0.006
4.0-5.0	0.935	12.979	83.056	19.009	4.249	0.707	0.145	0.016
5.0-6.0	0.338	3.077	19.009	76.961	17.936	2.974	0.414	0.049
6.0-7.0	0.170	0.916	4.249	17.936	52.187	8.527	1.138	0.061
7.0-8.5	0.049	0.225	0.707	2.974	8.527	15.067	1.952	0.104
8.5-10.0	0.020	0.043	0.145	0.414	1.138	1.952	4.444	0.153
10.0-20.0	0.002	0.006	0.016	0.049	0.061	0.104	0.153	0.190

TABLE Supp.VII. Systematic covariance matrix of measured cross section in p_μ on scintillator, in units of $10^{-84} (\text{cm}^2/\text{GeV}/c/\text{nucleon})^2$

Bin edges (GeV/c)	1.5-3.0	3.0-4.0	4.0-5.0	5.0-6.0	6.0-7.0	7.0-8.5	8.5-10.0	10.0-20.0
1.5-3.0	82.125	213.956	314.097	329.205	240.409	106.454	32.919	5.696
3.0-4.0	213.956	590.438	854.841	906.030	662.006	293.496	94.406	15.869
4.0-5.0	314.097	854.841	1292.343	1361.955	1020.144	458.089	144.301	24.963
5.0-6.0	329.205	906.030	1361.955	1461.454	1099.429	498.336	156.016	26.910
6.0-7.0	240.409	662.006	1020.144	1099.429	859.179	394.495	122.519	21.348
7.0-8.5	106.454	293.496	458.089	498.336	394.495	189.709	57.596	10.355
8.5-10.0	32.919	94.406	144.301	156.016	122.519	57.596	19.425	3.242
10.0-20.0	5.696	15.869	24.963	26.910	21.348	10.355	3.242	0.618

TABLE Supp.VIII. Measured cross section as function of θ_μ on scintillator, in units of $10^{-42} \text{cm}^2/\text{degree}/\text{nucleon}$, and the absolute and fractional cross section uncertainties

Bin edges (degree)	σ	Abs. Unc.	Frac. Stat. Unc.	Frac. Sys. Unc.	Frac. Flux Unc.
0-2	93.64	6.19	0.023	0.062	0.033
2-3	226.67	15.25	0.025	0.063	0.035
3-4	276.53	18.89	0.025	0.063	0.035
4-5	278.12	22.02	0.028	0.074	0.036
5-6	262.12	25.46	0.031	0.092	0.038
6-8	232.61	21.04	0.027	0.086	0.038
8-10	167.48	16.70	0.038	0.092	0.041
10-13	114.14	13.91	0.047	0.112	0.046

TABLE Supp.IX. Statistical covariance matrix of measured cross section as function of θ_μ on scintillator, in units of $10^{-84} (\text{cm}^2/\text{degree}/\text{nucleon})^2$

Bin edges (degree)	0-2	2-3	3-4	4-5	5-6	6-8	8-10	10-13
0-2	4.693	-0.300	-0.494	-0.035	-0.001	-0.002	-0.002	-0.002
2-3	-0.300	31.566	0.489	-1.641	-0.173	-0.013	-0.015	-0.013
3-4	-0.494	0.489	49.367	1.222	-2.542	-0.137	0.002	-0.004
4-5	-0.035	-1.641	1.222	60.451	2.522	-1.709	-0.064	0.008
5-6	-0.001	-0.173	-2.542	2.522	68.064	-0.152	-1.074	-0.021
6-8	-0.002	-0.013	-0.137	-1.709	-0.152	39.575	-0.871	-0.601
8-10	-0.002	-0.015	0.002	-0.064	-1.074	-0.871	39.542	-1.187
10-13	-0.002	-0.013	-0.004	0.008	-0.021	-0.601	-1.187	28.649

TABLE Supp.X. Systematic covariance matrix of measured cross section in θ_μ on scintillator, in units of $10^{-84} (\text{cm}^2/\text{degree}/\text{nucleon})^2$

Bin edges (degree)	0-2	2-3	3-4	4-5	5-6	6-8	8-10	10-13
0-2	33.684	78.058	87.540	87.329	86.942	68.156	50.842	37.409
2-3	78.058	200.937	237.301	255.413	267.730	210.228	154.423	119.171
3-4	87.540	237.301	307.318	345.850	375.759	306.688	229.018	179.044
4-5	87.329	255.413	345.850	424.408	479.626	386.851	290.976	229.426
5-6	86.942	267.730	375.759	479.626	580.386	461.821	343.697	276.712
6-8	68.156	210.228	306.688	386.851	461.821	403.285	300.163	244.821
8-10	50.842	154.423	229.018	290.976	343.697	300.163	239.503	193.833
10-13	37.409	119.171	179.044	229.426	276.712	244.821	193.833	164.717

TABLE Supp.XI. Measured cross section as function of $p_{\mu,||}$ on scintillator, in units of 10^{-42} $\text{cm}^2/\text{GeV}/c/\text{nucleon}$, and the absolute and fractional cross section uncertainties

Bin edges (GeV/c)	σ	Abs. Unc.	Frac. Stat. Unc.	Frac. Sys. Unc.	Frac. Flux Unc.
1.5-3.0	137.27	10.42	0.030	0.070	0.037
3.0-4.0	347.62	25.93	0.022	0.071	0.037
4.0-5.0	494.41	37.52	0.018	0.074	0.037
5.0-6.0	518.20	38.78	0.017	0.073	0.037
6.0-7.0	386.60	29.60	0.018	0.074	0.036
7.0-8.5	173.45	14.06	0.022	0.078	0.035
8.5-10.0	52.71	4.76	0.040	0.081	0.033
10.0-20.0	9.44	0.89	0.046	0.082	0.035

TABLE Supp.XII. Statistical covariance matrix of measured cross section as function of $p_{\mu,||}$ on scintillator, in units of 10^{-84} $(\text{cm}^2/\text{GeV}/c/\text{nucleon})^2$

Bin edges (GeV/c)	1.5-3.0	3.0-4.0	4.0-5.0	5.0-6.0	6.0-7.0	7.0-8.5	8.5-10.0	10.0-20.0
1.5-3.0	17.281	4.316	0.981	0.386	0.175	0.047	0.019	0.002
3.0-4.0	4.316	59.783	13.377	3.199	0.890	0.225	0.042	0.006
4.0-5.0	0.981	13.377	83.368	19.478	4.159	0.688	0.142	0.016
5.0-6.0	0.386	3.199	19.478	76.300	17.415	2.887	0.399	0.049
6.0-7.0	0.175	0.890	4.159	17.415	50.714	8.346	1.129	0.062
7.0-8.5	0.047	0.225	0.688	2.887	8.346	14.498	1.871	0.101
8.5-10.0	0.019	0.042	0.142	0.399	1.129	1.871	4.343	0.147
10.0-20.0	0.002	0.006	0.016	0.049	0.062	0.101	0.147	0.188

TABLE Supp.XIII. Systematic covariance matrix of measured cross section in $p_{\mu,||}$ on scintillator, in units of $10^{-84} (\text{cm}^2/\text{GeV}/c/\text{nucleon})^2$

Bin edges (GeV/c)	1.5-3.0	3.0-4.0	4.0-5.0	5.0-6.0	6.0-7.0	7.0-8.5	8.5-10.0	10.0-20.0
1.5-3.0	91.226	229.520	338.349	347.709	251.637	112.813	34.549	6.067
3.0-4.0	229.520	612.679	877.172	909.191	657.101	291.505	93.008	15.804
4.0-5.0	338.349	877.172	1324.084	1362.526	1012.135	457.507	142.290	25.029
5.0-6.0	347.709	909.191	1362.526	1427.562	1062.163	483.211	149.666	26.138
6.0-7.0	251.637	657.101	1012.135	1062.163	825.422	380.578	117.151	20.653
7.0-8.5	112.813	291.505	457.507	483.211	380.578	183.242	55.337	10.013
8.5-10.0	34.549	93.008	142.290	149.666	117.151	55.337	18.344	3.110
10.0-20.0	6.067	15.804	25.029	26.138	20.653	10.013	3.110	0.598

TABLE Supp.XIV. Measured cross section as function of $p_{\mu,T}$ on scintillator, in units of $10^{-42} \text{cm}^2/\text{GeV}/c/\text{nucleon}$, and the absolute and fractional cross section uncertainties

Bin edges (GeV/c)	σ	Abs. Unc.	Frac. Stat. Unc.	Frac. Sys. Unc.	Frac. Flux Unc.
0.00-0.15	646.46	44.23	0.030	0.062	0.033
0.15-0.30	2212.06	141.95	0.019	0.061	0.033
0.30-0.45	3421.09	240.61	0.019	0.068	0.035
0.45-0.60	3545.67	308.07	0.022	0.084	0.036
0.60-0.75	2728.36	278.16	0.028	0.098	0.037
0.75-0.90	1665.26	200.09	0.041	0.113	0.041
0.90-1.25	559.10	97.31	0.065	0.161	0.045
1.25-2.50	19.99	5.98	0.221	0.202	0.045

TABLE Supp.XV. Statistical covariance matrix of measured cross section as function of $p_{\mu,T}$ on scintillator, in units of 10^{-84} ($\text{cm}^2/\text{GeV}/c/\text{nucleon}$)²

Bin edges (GeV/c)	0.00-0.15	0.15-0.30	0.30-0.45	0.45-0.60	0.60-0.75	0.75-0.90	0.90-1.25	1.25-2.50
0.00-0.15	375.058	-5.551	-47.201	-7.308	-0.821	-0.902	-0.344	-0.030
0.15-0.30	-5.551	1821.647	31.115	-156.758	-39.058	-9.338	-2.217	-0.043
0.30-0.45	-47.201	31.115	4348.247	269.040	-313.708	-92.462	-17.984	-0.914
0.45-0.60	-7.308	-156.758	269.040	5947.956	700.721	-342.839	-78.672	-2.713
0.60-0.75	-0.821	-39.058	-313.708	700.721	5878.758	1013.662	-145.751	-2.860
0.75-0.90	-0.902	-9.338	-92.462	-342.839	1013.662	4679.844	465.915	-9.180
0.90-1.25	-0.344	-2.217	-17.984	-78.672	-145.751	465.915	1335.605	34.903
1.25-2.50	-0.030	-0.043	-0.914	-2.713	-2.860	-9.180	34.903	19.497

TABLE Supp.XVI. Systematic covariance matrix of measured cross section in $p_{\mu,T}$ on scintillator, in units of 10^{-84} ($\text{cm}^2/\text{GeV}/c/\text{nucleon}$)²

Bin edges (GeV/c)	0.00-0.15	0.15-0.30	0.30-0.45	0.45-0.60	0.60-0.75	0.75-0.90	0.90-1.25	1.25-2.50
0.00-0.15	1581.186	5096.119	6401.031	6050.531	4214.151	2732.787	955.250	36.236
0.15-0.30	5096.119	18327.195	26728.571	28116.824	20742.179	13158.005	4370.207	161.226
0.30-0.45	6401.031	26728.571	53542.567	65838.516	54164.519	34609.724	11743.643	442.813
0.45-0.60	6050.531	28116.824	65838.516	88957.669	77342.326	50764.557	18249.458	689.458
0.60-0.75	4214.151	20742.179	54164.519	77342.326	71495.961	48206.936	18687.460	724.443
0.75-0.90	2732.787	13158.005	34609.724	50764.557	48206.936	35354.928	15091.296	591.143
0.90-1.25	955.250	4370.207	11743.643	18249.458	18687.460	15091.296	8133.526	341.419
1.25-2.50	36.236	161.226	442.813	689.458	724.443	591.143	341.419	16.250

TABLE Supp.XVII. Measured cross section as function of Q^2 on scintillator, in units of 10^{-42} $\text{cm}^2/\text{GeV}^2/c^2/\text{nucleon}$, and the absolute and fractional cross section uncertainties

Bin edges (GeV^2/c^2)	σ	Abs. Unc.	Frac. Stat. Unc.	Frac. Sys. Unc.	Frac. Flux Unc.
0.000-0.025	3825.00	261.09	0.029	0.062	0.033
0.025-0.050	4428.16	286.72	0.028	0.059	0.033
0.050-0.100	4535.82	301.52	0.023	0.062	0.034
0.100-0.200	4059.36	285.14	0.021	0.067	0.035
0.200-0.300	3452.35	286.17	0.024	0.079	0.036
0.300-0.400	2733.16	247.43	0.028	0.086	0.036
0.400-0.500	2103.42	214.43	0.033	0.096	0.037
0.500-0.700	1412.01	153.16	0.034	0.103	0.038
0.700-1.000	718.94	89.74	0.046	0.116	0.041
1.000-1.300	331.82	54.29	0.071	0.147	0.044
1.300-2.000	90.74	24.36	0.137	0.231	0.051
2.000-3.000	21.03	7.04	0.278	0.186	0.039

TABLE Supp.XVIII. Statistical covariance matrix of measured cross section as function of Q^2 on scintillator, in units of 10^{-84} $(\text{cm}^2/\text{GeV}^2/c^2/\text{nucleon})^2$

Bin edges (GeV^2/c^2)	0.000-0.025	0.025-0.050	0.050-0.100	0.100-0.200	0.200-0.300	0.300-0.400	0.400-0.500	0.500-0.700	0.700-1.000	1.000-1.300	1.300-2.000	2.000-3.000
0.000-0.025	12588.365	997.907	-805.851	-175.415	-12.014	-3.840	-2.954	-1.013	-1.935	-0.723	-0.531	-0.175
0.025-0.050	997.907	14929.823	1929.772	-589.284	-214.404	-36.350	-8.937	-5.562	-3.890	-1.779	-0.493	-0.030
0.050-0.100	-805.851	1929.772	10965.271	674.926	-508.532	-190.296	-62.976	-16.436	-3.694	-3.023	-1.259	-0.104
0.100-0.200	-175.415	-589.284	674.926	7118.253	814.386	-378.057	-250.650	-76.736	-19.479	-5.880	-2.364	-0.485
0.200-0.300	-12.014	-214.404	-508.532	814.386	6771.264	1416.831	-132.953	-214.847	-56.635	-19.106	-2.782	-1.670
0.300-0.400	-3.840	-36.350	-190.296	-378.057	1416.831	5865.008	1736.357	-24.934	-128.954	-45.772	-7.149	-2.457
0.400-0.500	-2.954	-8.937	-62.976	-250.650	-132.953	1736.357	4823.638	887.183	-77.544	-55.772	-11.482	0.465
0.500-0.700	-1.013	-5.562	-16.436	-76.736	-214.847	-24.934	887.183	2338.753	352.481	-49.685	-20.726	-1.956
0.700-1.000	-1.935	-3.890	-3.694	-19.479	-56.635	-128.954	-77.544	352.481	1092.546	239.344	3.234	-4.504
1.000-1.300	-0.723	-1.779	-3.023	-5.880	-19.106	-45.772	-55.772	-49.685	239.344	562.636	91.453	3.066
1.300-2.000	-0.531	-0.493	-1.259	-2.364	-2.782	-7.149	-11.482	-20.726	3.234	91.453	153.493	11.032
2.000-3.000	-0.175	-0.030	-0.104	-0.485	-1.670	-2.457	0.465	-1.956	-4.504	3.066	11.032	34.274

TABLE Supp.XIX. Systematic covariance matrix of measured cross section in Q^2 on scintillator, in units of $10^{-84} (\text{cm}^2/\text{GeV}^2/c^2/\text{nucleon})^2$

Bin edges (GeV^2/c^2)	0.000-0.025	0.025-0.050	0.050-0.100	0.100-0.200	0.200-0.300	0.300-0.400	0.400-0.500	0.500-0.700	0.700-1.000	1.000-1.300	1.300-2.000	2.000-3.000
0.000-0.025	55578.445	58860.557	60378.311	45220.647	34618.319	26584.728	20025.404	12986.738	6460.467	3981.279	829.538	205.817
0.025-0.050	58860.557	67278.874	71209.690	60105.923	50535.710	39818.233	31808.493	20735.959	10139.678	5164.600	1487.729	261.792
0.050-0.100	60378.311	71209.690	79947.393	69924.610	60147.726	47554.008	38176.351	25061.644	12064.101	6143.531	1774.373	308.808
0.100-0.200	45220.647	60105.923	69924.610	74185.188	71691.029	59199.546	49384.624	33309.494	16489.765	7198.661	2728.158	399.253
0.200-0.300	34618.319	50535.710	60147.726	71691.029	75124.673	63525.200	54225.183	37359.079	19135.220	8013.084	3474.311	468.633
0.300-0.400	26584.728	39818.233	47554.008	59199.546	63525.200	55354.698	46951.905	33113.395	17206.412	7264.286	3260.826	458.856
0.400-0.500	20025.404	31808.493	38176.351	49384.624	54225.183	46951.905	41157.215	28869.769	15207.015	6487.562	2953.839	418.405
0.500-0.700	12986.738	20735.959	25061.644	33309.494	37359.079	33113.395	28869.769	21118.541	11534.464	5238.876	2309.615	338.961
0.700-1.000	6460.467	10139.678	12064.101	16489.765	19135.220	17206.412	15207.015	11534.464	6960.978	3570.619	1531.486	228.184
1.000-1.300	3981.279	5164.600	6143.531	7198.661	8013.084	7264.286	6487.562	5238.876	3570.619	2385.019	913.026	154.129
1.300-2.000	829.538	1487.729	1774.373	2728.158	3474.311	3260.826	2953.839	2309.615	1531.486	913.026	439.729	62.254
2.000-3.000	205.817	261.792	308.808	399.253	468.633	458.856	418.405	338.961	228.184	154.129	62.254	15.245

TABLE Supp.XX. Measured cross section as function of W_{exp} on scintillator, in units of 10^{-42} $\text{cm}^2/\text{GeV}/c^2/\text{nucleon}$, and the absolute and fractional cross section uncertainties

Bin edges (GeV/c^2)	σ	Abs. Unc.	Frac. Stat. Unc.	Frac. Sys. Unc.	Frac. Flux Unc.
0.9-1.1	380.21	89.00	0.100	0.212	0.059
1.1-1.2	4969.82	394.14	0.026	0.075	0.038
1.2-1.3	10893.98	791.75	0.015	0.071	0.034
1.3-1.4	7534.12	786.69	0.031	0.100	0.033

TABLE Supp.XXI. Statistical covariance matrix of measured cross section as function of W_{exp} on scintillator, in units of 10^{-84} $(\text{cm}^2/\text{GeV}/c^2/\text{nucleon})^2$

Bin edges (GeV/c^2)	0.9-1.1	1.1-1.2	1.2-1.3	1.3-1.4
0.9-1.1	1434.912	298.236	-1959.309	-15.500
1.1-1.2	298.236	16108.522	-6199.017	-16343.752
1.2-1.3	-1959.309	-6199.017	28235.499	17223.717
1.3-1.4	-15.500	-16343.752	17223.717	53971.062

TABLE Supp.XXII. Systematic covariance matrix of measured cross section in W_{exp} on scintillator, in units of 10^{-84} $(\text{cm}^2/\text{GeV}/c^2/\text{nucleon})^2$

Bin edges (GeV/c^2)	0.9-1.1	1.1-1.2	1.2-1.3	1.3-1.4
0.9-1.1	6486.707	15615.022	35973.498	36397.745
1.1-1.2	15615.022	139234.924	211164.417	136341.941
1.2-1.3	35973.498	211164.417	598624.922	523114.324
1.3-1.4	36397.745	136341.941	523114.324	564914.576

TABLE Supp.XXIII. Measured cross section as function of T_π on scintillator, in units of 10^{-42} $\text{cm}^2/\text{GeV}/\text{nucleon}$, and the absolute and fractional cross section uncertainties

Bin edges (GeV)	σ	Abs. Unc.	Frac. Stat. Unc.	Frac. Sys. Unc.	Frac. Flux Unc.
0.035-0.100	13123.56	1025.94	0.016	0.076	0.037
0.100-0.150	9902.55	655.87	0.015	0.064	0.035
0.150-0.200	6746.23	521.56	0.023	0.074	0.035
0.200-0.350	3574.69	367.65	0.032	0.098	0.037

TABLE Supp.XXIV. Statistical covariance matrix of measured cross section as function of T_π on scintillator, in units of 10^{-84} $(\text{cm}^2/\text{GeV}/\text{nucleon})^2$

Bin edges (GeV)	0.035-0.100	0.100-0.150	0.150-0.200	0.200-0.350
0.035-0.100	46118.291	870.889	-2121.179	-1189.136
0.100-0.150	870.889	23295.488	2478.311	-458.209
0.150-0.200	-2121.179	2478.311	24009.621	3296.240
0.200-0.350	-1189.136	-458.209	3296.240	13381.849

TABLE Supp.XXV. Systematic covariance matrix of measured cross section in T_π on scintillator, in units of 10^{-84} $(\text{cm}^2/\text{GeV}/\text{nucleon})^2$

Bin edges (GeV)	0.035-0.100	0.100-0.150	0.150-0.200	0.200-0.350
0.035-0.100	1006425.993	600004.017	464834.038	298853.945
0.100-0.150	600004.017	406873.221	299782.750	190420.988
0.150-0.200	464834.038	299782.750	248015.149	165499.617
0.200-0.350	298853.945	190420.988	165499.617	121786.467

TABLE Supp.XXVI. Measured cross section as function of θ_π on scintillator, in units of 10^{-42} $\text{cm}^2/\text{degree}/\text{nucleon}$, and the absolute and fractional cross section uncertainties

Bin edges (degree)	σ	Abs. Unc.	Frac. Stat. Unc.	Frac. Sys. Unc.	Frac. Flux Unc.
0-10	3.46	0.45	0.079	0.102	0.039
10-20	10.35	1.05	0.041	0.092	0.037
20-30	15.83	1.50	0.032	0.089	0.036
30-40	19.13	1.65	0.027	0.082	0.037
40-50	21.54	1.81	0.026	0.080	0.038
50-60	23.20	1.83	0.026	0.074	0.037
60-120	19.20	1.53	0.019	0.077	0.035
120-135	9.30	0.69	0.027	0.069	0.033
135-150	6.21	0.46	0.031	0.068	0.034
150-165	3.20	0.30	0.049	0.079	0.035
165-180	0.78	0.10	0.110	0.074	0.037

TABLE Supp.XXVII. Statistical covariance matrix of measured cross section as function of θ_π on scintillator, in units of 10^{-84} ($\text{cm}^2/\text{degree/nucleon}$)²

Bin edges (degree)	0-10	10-20	20-30	30-40	40-50	50-60	60-120	120-135	135-150	150-165	165-180
0-10	0.074	0.022	-0.002	-0.003	-0.001	-0.001	-0.000	-0.001	-0.000	-0.000	0.005
10-20	0.022	0.183	0.029	-0.007	-0.004	-0.004	-0.003	-0.002	-0.002	0.002	0.005
20-30	-0.002	0.029	0.250	0.034	-0.009	-0.006	-0.003	-0.004	-0.003	0.005	-0.000
30-40	-0.003	-0.007	0.034	0.276	0.040	-0.011	-0.005	-0.006	0.002	0.002	-0.000
40-50	-0.001	-0.004	-0.009	0.040	0.323	0.044	-0.006	-0.004	0.002	-0.003	-0.001
50-60	-0.001	-0.004	-0.006	-0.011	0.044	0.376	0.020	0.002	-0.006	-0.002	-0.000
60-120	-0.000	-0.003	-0.003	-0.005	-0.006	0.020	0.133	0.007	-0.002	0.000	0.000
120-135	-0.001	-0.002	-0.004	-0.006	-0.004	0.002	0.007	0.064	0.009	-0.001	0.000
135-150	-0.000	-0.002	-0.003	0.002	0.002	-0.006	-0.002	0.009	0.036	0.008	0.001
150-165	-0.000	0.002	0.005	0.002	-0.003	-0.002	0.000	-0.001	0.008	0.024	0.001
165-180	0.005	0.005	-0.000	-0.000	-0.001	-0.000	0.000	0.000	0.001	0.001	0.007

TABLE Supp.XXVIII. Systematic covariance matrix of measured cross section in θ_π on scintillator, in units of 10^{-84} ($\text{cm}^2/\text{degree/nucleon}$)²

Bin edges (degree)	0-10	10-20	20-30	30-40	40-50	50-60	60-120	120-135	135-150	150-165	165-180
0-10	0.125	0.325	0.470	0.510	0.522	0.494	0.301	0.146	0.097	0.054	0.014
10-20	0.325	0.913	1.275	1.384	1.399	1.314	0.860	0.434	0.280	0.161	0.038
20-30	0.470	1.275	1.989	2.183	2.306	2.214	1.631	0.653	0.431	0.258	0.059
30-40	0.510	1.384	2.183	2.450	2.624	2.532	1.914	0.750	0.500	0.299	0.071
40-50	0.522	1.399	2.306	2.624	2.936	2.888	2.220	0.856	0.575	0.326	0.078
50-60	0.494	1.314	2.214	2.532	2.888	2.972	2.272	0.903	0.616	0.349	0.079
60-120	0.301	0.860	1.631	1.914	2.220	2.272	2.193	0.675	0.463	0.301	0.059
120-135	0.146	0.434	0.653	0.750	0.856	0.903	0.675	0.407	0.261	0.118	0.025
135-150	0.097	0.280	0.431	0.500	0.575	0.616	0.463	0.261	0.176	0.085	0.018
150-165	0.054	0.161	0.258	0.299	0.326	0.349	0.301	0.118	0.085	0.064	0.012
165-180	0.014	0.038	0.059	0.071	0.078	0.079	0.059	0.025	0.018	0.012	0.003

TABLE Supp.XXIX. Measured cross section as function of p_μ on carbon, in units of 10^{-42} $\text{cm}^2/\text{GeV}/c/\text{nucleon}$, and the absolute and fractional cross section uncertainties

Bin edges (GeV/c)	σ	Abs. Unc.	Frac. Stat. Unc.	Frac. Sys. Unc.	Frac. Flux Unc.
1.5-3.0	143.43	53.59	0.348	0.137	0.038
3.0-4.0	400.66	96.71	0.207	0.124	0.038
4.0-5.0	489.84	119.50	0.183	0.162	0.039
5.0-6.0	489.52	115.11	0.170	0.163	0.037
6.0-7.0	310.21	84.33	0.194	0.191	0.037
7.0-8.5	135.12	44.89	0.257	0.210	0.038
8.5-10.0	36.97	16.68	0.364	0.267	0.041
10.0-20.0	11.32	5.78	0.446	0.247	0.038

TABLE Supp.XXX. Statistical covariance matrix of measured cross section as function of p_μ on carbon, in units of 10^{-84} $(\text{cm}^2/\text{GeV}/c/\text{nucleon})^2$

Bin edges (GeV/c)	1.5-3.0	3.0-4.0	4.0-5.0	5.0-6.0	6.0-7.0	7.0-8.5	8.5-10.0	10.0-20.0
1.5-3.0	2487.306	783.530	123.415	78.780	75.516	20.167	1.410	1.759
3.0-4.0	783.530	6883.567	1843.185	398.312	105.427	9.190	0.161	0.000
4.0-5.0	123.415	1843.185	7998.915	2532.020	359.777	55.429	7.510	0.000
5.0-6.0	78.780	398.312	2532.020	6906.017	2408.268	351.079	61.864	4.991
6.0-7.0	75.516	105.427	359.777	2408.268	3610.355	1147.420	152.970	34.063
7.0-8.5	20.167	9.190	55.429	351.079	1147.420	1207.419	270.781	15.516
8.5-10.0	1.410	0.161	7.510	61.864	152.970	270.781	180.813	22.407
10.0-20.0	1.759	0.000	0.000	4.991	34.063	15.516	22.407	25.537

TABLE Supp.XXXI. Systematic covariance matrix of measured cross section in p_μ on carbon, in units of $10^{-84} (\text{cm}^2/\text{GeV}/c/\text{nucleon})^2$

Bin edges (GeV/c)	1.5-3.0	3.0-4.0	4.0-5.0	5.0-6.0	6.0-7.0	7.0-8.5	8.5-10.0	10.0-20.0
1.5-3.0	384.799	789.008	1193.866	1166.558	826.990	220.270	87.278	38.919
3.0-4.0	789.008	2468.666	3297.934	3441.037	2430.366	827.244	278.953	104.621
4.0-5.0	1193.866	3297.934	6281.017	5857.713	4182.090	1528.720	419.419	150.395
5.0-6.0	1166.558	3441.037	5857.713	6343.377	4461.196	1667.815	497.086	168.352
6.0-7.0	826.990	2430.366	4182.090	4461.196	3502.013	1401.819	439.792	128.544
7.0-8.5	220.270	827.244	1528.720	1667.815	1401.819	807.588	248.509	47.072
8.5-10.0	87.278	278.953	419.419	497.086	439.792	248.509	97.422	19.134
10.0-20.0	38.919	104.621	150.395	168.352	128.544	47.072	19.134	7.842

TABLE Supp.XXXII. Measured cross section as function of θ_μ on carbon, in units of $10^{-42} \text{cm}^2/\text{degree}/\text{nucleon}$, and the absolute and fractional cross section uncertainties

Bin edges (degree)	σ	Abs. Unc.	Frac. Stat. Unc.	Frac. Sys. Unc.	Frac. Flux Unc.
0-2	69.93	21.86	0.297	0.096	0.034
2-3	293.81	74.18	0.226	0.113	0.033
3-4	232.51	71.15	0.268	0.147	0.033
4-5	243.12	83.24	0.275	0.204	0.037
5-6	104.44	64.79	0.510	0.353	0.046
6-8	165.82	82.86	0.411	0.285	0.039
8-10	272.11	109.74	0.346	0.207	0.035
10-13	210.36	91.15	0.384	0.202	0.039

TABLE Supp.XXXIII. Statistical covariance matrix of measured cross section as function of θ_μ on carbon, in units of $10^{-84} (\text{cm}^2/\text{degree}/\text{nucleon})^2$

Bin edges (degree)	0-2	2-3	3-4	4-5	5-6	6-8	8-10	10-13
0-2	432.545	-42.190	-60.428	-10.381	0.256	0.206	-2.325	-2.718
2-3	-42.190	4402.124	227.802	-355.022	-55.531	-0.703	-21.100	-2.610
3-4	-60.428	227.802	3889.313	556.447	-267.531	-59.679	-5.042	-9.166
4-5	-10.381	-355.022	556.447	4479.508	604.254	-323.825	-38.103	3.448
5-6	0.256	-55.531	-267.531	604.254	2836.385	323.719	-183.679	-8.398
6-8	0.206	-0.703	-59.679	-323.825	323.719	4640.159	-126.552	-144.285
8-10	-2.325	-21.100	-5.042	-38.103	-183.679	-126.552	8881.099	-343.995
10-13	-2.718	-2.610	-9.166	3.448	-8.398	-144.285	-343.995	6510.178

TABLE Supp.XXXIV. Systematic covariance matrix of measured cross section in θ_μ on carbon, in units of $10^{-84} (\text{cm}^2/\text{degree}/\text{nucleon})^2$

Bin edges (degree)	0-2	2-3	3-4	4-5	5-6	6-8	8-10	10-13
0-2	45.099	92.411	103.281	114.507	74.645	105.557	149.681	52.143
2-3	92.411	1100.609	841.832	1222.754	769.793	961.137	1118.738	1053.933
3-4	103.281	841.832	1172.797	1542.172	1062.769	1138.866	1384.286	1145.364
4-5	114.507	1222.754	1542.172	2449.024	1531.587	1737.054	2156.829	1604.998
5-6	74.645	769.793	1062.769	1531.587	1361.346	1240.504	1502.525	1102.167
6-8	105.557	961.137	1138.866	1737.054	1240.504	2226.414	1880.519	1195.813
8-10	149.681	1118.738	1384.286	2156.829	1502.525	1880.519	3161.621	1418.018
10-13	52.143	1053.933	1145.364	1604.998	1102.167	1195.813	1418.018	1798.854

TABLE Supp.XXXV. Measured cross section as function of $p_{\mu,||}$ on carbon, in units of 10^{-42} $\text{cm}^2/\text{GeV}/c/\text{nucleon}$, and the absolute and fractional cross section uncertainties

Bin edges (GeV/c)	σ	Abs. Unc.	Frac. Stat. Unc.	Frac. Sys. Unc.	Frac. Flux Unc.
1.5-3.0	142.81	54.37	0.353	0.142	0.038
3.0-4.0	414.13	100.15	0.207	0.125	0.037
4.0-5.0	495.24	120.33	0.181	0.162	0.039
5.0-6.0	470.54	113.51	0.174	0.167	0.038
6.0-7.0	316.82	84.97	0.193	0.186	0.037
7.0-8.5	131.56	43.90	0.258	0.211	0.038
8.5-10.0	36.08	16.51	0.370	0.270	0.041
10.0-20.0	11.27	5.74	0.446	0.247	0.038

TABLE Supp.XXXVI. Statistical covariance matrix of measured cross section as function of $p_{\mu,||}$ on carbon, in units of 10^{-84} $(\text{cm}^2/\text{GeV}/c/\text{nucleon})^2$

Bin edges (GeV/c)	1.5-3.0	3.0-4.0	4.0-5.0	5.0-6.0	6.0-7.0	7.0-8.5	8.5-10.0	10.0-20.0
1.5-3.0	2545.244	728.621	120.277	77.608	72.794	19.444	1.364	1.702
3.0-4.0	728.621	7370.998	1832.106	356.992	93.965	8.392	0.052	0.000
4.0-5.0	120.277	1832.106	8057.985	2544.775	374.057	53.227	7.161	0.000
5.0-6.0	77.608	356.992	2544.775	6684.440	2431.505	348.631	58.569	4.882
6.0-7.0	72.794	93.965	374.057	2431.505	3735.052	1088.284	140.039	33.362
7.0-8.5	19.444	8.392	53.227	348.631	1088.284	1156.326	260.739	15.362
8.5-10.0	1.364	0.052	7.161	58.569	140.039	260.739	177.793	22.270
10.0-20.0	1.702	0.000	0.000	4.882	33.362	15.362	22.270	25.211

TABLE Supp.XXXVII. Systematic covariance matrix of measured cross section in $p_{\mu,||}$ on carbon, in units of $10^{-84} (\text{cm}^2/\text{GeV}/c/\text{nucleon})^2$

Bin edges (GeV/c)	1.5-3.0	3.0-4.0	4.0-5.0	5.0-6.0	6.0-7.0	7.0-8.5	8.5-10.0	10.0-20.0
1.5-3.0	410.793	807.898	1244.792	1207.063	865.339	222.378	85.770	40.987
3.0-4.0	807.898	2659.590	3370.825	3460.466	2460.014	783.208	264.051	103.430
4.0-5.0	1244.792	3370.825	6421.428	5800.897	4234.157	1488.178	408.526	149.058
5.0-6.0	1207.063	3460.466	5800.897	6199.385	4432.492	1594.078	488.891	166.781
6.0-7.0	865.339	2460.014	4234.157	4432.492	3484.686	1332.120	428.733	129.620
7.0-8.5	222.378	783.208	1488.178	1594.078	1332.120	770.937	239.169	44.936
8.5-10.0	85.770	264.051	408.526	488.891	428.733	239.169	94.943	18.573
10.0-20.0	40.987	103.430	149.058	166.781	129.620	44.936	18.573	7.764

TABLE Supp.XXXVIII. Measured cross section as function of $p_{\mu,T}$ on carbon, in units of $10^{-42} \text{cm}^2/\text{GeV}/c/\text{nucleon}$, and the absolute and fractional cross section uncertainties

Bin edges (GeV/c)	σ	Abs. Unc.	Frac. Stat. Unc.	Frac. Sys. Unc.	Frac. Flux Unc.
0.00-0.15	677.76	225.45	0.321	0.087	0.034
0.15-0.30	1738.89	427.93	0.225	0.100	0.034
0.30-0.45	3334.80	784.27	0.200	0.124	0.035
0.45-0.60	3255.16	968.88	0.227	0.193	0.037
0.60-0.75	2354.67	914.93	0.305	0.241	0.037
0.75-0.90	1095.46	966.59	0.687	0.554	0.049
0.90-1.25	732.87	537.65	0.581	0.448	0.048
1.25-2.50	41.20	64.42	1.409	0.678	0.036

TABLE Supp.XXXIX. Statistical covariance matrix of measured cross section as function of $p_{\mu,T}$ on carbon, in units of 10^{-84} ($\text{cm}^2/\text{GeV}/c/\text{nucleon}$)²

Bin edges (GeV/c)	0.00-0.15	0.15-0.30	0.30-0.45	0.45-0.60	0.60-0.75	0.75-0.90	0.90-1.25	1.25-2.50
0.00-0.15	47345.844	489.515	-9627.274	-1191.565	-50.835	695.864	-132.553	-2.979
0.15-0.30	489.515	152597.493	15878.159	-24434.942	-4415.122	-2630.600	-338.305	-26.218
0.30-0.45	-9627.274	15878.159	442805.481	56960.571	-47584.361	-18432.176	-3106.294	-512.456
0.45-0.60	-1191.565	-24434.942	56960.571	545345.745	82151.510	-38191.909	-22415.638	566.213
0.60-0.75	-50.835	-4415.122	-47584.361	82151.510	514382.100	160232.420	-4248.074	-2161.159
0.75-0.90	695.864	-2630.600	-18432.176	-38191.909	160232.420	565653.640	116267.363	-433.914
0.90-1.25	-132.553	-338.305	-3106.294	-22415.638	-4248.074	116267.363	181284.881	-260.193
1.25-2.50	-2.979	-26.218	-512.456	566.213	-2161.159	-433.914	-260.193	3369.229

TABLE Supp.XL. Systematic covariance matrix of measured cross section in $p_{\mu,T}$ on carbon, in units of 10^{-84} ($\text{cm}^2/\text{GeV}/c/\text{nucleon}$)²

Bin edges (GeV/c)	0.00-0.15	0.15-0.30	0.30-0.45	0.45-0.60	0.60-0.75	0.75-0.90	0.90-1.25	1.25-2.50
0.00-0.15	3483.817	7652.058	8866.626	10183.622	11849.515	6912.592	2468.776	265.614
0.15-0.30	7652.058	30530.330	51863.562	66554.567	71581.100	50684.480	18484.932	1839.939
0.30-0.45	8866.626	51863.562	172270.470	234351.239	208147.109	144317.649	56989.645	6228.014
0.45-0.60	10183.622	66554.567	234351.239	393376.163	322202.135	212486.586	91525.906	9190.991
0.60-0.75	11849.515	71581.100	208147.109	322202.135	322712.829	223779.297	80646.181	9352.017
0.75-0.90	6912.592	50684.480	144317.649	212486.586	223779.297	368643.495	152778.165	12440.530
0.90-1.25	2468.776	18484.932	56989.645	91525.906	80646.181	152778.165	107781.804	5769.398
1.25-2.50	265.614	1839.939	6228.014	9190.991	9352.017	12440.530	5769.398	780.369

TABLE Supp.XLI. Measured cross section as function of Q^2 on carbon, in units of 10^{-42} $\text{cm}^2/\text{GeV}^2/c^2/\text{nucleon}$, and the absolute and fractional cross section uncertainties

Bin edges (GeV^2/c^2)	σ	Abs. Unc.	Frac. Stat. Unc.	Frac. Sys. Unc.	Frac. Flux Unc.
0.000-0.025	4110.92	1313.92	0.309	0.082	0.034
0.025-0.050	3738.85	1125.78	0.289	0.086	0.035
0.050-0.100	3372.90	968.01	0.257	0.127	0.033
0.100-0.200	4499.60	1037.27	0.198	0.119	0.035
0.200-0.300	2654.05	855.20	0.271	0.175	0.036
0.300-0.400	2401.01	861.33	0.280	0.224	0.039
0.400-0.500	1622.89	738.87	0.352	0.289	0.042
0.500-0.700	934.89	545.84	0.465	0.353	0.040
0.700-1.000	786.73	497.09	0.515	0.366	0.039
1.000-1.300	508.34	308.25	0.541	0.274	0.040
1.300-2.000	104.02	162.03	1.255	0.923	0.059
2.000-3.000	43.44	76.15	1.619	0.673	0.050

TABLE Supp.XLII. Statistical covariance matrix of measured cross section as function of Q^2 on carbon, in units of 10^{-84} $(\text{cm}^2/\text{GeV}^2/c^2/\text{nucleon})^2$

Bin edges (GeV^2/c^2)	0.000-0.025	0.025-0.050	0.050-0.100	0.100-0.200	0.200-0.300	0.300-0.400	0.400-0.500	0.500-0.700	0.700-1.000	1.000-1.300	1.300-2.000	2.000-3.000
0.000-0.025	1612047.844	133164.747	-109292.560	-38037.712	-210.854	-289.388	-431.586	-381.587	1410.826	-116.093	-134.401	-15.298
0.025-0.050	133164.747	1163631.354	296929.122	-89658.591	-29868.450	-4855.439	-2137.794	-1577.626	-2178.074	-485.529	-223.131	12.313
0.050-0.100	-109292.560	296929.122	753462.588	147506.891	-58070.191	-21930.282	-6742.827	-1558.373	317.631	-580.345	-609.480	-76.275
0.100-0.200	-38037.712	-89658.591	147506.891	790275.558	111043.502	-56840.469	-38915.673	-5121.184	-3538.403	-2738.221	-473.804	-314.496
0.200-0.300	-210.854	-29868.450	-58070.191	111043.502	516648.021	193831.617	-9914.202	-26131.027	-9527.948	-4605.887	-2429.364	-225.566
0.300-0.400	-289.388	-4855.439	-21930.282	-56840.469	193831.617	453257.205	226912.682	727.533	-25604.708	-10358.162	2497.816	-92.988
0.400-0.500	-431.586	-2137.794	-6742.827	-38915.673	-9914.202	226912.682	325672.916	114465.431	-2753.532	-9681.002	-1603.063	-511.652
0.500-0.700	-381.587	-1577.626	-1558.373	-5121.184	-26131.027	727.533	114465.431	188992.547	64966.679	-2230.532	-223.786	-666.490
0.700-1.000	1410.826	-2178.074	317.631	-3538.403	-9527.948	-25604.708	-2753.532	64966.679	163968.352	51804.379	591.175	-1196.626
1.000-1.300	-116.093	-485.529	-580.345	-2738.221	-4605.887	-10358.162	-9681.002	-2230.532	51804.379	75645.608	8609.031	-672.953
1.300-2.000	-134.401	-223.131	-609.480	-473.804	-2429.364	2497.816	-1603.063	-223.786	591.175	8609.031	17036.574	2099.067
2.000-3.000	-15.298	12.313	-76.275	-314.496	-225.566	-92.988	-511.652	-666.490	-1196.626	-672.953	2099.067	4943.006

TABLE Supp.XLIII. Systematic covariance matrix of measured cross section in Q^2 on carbon, in units of $10^{-84} \text{ (cm}^2/\text{GeV}^2/c^2/\text{nucleon})^2$

Bin edges (GeV^2/c^2)	0.000-0.025	0.025-0.050	0.050-0.100	0.100-0.200	0.200-0.300	0.300-0.400	0.400-0.500	0.500-0.700	0.700-1.000	1.000-1.300	1.300-2.000	2.000-3.000
0.000-0.025	114340.749	63203.907	97883.668	69702.441	50788.032	44606.610	50119.145	27594.492	15002.767	9359.854	2927.239	1444.850
0.025-0.050	63203.907	103757.689	84392.474	109039.744	61996.950	53071.693	63755.278	53044.149	28270.909	14167.656	3437.170	2164.095
0.050-0.100	97883.668	84392.474	183575.702	170724.672	142519.813	153118.040	139533.540	99833.908	67543.256	30334.664	12124.226	4509.597
0.100-0.200	69702.441	109039.744	170724.672	285646.828	223066.738	226804.698	203762.849	146664.829	78950.233	38488.714	19109.338	6346.318
0.200-0.300	50788.032	61996.950	142519.813	223066.738	214718.388	225859.884	194853.625	120137.142	64661.826	32947.723	16705.759	4606.379
0.300-0.400	44606.610	53071.693	153118.040	226804.698	225859.884	288638.745	230674.942	132653.732	72541.441	34292.653	21857.936	5416.617
0.400-0.500	50119.145	63755.278	139533.540	203762.849	194853.625	230674.942	220250.698	124449.181	63894.843	32171.484	19459.809	5250.944
0.500-0.700	27594.492	53044.149	99833.908	146664.829	120137.142	132653.732	124449.181	108949.639	72984.339	34427.668	17917.460	5931.924
0.700-1.000	15002.767	28270.909	67543.256	78950.233	64661.826	72541.441	63894.843	72984.339	83134.974	34268.597	17608.447	5894.400
1.000-1.300	9359.854	14167.656	30334.664	38488.714	32947.723	34292.653	32171.484	34427.668	34268.597	19372.429	10260.940	3053.558
1.300-2.000	2927.239	3437.170	12124.226	19109.338	16705.759	21857.936	19459.809	17917.460	17608.447	10260.940	9218.640	1777.178
2.000-3.000	1444.850	2164.095	4509.597	6346.318	4606.379	5416.617	5250.944	5931.924	5894.400	3053.558	1777.178	855.347

TABLE Supp.XLIV. Measured cross section as function of W_{exp} on carbon, in units of 10^{-42} $\text{cm}^2/\text{GeV}/c^2/\text{nucleon}$, and the absolute and fractional cross section uncertainties

Bin edges (GeV/c^2)	σ	Abs. Unc.	Frac. Stat. Unc.	Frac. Sys. Unc.	Frac. Flux Unc.
0.9-1.1	935.92	613.41	0.627	0.191	0.043
1.1-1.2	5238.76	1031.06	0.175	0.091	0.036
1.2-1.3	8434.70	2309.31	0.200	0.187	0.033
1.3-1.4	4744.74	3791.22	0.529	0.599	0.033

TABLE Supp.XLV. Statistical covariance matrix of measured cross section as function of W_{exp} on carbon, in units of 10^{-84} $(\text{cm}^2/\text{GeV}/c^2/\text{nucleon})^2$

Bin edges (GeV/c^2)	0.9-1.1	1.1-1.2	1.2-1.3	1.3-1.4
0.9-1.1	344280.921	-5955.534	-433736.932	-328835.505
1.1-1.2	-5955.534	837000.556	82998.926	-910335.711
1.2-1.3	-433736.932	82998.926	2848202.794	1532250.771
1.3-1.4	-328835.505	-910335.711	1532250.771	6306221.739

TABLE Supp.XLVI. Systematic covariance matrix of measured cross section in W_{exp} on carbon, in units of 10^{-84} $(\text{cm}^2/\text{GeV}/c^2/\text{nucleon})^2$

Bin edges (GeV/c^2)	0.9-1.1	1.1-1.2	1.2-1.3	1.3-1.4
0.9-1.1	31991.340	34754.971	26908.976	39260.342
1.1-1.2	34754.971	226074.839	269792.794	290485.892
1.2-1.3	26908.976	269792.794	2484692.008	4127535.293
1.3-1.4	39260.342	290485.892	4127535.293	8067146.466

TABLE Supp.XLVII. Measured cross section as function of T_π on carbon, in units of 10^{-42} $\text{cm}^2/\text{GeV}/\text{nucleon}$, and the absolute and fractional cross section uncertainties

Bin edges (GeV)	σ	Abs. Unc.	Frac. Stat. Unc.	Frac. Sys. Unc.	Frac. Flux Unc.
0.035-0.100	11544.77	2671.16	0.176	0.151	0.036
0.100-0.150	9366.27	1783.83	0.132	0.137	0.034
0.150-0.200	5705.08	1763.73	0.226	0.211	0.033
0.200-0.350	2730.47	1583.72	0.425	0.394	0.040

TABLE Supp.XLVIII. Statistical covariance matrix of measured cross section as function of T_π on carbon, in units of 10^{-84} $(\text{cm}^2/\text{GeV}/\text{nucleon})^2$

Bin edges (GeV)	0.035-0.100	0.100-0.150	0.150-0.200	0.200-0.350
0.035-0.100	4110120.545	450633.521	-366102.636	-6362.214
0.100-0.150	450633.521	1529252.308	596865.376	246606.388
0.150-0.200	-366102.636	596865.376	1657591.298	826260.188
0.200-0.350	-6362.214	246606.388	826260.188	1349320.553

TABLE Supp.XLIX. Systematic covariance matrix of measured cross section in T_π on carbon, in units of 10^{-84} $(\text{cm}^2/\text{GeV}/\text{nucleon})^2$

Bin edges (GeV)	0.035-0.100	0.100-0.150	0.150-0.200	0.200-0.350
0.035-0.100	3024981.510	1978891.970	1702989.640	1319045.699
0.100-0.150	1978891.970	1652801.001	1398786.930	954689.298
0.150-0.200	1702989.640	1398786.930	1453140.559	1071815.858
0.200-0.350	1319045.699	954689.298	1071815.858	1158852.632

TABLE Supp.L. Measured cross section as function of θ_π on carbon, in units of 10^{-42} $\text{cm}^2/\text{degree}/\text{nucleon}$, and the absolute and fractional cross section uncertainties

Bin edges (degree)	σ	Abs. Unc.	Frac. Stat. Unc.	Frac. Sys. Unc.	Frac. Flux Unc.
0-10	3.68	5.99	1.483	0.671	0.045
10-20	9.04	6.38	0.627	0.325	0.040
20-30	14.15	5.91	0.339	0.244	0.035
30-40	16.26	5.52	0.279	0.194	0.037
40-50	21.86	6.14	0.228	0.163	0.036
50-60	18.12	5.63	0.256	0.176	0.034
60-120	17.45	4.32	0.207	0.135	0.035
120-135	9.75	3.15	0.291	0.141	0.033
135-150	8.14	2.79	0.310	0.146	0.033
150-165	5.01	3.21	0.556	0.319	0.039
165-180	1.05	0.91	0.768	0.395	0.036

TABLE Supp.LI. Statistical covariance matrix of measured cross section as function of θ_π on carbon, in units of $10^{-84} (\text{cm}^2/\text{degree/nucleon})^2$

Bin edges (degree)	0-10	10-20	20-30	30-40	40-50	50-60	60-120	120-135	135-150	150-165	165-180
0-10	29.766	12.455	4.832	-1.353	2.463	-0.442	-0.606	-0.302	-0.460	-0.539	0.102
10-20	12.455	32.119	11.299	-0.769	-0.780	-1.218	-0.439	0.010	-0.135	0.286	2.196
20-30	4.832	11.299	23.034	5.013	-1.963	-1.259	-0.814	-0.799	-0.565	0.421	0.728
30-40	-1.353	-0.769	5.013	20.496	7.417	-0.553	-0.845	-0.311	0.136	-0.222	-0.201
40-50	2.463	-0.780	-1.963	7.417	24.897	6.425	-0.456	-0.672	-0.583	-1.089	-0.313
50-60	-0.442	-1.218	-1.259	-0.553	6.425	21.543	4.262	-0.433	-0.423	-0.570	-0.167
60-120	-0.606	-0.439	-0.814	-0.845	-0.456	4.262	13.098	1.406	-0.111	-0.194	-0.021
120-135	-0.302	0.010	-0.799	-0.311	-0.672	-0.433	1.406	8.040	1.280	0.071	0.060
135-150	-0.460	-0.135	-0.565	0.136	-0.583	-0.423	-0.111	1.280	6.378	4.357	0.394
150-165	-0.539	0.286	0.421	-0.222	-1.089	-0.570	-0.194	4.357	7.762	0.096	
165-180	0.102	2.196	0.728	-0.201	-0.313	-0.167	-0.021	0.060	0.394	0.096	0.653

TABLE Supp.LII. Systematic covariance matrix of measured cross section in θ_π on carbon, in units of 10^{-84} ($\text{cm}^2/\text{degree/nucleon}$)²

Bin edges (degree)	0-10	10-20	20-30	30-40	40-50	50-60	60-120	120-135	135-150	150-165	165-180
0-10	6.099	2.112	3.025	2.738	2.224	2.087	1.429	1.276	1.283	1.506	0.034
10-20	2.112	8.617	9.250	7.393	8.503	7.705	4.256	2.782	2.277	1.852	0.710
20-30	3.025	9.250	11.938	9.913	10.228	8.821	5.209	3.110	2.750	1.823	0.670
30-40	2.738	7.393	9.913	9.939	8.952	7.789	4.739	2.801	2.587	1.857	0.574
40-50	2.224	8.503	10.228	8.952	12.744	10.942	6.933	3.974	3.154	1.512	0.677
50-60	2.087	7.705	8.821	7.789	10.942	10.147	6.381	3.840	2.837	1.708	0.712
60-120	1.429	4.256	5.209	4.739	6.933	6.381	5.548	2.655	1.714	0.957	0.559
120-135	1.276	2.782	3.110	2.801	3.974	3.840	2.655	1.883	1.275	1.207	0.335
135-150	1.283	2.277	2.750	2.587	3.154	2.837	1.714	1.275	1.417	0.745	0.186
150-165	1.506	1.852	1.823	1.857	1.512	1.708	0.957	1.207	0.745	2.546	0.259
165-180	0.034	0.710	0.670	0.574	0.677	0.712	0.559	0.335	0.186	0.259	0.173

TABLE Supp.LIII. Measured cross section as function of p_μ on water, in units of 10^{-42} $\text{cm}^2/\text{GeV}/c/\text{nucleon}$, and the absolute and fractional cross section uncertainties

Bin edges (GeV/c)	σ	Abs. Unc.	Frac. Stat. Unc.	Frac. Sys. Unc.	Frac. Flux Unc.
1.5-3.0	117.95	52.87	0.410	0.180	0.035
3.0-4.0	185.58	88.01	0.386	0.276	0.048
4.0-5.0	457.01	118.99	0.211	0.153	0.041
5.0-6.0	476.40	113.68	0.187	0.148	0.037
6.0-7.0	340.82	84.27	0.207	0.135	0.035
7.0-8.5	162.09	46.27	0.233	0.165	0.032
8.5-10.0	46.21	16.77	0.317	0.176	0.031
10.0-20.0	6.09	2.91	0.438	0.192	0.037

TABLE Supp.LIV. Statistical covariance matrix of measured cross section as function of p_μ on water, in units of 10^{-84} $(\text{cm}^2/\text{GeV}/c/\text{nucleon})^2$

Bin edges (GeV/c)	1.5-3.0	3.0-4.0	4.0-5.0	5.0-6.0	6.0-7.0	7.0-8.5	8.5-10.0	10.0-20.0
1.5-3.0	2344.004	445.008	69.019	37.629	28.309	10.974	8.907	0.011
3.0-4.0	445.008	5127.450	2079.943	557.499	60.656	35.261	3.708	1.132
4.0-5.0	69.019	2079.943	9264.813	3453.632	698.630	141.989	30.908	2.745
5.0-6.0	37.629	557.499	3453.632	7926.040	3136.162	481.482	55.213	7.682
6.0-7.0	28.309	60.656	698.630	3136.162	4992.546	1267.690	85.475	1.391
7.0-8.5	10.974	35.261	141.989	481.482	1267.690	1425.398	217.459	10.233
8.5-10.0	8.907	3.708	30.908	55.213	85.475	217.459	215.068	20.762
10.0-20.0	0.011	1.132	2.745	7.682	1.391	10.233	20.762	7.127

TABLE Supp.LV. Systematic covariance matrix of measured cross section in p_μ on water, in units of $10^{-84} (\text{cm}^2/\text{GeV}/c/\text{nucleon})^2$

Bin edges (GeV/c)	1.5-3.0	3.0-4.0	4.0-5.0	5.0-6.0	6.0-7.0	7.0-8.5	8.5-10.0	10.0-20.0
1.5-3.0	451.412	564.022	898.038	799.031	682.157	419.447	119.619	9.347
3.0-4.0	564.022	2619.122	2753.930	2802.366	1580.375	770.858	208.530	26.336
4.0-5.0	898.038	2753.930	4893.632	4338.470	2681.647	1244.144	288.103	47.295
5.0-6.0	799.031	2802.366	4338.470	4998.182	2697.240	1079.987	305.276	52.912
6.0-7.0	682.157	1580.375	2681.647	2697.240	2109.131	974.516	247.648	36.237
7.0-8.5	419.447	770.858	1244.144	1079.987	974.516	715.744	182.693	18.250
8.5-10.0	119.619	208.530	288.103	305.276	247.648	182.693	66.308	4.025
10.0-20.0	9.347	26.336	47.295	52.912	36.237	18.250	4.025	1.361

TABLE Supp.LVI. Measured cross section as function of θ_μ on water, in units of $10^{-42} \text{cm}^2/\text{degree}/\text{nucleon}$, and the absolute and fractional cross section uncertainties

Bin edges (degree)	σ	Abs. Unc.	Frac. Stat. Unc.	Frac. Sys. Unc.	Frac. Flux Unc.
0-2	63.72	18.14	0.260	0.117	0.031
2-3	217.48	63.11	0.271	0.103	0.035
3-4	246.44	72.74	0.267	0.125	0.033
4-5	207.57	88.04	0.382	0.184	0.034
5-6	136.66	83.70	0.536	0.296	0.037
6-8	236.70	102.60	0.366	0.233	0.040
8-10	290.88	114.06	0.340	0.195	0.039
10-13	14.67	57.44	3.399	1.945	0.181

TABLE Supp.LVII. Statistical covariance matrix of measured cross section as function of θ_μ on water, in units of $10^{-84} (\text{cm}^2/\text{degree}/\text{nucleon})^2$

Bin edges (degree)	0-2	2-3	3-4	4-5	5-6	6-8	8-10	10-13
0-2	273.470	54.585	-101.543	-17.484	-0.727	-4.685	-0.455	0.011
2-3	54.585	3478.295	496.736	-513.517	-80.607	-13.769	-12.044	0.139
3-4	-101.543	496.736	4336.745	942.105	-394.960	-115.405	5.655	0.149
4-5	-17.484	-513.517	942.105	6294.647	1188.026	-463.504	-39.117	0.892
5-6	-0.727	-80.607	-394.960	1188.026	5373.660	607.700	-342.608	-2.822
6-8	-4.685	-13.769	-115.405	-463.504	607.700	7487.508	-398.111	-72.215
8-10	-0.455	-12.044	5.655	-39.117	-342.608	-398.111	9799.885	587.996
10-13	0.011	0.139	0.149	0.892	-2.822	-72.215	587.996	2485.525

TABLE Supp.LVIII. Systematic covariance matrix of measured cross section in θ_μ on water, in units of $10^{-84} (\text{cm}^2/\text{degree}/\text{nucleon})^2$

Bin edges (degree)	0-2	2-3	3-4	4-5	5-6	6-8	8-10	10-13
0-2	55.609	108.738	139.883	81.848	35.719	28.759	40.840	-6.741
2-3	108.738	504.494	552.733	601.157	570.449	631.701	410.197	287.381
3-4	139.883	552.733	954.832	802.914	660.357	1116.479	944.109	450.452
4-5	81.848	601.157	802.914	1456.929	1320.732	1478.837	1299.382	751.433
5-6	35.719	570.449	660.357	1320.732	1632.620	1328.831	1269.663	881.853
6-8	28.759	631.701	1116.479	1478.837	1328.831	3040.213	1943.068	1180.314
8-10	40.840	410.197	944.109	1299.382	1269.663	1943.068	3209.779	1043.855
10-13	-6.741	287.381	450.452	751.433	881.853	1180.314	1043.855	814.089

TABLE Supp.LIX. Measured cross section as function of $p_{\mu,||}$ on water, in units of 10^{-42} $\text{cm}^2/\text{GeV}/c/\text{nucleon}$, and the absolute and fractional cross section uncertainties

Bin edges (GeV/c)	σ	Abs. Unc.	Frac. Stat. Unc.	Frac. Sys. Unc.	Frac. Flux Unc.
1.5-3.0	136.29	60.24	0.389	0.210	0.035
3.0-4.0	209.53	91.74	0.357	0.253	0.046
4.0-5.0	467.09	122.37	0.211	0.155	0.041
5.0-6.0	454.55	110.72	0.192	0.149	0.037
6.0-7.0	332.04	82.82	0.211	0.134	0.034
7.0-8.5	150.87	44.38	0.239	0.171	0.032
8.5-10.0	44.53	16.29	0.319	0.180	0.031
10.0-20.0	6.13	2.91	0.436	0.189	0.037

TABLE Supp.LX. Statistical covariance matrix of measured cross section as function of $p_{\mu,||}$ on water, in units of 10^{-84} $(\text{cm}^2/\text{GeV}/c/\text{nucleon})^2$

Bin edges (GeV/c)	1.5-3.0	3.0-4.0	4.0-5.0	5.0-6.0	6.0-7.0	7.0-8.5	8.5-10.0	10.0-20.0
1.5-3.0	2806.437	504.890	73.486	37.165	29.685	10.703	9.867	0.011
3.0-4.0	504.890	5594.629	2192.711	520.469	52.881	35.865	3.809	1.132
4.0-5.0	73.486	2192.711	9743.624	3427.026	667.524	136.501	30.407	2.822
5.0-6.0	37.165	520.469	3427.026	7644.453	2938.764	447.993	53.709	7.692
6.0-7.0	29.685	52.881	667.524	2938.764	4887.686	1195.760	81.566	1.344
7.0-8.5	10.703	35.865	136.501	447.993	1195.760	1302.963	209.148	9.855
8.5-10.0	9.867	3.809	30.407	53.709	81.566	209.148	201.152	20.494
10.0-20.0	0.011	1.132	2.822	7.692	1.344	9.855	20.494	7.146

TABLE Supp.LXI. Systematic covariance matrix of measured cross section in $p_{\mu,||}$ on water, in units of $10^{-84} (\text{cm}^2/\text{GeV}/c/\text{nucleon})^2$

Bin edges (GeV/c)	1.5-3.0	3.0-4.0	4.0-5.0	5.0-6.0	6.0-7.0	7.0-8.5	8.5-10.0	10.0-20.0
1.5-3.0	822.289	462.724	1028.704	801.765	665.651	470.679	127.720	9.731
3.0-4.0	462.724	2820.764	2891.273	2824.462	1605.847	795.496	223.430	27.984
4.0-5.0	1028.704	2891.273	5230.407	4401.956	2668.438	1195.644	289.928	49.303
5.0-6.0	801.765	2824.462	4401.956	4615.427	2549.872	1005.696	294.413	50.238
6.0-7.0	665.651	1605.847	2668.438	2549.872	1972.173	891.953	230.546	34.929
7.0-8.5	470.679	795.496	1195.644	1005.696	891.953	666.928	168.923	17.475
8.5-10.0	127.720	223.430	289.928	294.413	230.546	168.923	64.052	3.808
10.0-20.0	9.731	27.984	49.303	50.238	34.929	17.475	3.808	1.345

TABLE Supp.LXII. Measured cross section as function of $p_{\mu,T}$ on water, in units of $10^{-42} \text{cm}^2/\text{GeV}/c/\text{nucleon}$, and the absolute and fractional cross section uncertainties

Bin edges (GeV/c)	σ	Abs. Unc.	Frac. Stat. Unc.	Frac. Sys. Unc.	Frac. Flux Unc.
0.00-0.15	427.07	156.83	0.350	0.110	0.031
0.15-0.30	1552.75	434.21	0.252	0.122	0.030
0.30-0.45	3698.80	892.81	0.212	0.115	0.035
0.45-0.60	3113.42	1107.87	0.288	0.209	0.035
0.60-0.75	762.06	764.44	0.739	0.678	0.047
0.75-0.90	2313.61	1115.44	0.419	0.239	0.032
0.90-1.25	1015.62	585.68	0.541	0.201	0.038
1.25-2.50	61.79	101.64	0.926	1.360	0.066

TABLE Supp.LXIII. Statistical covariance matrix of measured cross section as function of $p_{\mu,T}$ on water, in units of 10^{-84} ($\text{cm}^2/\text{GeV}/c/\text{nucleon}$)²

Bin edges (GeV/c)	0.00-0.15	0.15-0.30	0.30-0.45	0.45-0.60	0.60-0.75	0.75-0.90	0.90-1.25	1.25-2.50
0.00-0.15	22384.290	309.360	-7344.185	-1230.080	-94.202	-98.135	-6.266	1.649
0.15-0.30	309.360	152790.960	14256.803	-30091.672	-6430.353	-2133.393	-3061.313	-32.386
0.30-0.45	-7344.185	14256.803	617215.664	92003.011	-20825.426	-38780.595	-3925.249	-1075.423
0.45-0.60	-1230.080	-30091.672	92003.011	805716.499	171697.794	-44210.017	-7286.457	778.975
0.60-0.75	-94.202	-6430.353	-20825.426	171697.794	317423.898	241253.824	4577.656	-1266.640
0.75-0.90	-98.135	-2133.393	-38780.595	-44210.017	241253.824	938404.156	35594.495	-1501.990
0.90-1.25	-6.266	-3061.313	-3925.249	-7286.457	4577.656	35594.495	301365.386	99.880
1.25-2.50	1.649	-32.386	-1075.423	778.975	-1266.640	-1501.990	99.880	3273.325

TABLE Supp.LXIV. Systematic covariance matrix of measured cross section in $p_{\mu,T}$ on water, in units of 10^{-84} ($\text{cm}^2/\text{GeV}/c/\text{nucleon}$)²

Bin edges (GeV/c)	0.00-0.15	0.15-0.30	0.30-0.45	0.45-0.60	0.60-0.75	0.75-0.90	0.90-1.25	1.25-2.50
0.00-0.15	2212.331	7014.185	6289.850	3963.270	-1784.760	340.915	597.445	-91.941
0.15-0.30	7014.185	35749.178	50405.043	58067.522	33792.236	35975.418	6890.791	1602.846
0.30-0.45	6289.850	50405.043	179890.379	203145.934	115557.035	120354.622	27245.951	10487.937
0.45-0.60	3963.270	58067.522	203145.934	421666.486	253933.394	248251.930	32377.946	25258.683
0.60-0.75	-1784.760	33792.236	115557.035	253933.394	266938.915	244228.251	45765.171	16013.665
0.75-0.90	340.915	35975.418	120354.622	248251.930	244228.251	305802.129	47834.834	14707.867
0.90-1.25	597.445	6890.791	27245.951	32377.946	45765.171	47834.834	41657.051	893.402
1.25-2.50	-91.941	1602.846	10487.937	25258.683	16013.665	14707.867	893.402	7058.065

TABLE Supp.LXV. Measured cross section as function of Q^2 on water, in units of 10^{-42} $\text{cm}^2/\text{GeV}^2/c^2/\text{nucleon}$, and the absolute and fractional cross section uncertainties

Bin edges (GeV^2/c^2)	σ	Abs. Unc.	Frac. Stat. Unc.	Frac. Sys. Unc.	Frac. Flux Unc.
0.000-0.025	2480.15	898.11	0.346	0.106	0.031
0.025-0.050	2698.62	1003.28	0.330	0.171	0.033
0.050-0.100	3608.06	1040.14	0.268	0.106	0.028
0.100-0.200	4573.34	1179.68	0.224	0.127	0.034
0.200-0.300	3545.20	1057.43	0.253	0.158	0.034
0.300-1.300	638.77	323.90	0.375	0.341	0.038
1.300-2.000	563.66	378.38	0.613	0.275	0.035
2.000-3.000	60.16	107.17	0.885	1.546	0.072

TABLE Supp.LXVI. Statistical covariance matrix of measured cross section as function of Q^2 on water, in units of 10^{-84} ($\text{cm}^2/\text{GeV}^2/c^2/\text{nucleon}$)²

Bin edges (GeV^2/c^2)	0.000-0.025	0.025-0.050	0.050-0.100	0.100-0.200	0.200-0.300	0.300-1.300	1.300-2.000	2.000-3.000
0.000-0.025	737910.311	134711.025	-89360.998	-31088.514	-2618.557	-324.926	-0.770	-1.189
0.025-0.050	134711.025	793841.706	333689.764	-89325.086	-44223.884	-952.144	-494.547	-5.120
0.050-0.100	-89360.998	333689.764	936646.336	126010.540	-86362.695	-7058.249	-2918.545	-90.130
0.100-0.200	-31088.514	-89325.086	126010.540	1051659.826	307358.275	-24755.356	-6781.373	-690.978
0.200-0.300	-2618.557	-44223.884	-86362.695	307358.275	803030.467	25543.239	-13033.818	172.523
0.300-1.300	-324.926	-952.144	-7058.249	-24755.356	25543.239	57416.252	1624.192	-345.051
1.300-2.000	-0.770	-494.547	-2918.545	-6781.373	-13033.818	1624.192	119223.261	93.238
2.000-3.000	-1.189	-5.120	-90.130	-690.978	172.523	-345.051	93.238	2834.882

TABLE Supp.LXVII. Systematic covariance matrix of measured cross section in Q^2 on water, in units of $10^{-84} \text{ (cm}^2/\text{GeV}^2/c^2/\text{nucleon})^2$

Bin edges (GeV^2/c^2)	0.000-0.025	0.025-0.050	0.050-0.100	0.100-0.200	0.200-0.300	0.300-1.300	1.300-2.000	2.000-3.000
0.000-0.025	68685.777	99092.605	67287.625	59917.695	30844.096	-1265.600	8783.647	-575.413
0.025-0.050	99092.605	212727.324	129946.537	151239.000	86775.289	14457.069	1406.976	-268.952
0.050-0.100	67287.625	129946.537	145254.442	131364.523	127635.806	43360.984	15481.951	5821.559
0.100-0.200	59917.695	151239.000	131364.523	339983.217	241123.764	58008.934	7571.832	14480.329
0.200-0.300	30844.096	86775.289	127635.806	241123.764	315118.422	84308.069	15162.848	18844.419
0.300-1.300	-1265.600	14457.069	43360.984	58008.934	84308.069	47496.488	14950.425	7426.101
1.300-2.000	8783.647	1406.976	15481.951	7571.832	15162.848	14950.425	23946.121	3237.185
2.000-3.000	-575.413	-268.952	5821.559	14480.329	18844.419	7426.101	3237.185	8651.566

TABLE Supp.LXVIII. Measured cross section as function of W_{exp} on water, in units of 10^{-42} $\text{cm}^2/\text{GeV}/\text{c}^2/\text{nucleon}$, and the absolute and fractional cross section uncertainties

Bin edges (GeV/c^2)	σ	Abs. Unc.	Frac. Stat. Unc.	Frac. Sys. Unc.	Frac. Flux Unc.
0.9-1.1	1604.24	1413.62	0.847	0.242	0.037
1.1-1.2	7771.74	1887.69	0.206	0.129	0.034
1.2-1.3	5069.96	2456.47	0.368	0.315	0.033
1.3-1.4	1635.65	1510.53	0.665	0.641	0.035

TABLE Supp.LXIX. Statistical covariance matrix of measured cross section as function of W_{exp} on water, in units of 10^{-84} $(\text{cm}^2/\text{GeV}/\text{c}^2/\text{nucleon})^2$

Bin edges (GeV/c^2)	0.9-1.1	1.1-1.2	1.2-1.3	1.3-1.4
0.9-1.1	1847344.362	-656709.599	-543616.547	-214453.239
1.1-1.2	-656709.599	2563274.464	-922303.488	-458316.063
1.2-1.3	-543616.547	-922303.488	3484780.550	1620816.512
1.3-1.4	-214453.239	-458316.063	1620816.512	1183090.426

TABLE Supp.LXX. Systematic covariance matrix of measured cross section in W_{exp} on water, in units of 10^{-84} $(\text{cm}^2/\text{GeV}/\text{c}^2/\text{nucleon})^2$

Bin edges (GeV/c^2)	0.9-1.1	1.1-1.2	1.2-1.3	1.3-1.4
0.9-1.1	150974.241	50687.062	58336.608	39527.718
1.1-1.2	50687.062	1000092.261	133191.537	-6137.137
1.2-1.3	58336.608	133191.537	2549465.255	1600707.642
1.3-1.4	39527.718	-6137.137	1600707.642	1098601.315

TABLE Supp.LXXI. Measured cross section as function of T_π on water, in units of 10^{-42} $\text{cm}^2/\text{GeV}/\text{nucleon}$, and the absolute and fractional cross section uncertainties

Bin edges (GeV)	σ	Abs. Unc.	Frac. Stat. Unc.	Frac. Sys. Unc.	Frac. Flux Unc.
0.035-0.100	14951.68	3806.97	0.227	0.116	0.032
0.100-0.150	8200.70	1951.07	0.194	0.137	0.035
0.150-0.200	6207.98	1941.76	0.264	0.168	0.034
0.200-0.350	2966.39	1310.43	0.348	0.272	0.033

TABLE Supp.LXXII. Statistical covariance matrix of measured cross section as function of T_π on water, in units of 10^{-84} $(\text{cm}^2/\text{GeV}/\text{nucleon})^2$

Bin edges (GeV)	0.035-0.100	0.100-0.150	0.150-0.200	0.200-0.350
0.035-0.100	11487318.614	868059.738	-673181.424	-199663.456
0.100-0.150	868059.738	2541618.601	323855.531	-105323.874
0.150-0.200	-673181.424	323855.531	2681915.718	246201.197
0.200-0.350	-199663.456	-105323.874	246201.197	1065321.825

TABLE Supp.LXXIII. Systematic covariance matrix of measured cross section in T_π on water, in units of 10^{-84} $(\text{cm}^2/\text{GeV}/\text{nucleon})^2$

Bin edges (GeV)	0.035-0.100	0.100-0.150	0.150-0.200	0.200-0.350
0.035-0.100	3005725.726	1539098.927	915615.078	671957.761
0.100-0.150	1539098.927	1265067.788	828750.051	606538.898
0.150-0.200	915615.078	828750.051	1088524.206	692340.688
0.200-0.350	671957.761	606538.898	692340.688	651915.142

TABLE Supp.LXXIV. Measured cross section as function of θ_π on water, in units of 10^{-42} $\text{cm}^2/\text{degree}/\text{nucleon}$, and the absolute and fractional cross section uncertainties

Bin edges (degree)	σ	Abs. Unc.	Frac. Stat. Unc.	Frac. Sys. Unc.	Frac. Flux Unc.
0-10	3.73	3.47	0.897	0.251	0.036
10-20	6.29	3.35	0.480	0.232	0.032
20-30	11.59	4.24	0.306	0.201	0.037
30-40	13.14	5.19	0.324	0.227	0.035
40-50	19.07	5.60	0.258	0.139	0.032
50-60	31.04	8.12	0.241	0.101	0.033
60-120	20.46	6.10	0.279	0.106	0.035
120-135	10.15	5.48	0.502	0.198	0.035
135-150	7.81	3.50	0.428	0.134	0.029
150-165	2.83	2.64	0.851	0.380	0.030
165-180	0.34	0.50	1.418	0.484	0.036

TABLE Supp.LXXV. Statistical covariance matrix of measured cross section as function of θ_π on water, in units of 10^{-84} ($\text{cm}^2/\text{degree}/\text{nucleon}$)²

Bin edges (degree)	0-10	10-20	20-30	30-40	40-50	50-60	60-120	120-135	135-150	150-165	165-180
0-10	11.170	2.498	-1.025	0.144	-0.368	-0.392	-0.315	-0.144	-0.110	-0.033	0.073
10-20	2.498	9.112	2.790	-0.615	-0.690	0.290	-1.038	-0.391	0.180	-0.065	0.913
20-30	-1.025	2.790	12.590	2.532	-0.610	-1.929	-0.328	-0.119	-0.338	-0.210	-0.030
30-40	0.144	-0.615	2.532	18.112	4.371	-1.711	1.058	-1.156	-0.422	-0.142	-0.096
40-50	-0.368	-0.690	-0.610	4.371	24.296	7.335	0.049	-0.432	0.437	-0.855	-0.024
50-60	-0.392	0.290	-1.929	-1.711	7.335	55.983	12.473	-1.267	-2.303	-1.089	0.105
60-120	-0.315	-1.038	-0.328	1.058	0.049	12.473	32.466	2.691	0.102	0.512	-0.095
120-135	-0.144	-0.391	-0.119	-1.156	-0.432	-1.267	2.691	25.957	4.903	0.174	-0.033
135-150	-0.110	0.180	-0.338	-0.422	0.437	-2.303	0.102	4.903	11.147	4.975	0.011
150-165	-0.033	-0.065	-0.210	-0.142	-0.855	-1.089	0.512	4.975	5.814	5.814	-0.011
165-180	0.073	0.913	-0.030	-0.096	-0.024	0.105	-0.095	-0.033	0.011	-0.011	0.226

TABLE Supp.LXXVI. Systematic covariance matrix of measured cross section in θ_π on water, in units of 10^{-84} ($\text{cm}^2/\text{degree/nucleon}$)²

Bin edges (degree)	0-10	10-20	20-30	30-40	40-50	50-60	60-120	120-135	135-150	150-165	165-180
0-10	0.874	0.417	0.892	1.532	1.083	0.835	0.382	0.989	0.189	-0.067	0.056
10-20	0.417	2.131	2.779	2.292	2.270	2.104	1.702	1.130	0.512	0.455	0.120
20-30	0.892	2.779	5.418	4.935	4.810	4.863	3.200	2.073	1.203	1.039	0.166
30-40	1.532	2.292	4.935	8.866	6.480	4.936	3.897	1.623	1.690	0.872	0.117
40-50	1.083	2.270	4.810	6.480	7.040	6.230	4.455	2.552	1.932	1.482	0.155
50-60	0.835	2.104	4.863	4.936	6.230	9.898	4.975	3.563	1.863	2.035	0.116
60-120	0.382	1.702	3.200	3.897	4.455	4.975	4.694	1.217	1.618	1.141	0.036
120-135	0.989	1.130	2.073	1.623	2.552	3.563	1.217	4.038	0.640	0.662	0.127
135-150	0.189	0.512	1.203	1.690	1.932	1.863	1.618	0.640	1.099	0.818	-0.040
150-165	-0.067	0.455	1.039	0.872	1.482	2.035	1.141	0.662	0.818	1.159	-0.015
165-180	0.056	0.120	0.166	0.117	0.155	0.116	0.036	0.127	-0.040	-0.015	0.026

TABLE Supp.LXXVII. Measured cross section as function of p_μ on iron, in units of 10^{-42} $\text{cm}^2/\text{GeV}/c/\text{nucleon}$, and the absolute and fractional cross section uncertainties

Bin edges (GeV/c)	σ	Abs. Unc.	Frac. Stat. Unc.	Frac. Sys. Unc.	Frac. Flux Unc.
1.5-3.0	116.83	22.82	0.152	0.123	0.039
3.0-4.0	268.85	46.29	0.106	0.136	0.041
4.0-5.0	301.84	55.47	0.097	0.156	0.045
5.0-6.0	322.48	57.36	0.088	0.155	0.043
6.0-7.0	236.20	43.60	0.092	0.160	0.038
7.0-8.5	104.17	22.50	0.117	0.182	0.037
8.5-10.0	35.62	8.17	0.141	0.181	0.037
10.0-20.0	8.56	1.97	0.165	0.160	0.036

TABLE Supp.LXXVIII. Statistical covariance matrix of measured cross section as function of p_μ on iron, in units of 10^{-84} $(\text{cm}^2/\text{GeV}/c/\text{nucleon})^2$

Bin edges (GeV/c)	1.5-3.0	3.0-4.0	4.0-5.0	5.0-6.0	6.0-7.0	7.0-8.5	8.5-10.0	10.0-20.0
1.5-3.0	315.869	105.314	22.345	15.804	2.906	0.259	1.159	0.243
3.0-4.0	105.314	814.581	220.469	53.732	12.553	6.185	1.503	0.499
4.0-5.0	22.345	220.469	849.305	333.122	68.504	9.452	1.780	0.440
5.0-6.0	15.804	53.732	333.122	797.696	292.874	34.524	5.772	0.967
6.0-7.0	2.906	12.553	68.504	292.874	474.114	123.750	15.375	1.503
7.0-8.5	0.259	6.185	9.452	34.524	123.750	148.134	32.875	2.247
8.5-10.0	1.159	1.503	1.780	5.772	15.375	32.875	25.134	2.980
10.0-20.0	0.243	0.499	0.440	0.967	1.503	2.247	2.980	2.002

TABLE Supp.LXXIX. Systematic covariance matrix of measured cross section in p_μ on iron, in units of $10^{-84} (\text{cm}^2/\text{GeV}/c/\text{nucleon})^2$

Bin edges (GeV/c)	1.5-3.0	3.0-4.0	4.0-5.0	5.0-6.0	6.0-7.0	7.0-8.5	8.5-10.0	10.0-20.0
1.5-3.0	205.057	411.198	522.643	525.671	357.844	147.293	50.865	11.924
3.0-4.0	411.198	1328.219	1622.646	1716.459	1223.345	569.854	192.684	40.675
4.0-5.0	522.643	1622.646	2228.071	2298.227	1665.093	757.015	247.266	52.499
5.0-6.0	525.671	1716.459	2298.227	2492.373	1826.680	857.130	280.167	59.245
6.0-7.0	357.844	1223.345	1665.093	1826.680	1426.702	679.134	220.834	47.548
7.0-8.5	147.293	569.854	757.015	857.130	679.134	358.258	117.038	23.759
8.5-10.0	50.865	192.684	247.266	280.167	220.834	117.038	41.591	8.067
10.0-20.0	11.924	40.675	52.499	59.245	47.548	23.759	8.067	1.888

TABLE Supp.LXXX. Measured cross section as function of θ_μ on iron, in units of $10^{-42} \text{cm}^2/\text{degree}/\text{nucleon}$, and the absolute and fractional cross section uncertainties

Bin edges (degree)	σ	Abs. Unc.	Frac. Stat. Unc.	Frac. Sys. Unc.	Frac. Flux Unc.
0-2	57.81	9.20	0.127	0.096	0.034
2-3	134.08	21.30	0.128	0.094	0.036
3-4	170.17	29.69	0.130	0.117	0.036
4-5	150.80	34.52	0.157	0.167	0.037
5-6	128.51	41.05	0.203	0.247	0.039
6-8	163.18	39.09	0.139	0.195	0.041
8-10	150.52	40.93	0.175	0.208	0.045
10-13	97.89	37.08	0.268	0.268	0.053

TABLE Supp.LXXXI. Statistical covariance matrix of measured cross section as function of θ_μ on iron, in units of $10^{-84} (\text{cm}^2/\text{degree}/\text{nucleon})^2$

Bin edges (degree)	0-2	2-3	3-4	4-5	5-6	6-8	8-10	10-13
0-2	54.038	1.548	-13.083	-2.225	0.045	0.009	-0.008	-0.560
2-3	1.548	294.722	47.593	-35.823	-9.843	-0.361	-0.634	-1.134
3-4	-13.083	47.593	486.432	77.132	-48.142	-8.617	-0.080	-1.852
4-5	-2.225	-35.823	77.132	560.801	117.294	-35.313	-5.619	0.001
5-6	0.045	-9.843	-48.142	117.294	680.720	38.411	-31.330	-1.575
6-8	0.009	-0.361	-8.617	-35.313	38.411	516.629	-8.166	-21.606
8-10	-0.008	-0.634	-0.080	-5.619	-31.330	-8.166	691.011	-15.851
10-13	-0.560	-1.134	-1.852	0.001	-1.575	-21.606	-15.851	687.894

TABLE Supp.LXXXII. Systematic covariance matrix of measured cross section in θ_μ on iron, in units of $10^{-84} (\text{cm}^2/\text{degree}/\text{nucleon})^2$

Bin edges (degree)	0-2	2-3	3-4	4-5	5-6	6-8	8-10	10-13
0-2	30.528	50.989	58.155	52.156	59.051	67.665	66.932	55.487
2-3	50.989	159.060	212.872	252.762	318.832	308.256	309.224	236.358
3-4	58.155	212.872	395.244	445.472	555.057	563.320	551.134	454.471
4-5	52.156	252.762	445.472	630.696	755.249	745.566	720.905	569.497
5-6	59.051	318.832	555.057	755.249	1004.354	944.544	929.399	724.968
6-8	67.665	308.256	563.320	745.566	944.544	1011.501	961.363	765.424
8-10	66.932	309.224	551.134	720.905	929.399	961.363	984.233	773.472
10-13	55.487	236.358	454.471	569.497	724.968	765.424	773.472	686.724

TABLE Supp.LXXXIII. Measured cross section as function of $p_{\mu,||}$ on iron, in units of 10^{-42} $\text{cm}^2/\text{GeV}/c/\text{nucleon}$, and the absolute and fractional cross section uncertainties

Bin edges (GeV/c)	σ	Abs. Unc.	Frac. Stat. Unc.	Frac. Sys. Unc.	Frac. Flux Unc.
1.5-3.0	114.93	23.86	0.160	0.133	0.040
3.0-4.0	285.09	47.81	0.103	0.132	0.041
4.0-5.0	300.20	55.34	0.097	0.157	0.045
5.0-6.0	315.62	56.79	0.089	0.156	0.043
6.0-7.0	232.29	42.91	0.092	0.160	0.038
7.0-8.5	102.57	22.26	0.116	0.183	0.037
8.5-10.0	34.29	7.68	0.143	0.172	0.037
10.0-20.0	8.70	1.97	0.164	0.156	0.036

TABLE Supp.LXXXIV. Statistical covariance matrix of measured cross section as function of $p_{\mu,||}$ on iron, in units of 10^{-84} $(\text{cm}^2/\text{GeV}/c/\text{nucleon})^2$

Bin edges (GeV/c)	1.5-3.0	3.0-4.0	4.0-5.0	5.0-6.0	6.0-7.0	7.0-8.5	8.5-10.0	10.0-20.0
1.5-3.0	336.966	105.591	21.222	16.807	2.719	0.226	1.198	0.310
3.0-4.0	105.591	860.377	225.133	54.398	11.506	5.621	1.457	0.513
4.0-5.0	21.222	225.133	852.767	332.012	69.832	9.101	1.624	0.369
5.0-6.0	16.807	54.398	332.012	789.184	285.431	34.752	6.190	0.965
6.0-7.0	2.719	11.506	69.832	285.431	456.056	120.873	15.158	1.557
7.0-8.5	0.226	5.621	9.101	34.752	120.873	142.721	30.721	2.031
8.5-10.0	1.198	1.457	1.624	6.190	15.158	30.721	24.113	2.917
10.0-20.0	0.310	0.513	0.369	0.965	1.557	2.031	2.917	2.045

TABLE Supp.LXXXV. Systematic covariance matrix of measured cross section in $p_{\mu,||}$ on iron, in units of $10^{-84} (\text{cm}^2/\text{GeV}/c/\text{nucleon})^2$

Bin edges (GeV/c)	1.5-3.0	3.0-4.0	4.0-5.0	5.0-6.0	6.0-7.0	7.0-8.5	8.5-10.0	10.0-20.0
1.5-3.0	232.325	457.975	581.593	576.180	381.001	165.652	55.418	13.358
3.0-4.0	457.975	1425.191	1674.184	1767.028	1267.987	602.910	194.546	43.654
4.0-5.0	581.593	1674.184	2209.657	2242.767	1589.613	712.797	227.146	51.563
5.0-6.0	576.180	1767.028	2242.767	2435.665	1763.682	826.869	259.459	57.703
6.0-7.0	381.001	1267.987	1589.613	1763.682	1385.463	664.782	203.946	46.508
7.0-8.5	165.652	602.910	712.797	826.869	664.782	352.611	106.696	23.186
8.5-10.0	55.418	194.546	227.146	259.459	203.946	106.696	34.872	7.187
10.0-20.0	13.358	43.654	51.563	57.703	46.508	23.186	7.187	1.851

TABLE Supp.LXXXVI. Measured cross section as function of $p_{\mu,T}$ on iron, in units of $10^{-42} \text{cm}^2/\text{GeV}/c/\text{nucleon}$, and the absolute and fractional cross section uncertainties

Bin edges (GeV/c)	σ	Abs. Unc.	Frac. Stat. Unc.	Frac. Sys. Unc.	Frac. Flux Unc.
0.00-0.15	383.24	78.77	0.175	0.108	0.036
0.15-0.30	1292.12	180.71	0.108	0.089	0.034
0.30-0.45	2057.62	342.26	0.108	0.126	0.036
0.45-0.60	2510.77	486.56	0.108	0.161	0.038
0.60-0.75	1657.69	500.94	0.157	0.258	0.040
0.75-0.90	1144.28	456.20	0.209	0.339	0.044
0.90-1.25	537.52	222.14	0.280	0.304	0.049
1.25-2.50	30.88	29.66	0.858	0.432	0.044

TABLE Supp.LXXXVII. Statistical covariance matrix of measured cross section as function of $p_{\mu,T}$ on iron, in units of 10^{-84} $(\text{cm}^2/\text{GeV}/c/\text{nucleon})^2$

Bin edges (GeV/c)	0.00-0.15	0.15-0.30	0.30-0.45	0.45-0.60	0.60-0.75	0.75-0.90	0.90-1.25	1.25-2.50
0.00-0.15	4508.029	200.588	-1057.726	-151.445	-11.493	-13.006	-3.431	-0.124
0.15-0.30	200.588	19354.213	2200.287	-3066.130	-782.930	-151.086	-68.478	-17.264
0.30-0.45	-1057.726	2200.287	49488.545	5599.511	-4144.878	-1804.099	-554.261	-9.056
0.45-0.60	-151.445	-3066.130	5599.511	73629.427	11005.561	-5077.959	-1892.165	-35.771
0.60-0.75	-11.493	-782.930	-4144.878	11005.561	67610.981	16189.200	-3072.318	-34.839
0.75-0.90	-13.006	-151.086	-1804.099	-5077.959	16189.200	57364.592	12622.564	-456.645
0.90-1.25	-3.431	-68.478	-554.261	-1892.165	-3072.318	12622.564	22709.915	626.156
1.25-2.50	-0.124	-17.264	-9.056	-35.771	-34.839	-456.645	626.156	701.992

TABLE Supp.LXXXVIII. Systematic covariance matrix of measured cross section in $p_{\mu,T}$ on iron, in units of 10^{-84} ($\text{cm}^2/\text{GeV}/c/\text{nucleon}$)²

Bin edges (GeV/c)	0.00-0.15	0.15-0.30	0.30-0.45	0.45-0.60	0.60-0.75	0.75-0.90	0.90-1.25	1.25-2.50
0.00-0.15	1697.438	3083.106	1352.142	982.632	1042.083	-44.294	526.367	59.871
0.15-0.30	3083.106	13303.600	22528.156	32586.614	29441.668	25380.953	9590.877	498.537
0.30-0.45	1352.142	22528.156	67655.950	99661.336	101743.975	87615.854	33418.402	1559.410
0.45-0.60	982.632	32586.614	99661.336	163108.310	160333.855	143991.058	52913.450	2540.412
0.60-0.75	1042.083	29441.668	101743.975	160333.855	183327.323	157677.680	64102.260	3163.920
0.75-0.90	-44.294	25380.953	87615.854	143991.058	157677.680	150753.848	59087.249	3359.485
0.90-1.25	526.367	9590.877	33418.402	52913.450	64102.260	59087.249	26635.988	1593.865
1.25-2.50	59.871	498.537	1559.410	2540.412	3163.920	3359.485	1593.865	177.810

TABLE Supp.LXXXIX. Measured cross section as function of Q^2 on iron, in units of 10^{-42} $\text{cm}^2/\text{GeV}^2/c^2/\text{nucleon}$, and the absolute and fractional cross section uncertainties

Bin edges (GeV^2/c^2)	σ	Abs. Unc.	Frac. Stat. Unc.	Frac. Sys. Unc.	Frac. Flux Unc.
0.000-0.025	2203.06	440.60	0.169	0.108	0.036
0.025-0.050	2393.39	403.92	0.143	0.090	0.036
0.050-0.100	2621.21	406.66	0.124	0.094	0.034
0.100-0.200	2548.13	407.20	0.106	0.120	0.036
0.200-0.300	2512.02	439.28	0.120	0.127	0.037
0.300-0.400	1831.97	413.22	0.137	0.179	0.038
0.400-0.500	1192.24	352.42	0.168	0.243	0.040
0.500-0.700	857.58	322.78	0.198	0.320	0.042
0.700-1.000	571.66	224.01	0.223	0.323	0.044
1.000-1.300	314.24	136.57	0.325	0.289	0.048
1.300-2.000	70.95	65.02	0.684	0.610	0.075
2.000-3.000	29.19	30.93	0.929	0.509	0.047

TABLE Supp.XC. Statistical covariance matrix of measured cross section as function of Q^2 on iron, in units of $10^{-84} (\text{cm}^2/\text{GeV}^2/c^2/\text{nucleon})^2$

Bin edges (GeV^2/c^2)	0.000-0.025	0.025-0.050	0.050-0.100	0.100-0.200	0.200-0.300	0.300-0.400	0.400-0.500	0.500-0.700	0.700-1.000	1.000-1.300	1.300-2.000	2.000-3.000
0.000-0.025	137801.601	29581.907	-13084.445	-4487.854	-351.306	-215.348	-2.885	-7.405	-35.435	-7.505	-0.332	0.429
0.025-0.050	29581.907	116449.941	35811.441	-7818.177	-4115.050	-518.530	-213.727	-80.378	-16.845	-31.024	-30.061	-9.789
0.050-0.100	-13084.445	35811.441	105091.742	16546.048	-9383.267	-3935.939	-1127.083	-283.563	-95.588	-32.006	-96.217	-56.591
0.100-0.200	-4487.854	-7818.177	16546.048	72901.198	16065.321	-4398.396	-4091.900	-1297.178	-553.793	-505.000	45.509	40.002
0.200-0.300	-351.306	-4115.050	-9383.267	16065.321	91346.779	24554.767	187.068	-3523.817	-1354.187	-687.084	-330.202	-250.335
0.300-0.400	-215.348	-518.530	-3935.939	-4398.396	24554.767	63156.008	22886.304	-1436.591	-645.433	-61.612	260.211	
0.400-0.500	-2.885	-213.727	-1127.083	-4091.900	187.068	22886.304	40333.847	13802.060	-1188.428	-1911.245	-151.578	107.033
0.500-0.700	-7.405	-80.378	-283.563	-1297.178	-3523.817	-1436.591	13802.060	28940.832	6654.313	-614.375	-178.851	-102.142
0.700-1.000	-35.435	-16.845	-95.588	-553.793	-1354.187	-2212.579	-1188.428	6654.313	16190.031	6244.640	105.428	-42.257
1.000-1.300	-7.505	-31.024	-32.006	-505.000	-687.084	-645.433	-1911.245	-614.375	6244.640	10412.006	1945.571	-12.112
1.300-2.000	-0.332	-30.061	-96.217	45.509	-330.202	-61.612	-151.578	-178.851	105.428	1945.571	2354.592	478.895
2.000-3.000	0.429	-9.789	-56.591	40.002	-250.335	260.211	107.033	-102.142	-42.257	-12.112	478.895	735.750

TABLE Supp.XCI. Systematic covariance matrix of measured cross section in Q^2 on iron, in units of $10^{-84} \text{ (cm}^2/\text{GeV}^2/c^2/\text{nucleon})^2$

Bin edges (GeV^2/c^2)	0.000-0.025	0.025-0.050	0.050-0.100	0.100-0.200	0.200-0.300	0.300-0.400	0.400-0.500	0.500-0.700	0.700-1.000	1.000-1.300	1.300-2.000	2.000-3.000
0.000-0.025	56330.153	41854.391	28615.528	11777.222	8987.773	2808.922	3952.899	1414.203	-441.422	1719.485	404.092	-120.953
0.025-0.050	41854.391	46697.584	43841.747	39293.903	35734.056	34708.185	28744.777	26472.560	16308.957	7832.234	2691.034	871.441
0.050-0.100	28615.528	43841.747	60283.640	67369.854	63426.373	62541.414	53859.168	50007.653	31908.075	14771.552	5183.326	1710.945
0.100-0.200	11777.222	39293.903	67369.854	92910.828	88557.671	89883.663	78305.677	73333.008	45901.172	20886.720	7572.366	2500.306
0.200-0.300	8987.773	35734.056	63426.373	88557.671	101623.257	98829.623	86403.079	79752.621	51111.939	22341.626	8140.579	2902.191
0.300-0.400	2808.922	34708.185	62541.414	89883.663	98829.623	107593.652	90251.175	81170.858	53030.603	22342.842	8164.355	3128.716
0.400-0.500	3952.899	28744.777	53859.168	78305.677	86403.079	90251.175	83869.271	76341.753	49259.257	22398.760	9132.650	3139.109
0.500-0.700	1414.203	26472.560	50007.653	73333.008	79752.621	81170.858	76341.753	75245.661	48525.106	22687.294	9375.036	3072.433
0.700-1.000	-441.422	16308.957	31908.075	45901.172	51111.939	53030.603	49259.257	48525.106	33989.888	15320.991	6322.854	2224.255
1.000-1.300	1719.485	7832.234	14771.552	20886.720	22341.626	22342.842	22398.760	22687.294	15320.991	8239.954	3609.320	1099.543
1.300-2.000	404.092	2691.034	5183.326	7572.366	8140.579	8164.355	9132.650	9375.036	6322.854	3609.320	1872.378	567.369
2.000-3.000	-120.953	871.441	1710.945	2500.306	2902.191	3128.716	3139.109	3072.433	2224.255	1099.543	567.369	221.141

TABLE Supp.XCII. Measured cross section as function of W_{exp} on iron, in units of 10^{-42} $\text{cm}^2/\text{GeV}/c^2/\text{nucleon}$, and the absolute and fractional cross section uncertainties

Bin edges (GeV/c^2)	σ	Abs. Unc.	Frac. Stat. Unc.	Frac. Sys. Unc.	Frac. Flux Unc.
0.9-1.1	311.04	166.76	0.474	0.250	0.058
1.1-1.2	3578.05	568.58	0.132	0.089	0.037
1.2-1.3	6517.70	1370.61	0.096	0.187	0.037
1.3-1.4	4762.99	1879.65	0.178	0.352	0.037

TABLE Supp.XCIII. Statistical covariance matrix of measured cross section as function of W_{exp} on iron, in units of 10^{-84} $(\text{cm}^2/\text{GeV}/c^2/\text{nucleon})^2$

Bin edges (GeV/c^2)	0.9-1.1	1.1-1.2	1.2-1.3	1.3-1.4
0.9-1.1	21751.952	8816.208	-32096.118	-11418.298
1.1-1.2	8816.208	221945.211	-113809.407	-238691.744
1.2-1.3	-32096.118	-113809.407	388748.322	294208.988
1.3-1.4	-11418.298	-238691.744	294208.988	717522.632

TABLE Supp.XCIV. Systematic covariance matrix of measured cross section in W_{exp} on iron, in units of 10^{-84} $(\text{cm}^2/\text{GeV}/c^2/\text{nucleon})^2$

Bin edges (GeV/c^2)	0.9-1.1	1.1-1.2	1.2-1.3	1.3-1.4
0.9-1.1	6057.167	7556.637	35126.356	46543.098
1.1-1.2	7556.637	101332.959	-9217.793	-109601.685
1.2-1.3	35126.356	-9217.793	1489829.153	1981530.923
1.3-1.4	46543.098	-109601.685	1981530.923	2815551.855

TABLE Supp.XCV. Measured cross section as function of T_π on iron, in units of 10^{-42} $\text{cm}^2/\text{GeV}/\text{nucleon}$, and the absolute and fractional cross section uncertainties

Bin edges (GeV)	σ	Abs. Unc.	Frac. Stat. Unc.	Frac. Sys. Unc.	Frac. Flux Unc.
0.035-0.100	9611.08	1423.80	0.080	0.125	0.036
0.100-0.150	6490.73	926.72	0.067	0.126	0.037
0.150-0.200	4801.53	909.68	0.098	0.162	0.037
0.200-0.350	1964.13	829.17	0.206	0.368	0.042

TABLE Supp.XCVI. Statistical covariance matrix of measured cross section as function of T_π on iron, in units of 10^{-84} $(\text{cm}^2/\text{GeV}/\text{nucleon})^2$

Bin edges (GeV)	0.035-0.100	0.100-0.150	0.150-0.200	0.200-0.350
0.035-0.100	592308.755	144789.490	-51192.110	-29375.688
0.100-0.150	144789.490	190306.593	62421.208	-9576.103
0.150-0.200	-51192.110	62421.208	219623.729	60254.833
0.200-0.350	-29375.688	-9576.103	60254.833	163896.809

TABLE Supp.XCVII. Systematic covariance matrix of measured cross section in T_π on iron, in units of 10^{-84} $(\text{cm}^2/\text{GeV}/\text{nucleon})^2$

Bin edges (GeV)	0.035-0.100	0.100-0.150	0.150-0.200	0.200-0.350
0.035-0.100	1434906.838	857837.924	660551.198	539981.697
0.100-0.150	857837.924	668506.151	580579.025	474120.643
0.150-0.200	660551.198	580579.025	607902.437	539205.808
0.200-0.350	539981.697	474120.643	539205.808	523625.100

TABLE Supp.XCVIII. Measured cross section as function of θ_π on iron, in units of 10^{-42} $\text{cm}^2/\text{degree}/\text{nucleon}$, and the absolute and fractional cross section uncertainties

Bin edges (degree)	σ	Abs. Unc.	Frac. Stat. Unc.	Frac. Sys. Unc.	Frac. Flux Unc.
0-10	4.28	1.82	0.389	0.168	0.041
10-20	7.60	2.13	0.212	0.183	0.037
20-30	10.16	2.16	0.131	0.167	0.036
30-40	12.09	2.40	0.116	0.161	0.037
40-50	13.99	2.73	0.106	0.164	0.039
50-60	17.22	3.09	0.104	0.146	0.038
60-120	13.65	2.38	0.106	0.138	0.038
120-135	6.63	1.69	0.186	0.174	0.035
135-150	3.66	1.17	0.253	0.197	0.038
150-165	1.87	1.02	0.492	0.242	0.037
165-180	1.14	1.36	1.096	0.467	0.037

TABLE Supp.XCIX. Statistical covariance matrix of measured cross section as function of θ_π on iron, in units of 10^{-84} ($\text{cm}^2/\text{degree/nucleon}$)²

Bin edges (degree)	0-10	10-20	20-30	30-40	40-50	50-60	60-120	120-135	135-150	150-165	165-180
0-10	2.778	0.967	-0.097	-0.023	0.009	-0.055	-0.044	-0.026	0.019	0.025	-0.002
10-20	0.967	2.596	0.658	-0.123	-0.184	-0.099	-0.044	-0.046	-0.028	-0.018	-0.009
20-30	-0.097	0.658	1.783	0.606	-0.124	-0.171	-0.084	-0.066	-0.008	0.012	-0.018
30-40	-0.023	-0.123	0.606	1.968	0.855	-0.186	-0.160	-0.086	0.021	0.026	-0.030
40-50	0.009	-0.184	-0.124	0.855	2.216	1.051	-0.123	-0.053	-0.005	-0.029	-0.025
50-60	-0.055	-0.099	-0.171	-0.186	1.051	3.212	0.896	-0.133	-0.121	-0.077	0.003
60-120	-0.044	-0.044	-0.084	-0.160	-0.123	0.896	2.110	0.287	-0.036	-0.009	0.051
120-135	-0.026	-0.046	-0.066	-0.086	-0.053	-0.133	0.287	1.519	0.433	0.039	-0.130
135-150	0.019	-0.028	-0.008	0.021	-0.005	-0.121	-0.036	0.433	0.859	0.425	0.122
150-165	0.025	-0.018	0.012	0.026	-0.029	-0.077	-0.009	0.039	0.425	0.842	0.660
165-180	-0.002	-0.009	-0.018	-0.030	-0.025	0.003	0.051	-0.130	0.122	0.660	1.562

TABLE Supp.C. Systematic covariance matrix of measured cross section in θ_π on iron, in units of 10^{-84} ($\text{cm}^2/\text{degree/nucleon}$)²

Bin edges (degree)	0-10	10-20	20-30	30-40	40-50	50-60	60-120	120-135	135-150	150-165	165-180
0-10	0.519	0.817	0.997	1.074	1.244	1.284	0.896	0.666	0.352	0.211	-0.162
10-20	0.817	1.934	2.154	2.341	2.542	2.253	1.340	1.150	0.608	0.430	-0.239
20-30	0.997	2.154	2.885	3.148	3.495	3.379	2.171	1.630	0.949	0.583	-0.198
30-40	1.074	2.341	3.148	3.808	4.236	4.240	2.849	1.777	1.019	0.621	-0.090
40-50	1.244	2.542	3.495	4.236	5.253	5.456	3.638	2.285	1.325	0.718	-0.088
50-60	1.284	2.253	3.379	4.240	5.456	6.333	4.491	2.476	1.388	0.696	0.002
60-120	0.896	1.340	2.171	2.849	3.638	4.491	3.552	1.600	0.835	0.391	0.091
120-135	0.666	1.150	1.630	1.777	2.285	2.476	1.600	1.327	0.754	0.425	-0.112
135-150	0.352	0.608	0.949	1.019	1.325	1.388	0.835	0.754	0.520	0.270	-0.067
150-165	0.211	0.430	0.583	0.621	0.718	0.696	0.391	0.425	0.270	0.205	-0.028
165-180	-0.162	-0.239	-0.198	-0.090	-0.088	0.002	0.091	-0.112	-0.067	-0.028	0.284

TABLE Supp.CI. Measured cross section as function of p_μ on lead, in units of 10^{-42} $\text{cm}^2/\text{GeV}/c/\text{nucleon}$, and the absolute and fractional cross section uncertainties

Bin edges (GeV/c)	σ	Abs. Unc.	Frac. Stat. Unc.	Frac. Sys. Unc.	Frac. Flux Unc.
1.5-3.0	57.22	14.78	0.222	0.131	0.040
3.0-4.0	169.13	31.67	0.138	0.126	0.042
4.0-5.0	208.37	36.80	0.107	0.141	0.043
5.0-6.0	206.20	37.95	0.100	0.154	0.042
6.0-7.0	133.72	26.25	0.115	0.159	0.040
7.0-8.5	61.02	12.21	0.133	0.150	0.039
8.5-10.0	20.70	4.78	0.178	0.146	0.042
10.0-20.0	3.54	1.29	0.307	0.196	0.059

TABLE Supp.CII. Statistical covariance matrix of measured cross section as function of p_μ on lead, in units of 10^{-84} $(\text{cm}^2/\text{GeV}/c/\text{nucleon})^2$

Bin edges (GeV/c)	1.5-3.0	3.0-4.0	4.0-5.0	5.0-6.0	6.0-7.0	7.0-8.5	8.5-10.0	10.0-20.0
1.5-3.0	162.019	55.143	10.979	2.356	5.699	0.630	0.112	0.017
3.0-4.0	55.143	546.846	159.863	29.564	7.808	2.796	0.687	0.060
4.0-5.0	10.979	159.863	494.840	173.574	38.342	11.228	3.055	0.185
5.0-6.0	2.356	29.564	173.574	426.939	169.281	25.683	3.167	0.484
6.0-7.0	5.699	7.808	38.342	169.281	236.627	68.538	7.526	0.549
7.0-8.5	0.630	2.796	11.228	25.683	68.538	65.416	15.972	1.145
8.5-10.0	0.112	0.687	3.055	3.167	7.526	15.972	13.637	1.904
10.0-20.0	0.017	0.060	0.185	0.484	0.549	1.145	1.904	1.183

TABLE Supp.CIII. Systematic covariance matrix of measured cross section in p_μ on lead, in units of 10^{-84} ($\text{cm}^2/\text{GeV}/c/\text{nucleon}$)²

Bin edges (GeV/c)	1.5-3.0	3.0-4.0	4.0-5.0	5.0-6.0	6.0-7.0	7.0-8.5	8.5-10.0	10.0-20.0
1.5-3.0	56.444	138.926	180.808	195.336	116.599	37.107	11.447	3.040
3.0-4.0	138.926	456.300	585.215	618.568	366.751	130.067	36.735	9.805
4.0-5.0	180.808	585.215	859.583	899.855	540.719	203.785	51.933	14.063
5.0-6.0	195.336	618.568	899.855	1013.175	637.749	241.083	66.174	16.345
6.0-7.0	116.599	366.751	540.719	637.749	452.536	178.971	53.757	11.877
7.0-8.5	37.107	130.067	203.785	241.083	178.971	83.684	24.919	4.785
8.5-10.0	11.447	36.735	51.933	66.174	53.757	24.919	9.164	1.611
10.0-20.0	3.040	9.805	14.063	16.345	11.877	4.785	1.611	0.483

TABLE Supp.CIV. Measured cross section as function of θ_μ on lead, in units of 10^{-42} $\text{cm}^2/\text{degree}/\text{nucleon}$, and the absolute and fractional cross section uncertainties

Bin edges (degree)	σ	Abs. Unc.	Frac. Stat. Unc.	Frac. Sys. Unc.	Frac. Flux Unc.
0-2	32.71	6.87	0.179	0.110	0.035
2-3	83.11	16.21	0.166	0.103	0.036
3-4	81.92	17.97	0.176	0.131	0.036
4-5	93.94	21.24	0.177	0.141	0.036
5-6	82.57	23.50	0.218	0.183	0.038
6-8	83.06	22.10	0.190	0.187	0.042
8-10	96.34	26.31	0.201	0.185	0.045
10-13	88.49	28.00	0.250	0.194	0.045

TABLE Supp.CV. Statistical covariance matrix of measured cross section as function of θ_μ on lead, in units of $10^{-84} (\text{cm}^2/\text{degree}/\text{nucleon})^2$

Bin edges (degree)	0-2	2-3	3-4	4-5	5-6	6-8	8-10	10-13
0-2	34.123	1.170	-7.061	-1.132	0.053	-0.004	-0.048	-0.190
2-3	1.170	189.638	30.525	-21.629	-6.990	-0.080	-0.095	-0.407
3-4	-7.061	30.525	207.225	34.916	-21.579	-4.114	-0.110	-0.681
4-5	-1.132	-21.629	34.916	275.591	60.008	-17.741	-2.978	0.399
5-6	0.053	-6.990	-21.579	60.008	323.349	15.500	-15.806	-1.288
6-8	-0.004	-0.080	-4.114	-17.741	15.500	248.413	-1.075	-14.438
8-10	-0.048	-0.095	-0.110	-2.978	-15.806	-1.075	375.065	-9.371
10-13	-0.190	-0.407	-0.681	0.399	-1.288	-14.438	-9.371	489.807

TABLE Supp.CVI. Systematic covariance matrix of measured cross section in θ_μ on lead, in units of $10^{-84} (\text{cm}^2/\text{degree}/\text{nucleon})^2$

Bin edges (degree)	0-2	2-3	3-4	4-5	5-6	6-8	8-10	10-13
0-2	13.053	21.354	24.029	25.945	26.727	23.505	22.209	25.444
2-3	21.354	73.124	82.686	85.119	105.230	101.031	112.547	94.467
3-4	24.029	82.686	115.798	129.470	151.397	152.158	161.481	151.063
4-5	25.945	85.119	129.470	175.384	180.866	177.610	196.907	183.731
5-6	26.727	105.230	151.397	180.866	229.048	221.694	233.313	216.679
6-8	23.505	101.031	152.158	177.610	221.694	240.058	258.273	236.181
8-10	22.209	112.547	161.481	196.907	233.313	258.273	317.068	269.857
10-13	25.444	94.467	151.063	183.731	216.679	236.181	269.857	294.391

TABLE Supp.CVII. Measured cross section as function of $p_{\mu,||}$ on lead, in units of 10^{-42} $\text{cm}^2/\text{GeV}/c/\text{nucleon}$, and the absolute and fractional cross section uncertainties

Bin edges (GeV/c)	σ	Abs. Unc.	Frac. Stat. Unc.	Frac. Sys. Unc.	Frac. Flux Unc.
1.5-3.0	62.81	15.69	0.214	0.129	0.040
3.0-4.0	170.55	32.40	0.138	0.131	0.042
4.0-5.0	205.44	37.10	0.109	0.144	0.044
5.0-6.0	204.29	37.49	0.101	0.153	0.042
6.0-7.0	130.24	25.40	0.116	0.157	0.040
7.0-8.5	60.09	11.91	0.132	0.148	0.039
8.5-10.0	20.73	4.66	0.175	0.141	0.041
10.0-20.0	3.55	1.28	0.304	0.195	0.059

TABLE Supp.CVIII. Statistical covariance matrix of measured cross section as function of $p_{\mu,||}$ on lead, in units of 10^{-84} $(\text{cm}^2/\text{GeV}/c/\text{nucleon})^2$

Bin edges (GeV/c)	1.5-3.0	3.0-4.0	4.0-5.0	5.0-6.0	6.0-7.0	7.0-8.5	8.5-10.0	10.0-20.0
1.5-3.0	180.102	54.791	10.594	2.700	5.881	0.643	0.111	0.018
3.0-4.0	54.791	553.360	147.805	33.256	8.554	4.122	0.910	0.062
4.0-5.0	10.594	147.805	501.413	175.103	38.949	10.598	3.017	0.187
5.0-6.0	2.700	33.256	175.103	423.991	159.229	24.427	3.065	0.470
6.0-7.0	5.881	8.554	38.949	159.229	227.923	68.353	7.886	0.515
7.0-8.5	0.643	4.122	10.598	24.427	68.353	62.634	15.833	1.209
8.5-10.0	0.111	0.910	3.017	3.065	7.886	15.833	13.109	1.902
10.0-20.0	0.018	0.062	0.187	0.470	0.515	1.209	1.902	1.169

TABLE Supp.CIX. Systematic covariance matrix of measured cross section in $p_{\mu,||}$ on lead, in units of $10^{-84} \text{ (cm}^2/\text{GeV}/c/\text{nucleon})^2$

Bin edges (GeV/c)	1.5-3.0	3.0-4.0	4.0-5.0	5.0-6.0	6.0-7.0	7.0-8.5	8.5-10.0	10.0-20.0
1.5-3.0	65.945	156.648	196.080	208.037	121.268	40.055	12.698	3.241
3.0-4.0	156.648	496.145	613.874	627.753	362.434	128.593	36.249	9.914
4.0-5.0	196.080	613.874	875.271	890.815	528.535	204.789	52.470	14.028
5.0-6.0	208.037	627.753	890.815	981.148	610.077	238.019	65.819	16.173
6.0-7.0	121.268	362.434	528.535	610.077	417.195	168.414	50.493	11.430
7.0-8.5	40.055	128.593	204.789	238.019	168.414	79.260	23.105	4.764
8.5-10.0	12.698	36.249	52.470	65.819	50.493	23.105	8.596	1.597
10.0-20.0	3.241	9.914	14.028	16.173	11.430	4.764	1.597	0.479

TABLE Supp.CX. Measured cross section as function of $p_{\mu,T}$ on lead, in units of $10^{-42} \text{ cm}^2/\text{GeV}/c/\text{nucleon}$, and the absolute and fractional cross section uncertainties

Bin edges (GeV/c)	σ	Abs. Unc.	Frac. Stat. Unc.	Frac. Sys. Unc.	Frac. Flux Unc.
0.00-0.15	236.50	63.46	0.238	0.124	0.036
0.15-0.30	713.67	131.67	0.151	0.107	0.036
0.30-0.45	1294.09	207.18	0.114	0.112	0.036
0.45-0.60	1179.81	261.53	0.146	0.167	0.038
0.60-0.75	928.01	303.17	0.205	0.255	0.041
0.75-0.90	663.67	249.94	0.255	0.277	0.047
0.90-1.25	538.56	154.85	0.224	0.181	0.044
1.25-2.50	46.26	28.11	0.548	0.262	0.046

TABLE Supp.CXI. Statistical covariance matrix of measured cross section as function of $p_{\mu,T}$ on lead, in units of 10^{-84} ($\text{cm}^2/\text{GeV}/c/\text{nucleon}$)²

Bin edges (GeV/c)	0.00-0.15	0.15-0.30	0.30-0.45	0.45-0.60	0.60-0.75	0.75-0.90	0.90-1.25	1.25-2.50
0.00-0.15	3168.718	396.989	-682.793	-135.891	-4.150	-15.259	-2.058	-2.887
0.15-0.30	396.989	11544.339	1232.806	-1676.433	-454.364	-54.702	-41.615	-5.107
0.30-0.45	-682.793	1232.806	21839.737	3944.473	-2826.174	-928.275	-216.527	-6.595
0.45-0.60	-135.891	-1676.433	3944.473	29715.318	7674.514	-1779.356	-1087.723	-45.942
0.60-0.75	-4.150	-454.364	-2826.174	7674.514	36030.549	7778.024	-1015.831	-92.489
0.75-0.90	-15.259	-54.702	-928.275	-1779.356	7778.024	28589.494	5302.666	-387.123
0.90-1.25	-2.058	-41.615	-216.527	-1087.723	-1015.831	5302.666	14519.371	454.036
1.25-2.50	-2.887	-5.107	-6.595	-45.942	-92.489	-387.123	454.036	643.079

TABLE Supp.CXII. Systematic covariance matrix of measured cross section in $p_{\mu,T}$ on lead, in units of $10^{-84} \text{ (cm}^2/\text{GeV}/c/\text{nucleon})^2$

Bin edges (GeV/c)	0.00-0.15	0.15-0.30	0.30-0.45	0.45-0.60	0.60-0.75	0.75-0.90	0.90-1.25	1.25-2.50
0.00-0.15	858.314	1541.536	1477.698	858.624	566.947	760.244	425.940	31.396
0.15-0.30	1541.536	5793.906	9326.513	10708.725	10733.551	8355.208	3623.301	211.474
0.30-0.45	1477.698	9326.513	21083.833	26557.906	27334.872	20448.934	8612.808	492.206
0.45-0.60	858.624	10708.725	26557.906	38682.204	41349.523	30321.221	12514.317	663.020
0.60-0.75	566.947	10733.551	27334.872	41349.523	55883.369	40454.619	18278.196	831.407
0.75-0.90	760.244	8355.208	20448.934	30321.221	40454.619	33878.710	16027.219	756.951
0.90-1.25	425.940	3623.301	8612.808	12514.317	18278.196	16027.219	9459.079	337.098
1.25-2.50	31.396	211.474	492.206	663.020	831.407	756.951	337.098	147.264

TABLE Supp.CXIII. Measured cross section as function of Q^2 on lead, in units of 10^{-42} $\text{cm}^2/\text{GeV}^2/c^2/\text{nucleon}$, and the absolute and fractional cross section uncertainties

Bin edges (GeV^2/c^2)	σ	Abs. Unc.	Frac. Stat. Unc.	Frac. Sys. Unc.	Frac. Flux Unc.
0.000-0.025	1377.45	360.28	0.232	0.120	0.036
0.025-0.050	1545.90	318.03	0.180	0.099	0.035
0.050-0.100	1340.67	278.06	0.173	0.114	0.036
0.100-0.200	1540.32	254.33	0.120	0.113	0.036
0.200-0.300	1192.87	255.96	0.146	0.157	0.038
0.300-0.400	814.78	218.51	0.196	0.183	0.037
0.400-0.500	742.47	209.57	0.199	0.201	0.038
0.500-0.700	505.16	181.41	0.230	0.276	0.043
0.700-1.000	362.55	129.20	0.246	0.258	0.045
1.000-1.300	334.27	104.12	0.260	0.172	0.039
1.300-2.000	89.19	52.40	0.490	0.324	0.058
2.000-3.000	79.01	76.23	0.918	0.296	0.045

TABLE Supp.CXIV. Statistical covariance matrix of measured cross section as function of Q^2 on lead, in units of 10^{-84}
 $(\text{cm}^2/\text{GeV}^2/c^2/\text{nucleon})^2$

Bin edges (GeV^2/c^2)	0.000-0.025	0.025-0.050	0.050-0.100	0.100-0.200	0.200-0.300	0.300-0.400	0.400-0.500	0.500-0.700	0.700-1.000	1.000-1.300	1.300-2.000	2.000-3.000
0.000-0.025	102365.910	23995.884	-8159.314	-2931.052	-204.852	-174.866	-70.549	16.612	-62.726	20.284	-16.180	-17.044
0.025-0.050	23995.884	77779.070	23456.388	-4519.319	-2625.286	-478.484	-167.234	-45.000	-40.480	-32.874	-9.654	-3.802
0.050-0.100	-8159.314	23456.388	54101.847	9375.054	-4821.719	-1589.678	-712.645	-145.199	-39.017	-73.589	-28.538	1.758
0.100-0.200	-2931.052	-4519.319	9375.054	34308.499	8233.980	-2135.072	-2573.844	-749.455	-244.834	-143.762	-5.293	-19.055
0.200-0.300	-204.852	-2625.286	-4821.719	8233.980	30482.401	12298.839	895.149	-1464.890	-410.208	-23.786	-38.294	-19.719
0.300-0.400	-174.866	-478.484	-1589.678	-2135.072	12298.839	25629.989	14476.309	-2.271	-1103.469	-592.153	-234.311	-10.325
0.400-0.500	-70.549	-167.234	-712.645	-2573.844	895.149	14476.309	21746.274	8145.249	-370.599	-900.004	-166.443	-70.245
0.500-0.700	16.612	-45.000	-145.199	-749.455	-1464.890	-2.271	8145.249	13530.088	3797.890	-616.488	-17.299	-106.552
0.700-1.000	-62.726	-40.480	-39.017	-244.834	-410.208	-1103.469	-370.599	3797.890	7975.856	2679.136	-63.894	-319.962
1.000-1.300	20.284	-32.874	-73.589	-143.762	-23.786	-592.153	-900.004	-616.488	2679.136	7526.346	591.026	-223.317
1.300-2.000	-16.180	-9.654	-28.538	-5.293	-38.294	-234.311	-166.443	-17.299	-63.894	591.026	1912.384	306.063
2.000-3.000	-17.044	-3.802	1.758	-19.055	-19.719	-10.325	-70.245	-106.552	-319.962	-223.317	306.063	5262.012

TABLE Supp.CXV. Systematic covariance matrix of measured cross section in Q^2 on lead, in units of $10^{-84} \text{ (cm}^2/\text{GeV}^2/c^2/\text{nucleon})^2$

Bin edges (GeV^2/c^2)	0.000-0.025	0.025-0.050	0.050-0.100	0.100-0.200	0.200-0.300	0.300-0.400	0.400-0.500	0.500-0.700	0.700-1.000	1.000-1.300	1.300-2.000	2.000-3.000
0.000-0.025	27438.389	20614.170	15391.629	11891.348	4765.830	3573.036	3746.310	3030.552	2372.444	2054.434	-71.575	595.811
0.025-0.050	20614.170	23365.053	19586.410	18309.054	13307.121	10080.808	10051.827	9511.742	5927.853	4205.073	556.662	1133.213
0.050-0.100	15391.629	19586.410	23217.530	24616.084	22049.533	16620.749	16862.697	14612.344	8927.013	5825.351	994.784	995.743
0.100-0.200	11891.348	18309.054	24616.084	30375.661	27380.065	22412.748	22350.023	19200.507	11450.749	6802.159	1607.278	1210.251
0.200-0.300	4765.830	13307.121	22049.533	27380.065	35034.638	24271.171	23806.637	20699.693	12851.084	7331.150	2153.086	978.034
0.300-0.400	3573.036	10080.808	16620.749	22412.748	24271.171	22118.452	21160.786	18779.817	11030.151	6022.207	2193.369	719.037
0.400-0.500	3746.310	10051.827	16862.697	22350.023	23806.637	21160.786	22174.645	19688.088	11706.085	6521.884	2398.046	567.351
0.500-0.700	3030.552	9511.742	14612.344	19200.507	20699.693	18779.817	19688.088	19381.297	12112.459	6186.160	2733.678	593.115
0.700-1.000	2372.444	5927.853	8927.013	11450.749	12851.084	11030.151	11706.085	12112.459	8715.631	4576.629	2066.718	543.318
1.000-1.300	2054.434	4205.073	5825.351	6802.159	7331.150	6022.207	6521.884	6186.160	4576.629	3313.826	1091.299	224.801
1.300-2.000	-71.575	556.662	994.784	1607.278	2153.086	2193.369	2398.046	2733.678	2066.718	1091.299	833.186	15.014
2.000-3.000	595.811	1133.213	995.743	1210.251	978.034	719.037	567.351	593.115	543.318	224.801	15.014	548.266

TABLE Supp.CXVI. Measured cross section as function of W_{exp} on lead, in units of 10^{-42} $\text{cm}^2/\text{GeV}/\text{c}^2/\text{nucleon}$, and the absolute and fractional cross section uncertainties

Bin edges (GeV/c^2)	σ	Abs. Unc.	Frac. Stat. Unc.	Frac. Sys. Unc.	Frac. Flux Unc.
0.9-1.1	324.04	158.71	0.422	0.248	0.055
1.1-1.2	986.81	257.24	0.237	0.108	0.046
1.2-1.3	3802.07	617.99	0.091	0.135	0.037
1.3-1.4	5092.70	1400.14	0.161	0.223	0.032

TABLE Supp.CXVII. Statistical covariance matrix of measured cross section as function of W_{exp} on lead, in units of 10^{-84} $(\text{cm}^2/\text{GeV}/\text{c}^2/\text{nucleon})^2$

Bin edges (GeV/c^2)	0.9-1.1	1.1-1.2	1.2-1.3	1.3-1.4
0.9-1.1	18723.909	10639.010	-18411.776	-28099.433
1.1-1.2	10639.010	54830.704	23209.963	-124904.569
1.2-1.3	-18411.776	23209.963	119494.363	55595.419
1.3-1.4	-28099.433	-124904.569	55595.419	674041.129

TABLE Supp.CXVIII. Systematic covariance matrix of measured cross section in W_{exp} on lead, in units of 10^{-84} $(\text{cm}^2/\text{GeV}/\text{c}^2/\text{nucleon})^2$

Bin edges (GeV/c^2)	0.9-1.1	1.1-1.2	1.2-1.3	1.3-1.4
0.9-1.1	6465.812	5506.681	2629.126	6224.264
1.1-1.2	5506.681	11343.237	18638.835	14533.237
1.2-1.3	2629.126	18638.835	262420.462	543487.733
1.3-1.4	6224.264	14533.237	543487.733	1286338.954

TABLE Supp.CXIX. Measured cross section as function of T_π on lead, in units of 10^{-42} $\text{cm}^2/\text{GeV}/\text{nucleon}$, and the absolute and fractional cross section uncertainties

Bin edges (GeV)	σ	Abs. Unc.	Frac. Stat. Unc.	Frac. Sys. Unc.	Frac. Flux Unc.
0.035-0.100	5058.30	762.04	0.113	0.099	0.037
0.100-0.150	3560.00	528.69	0.091	0.117	0.038
0.150-0.200	2718.88	550.67	0.126	0.158	0.038
0.200-0.350	2145.01	624.92	0.169	0.237	0.038

TABLE Supp.CXX. Statistical covariance matrix of measured cross section as function of T_π on lead, in units of 10^{-84} $(\text{cm}^2/\text{GeV}/\text{nucleon})^2$

Bin edges (GeV)	0.035-0.100	0.100-0.150	0.150-0.200	0.200-0.350
0.035-0.100	327493.820	72027.359	-23454.488	-22608.464
0.100-0.150	72027.359	104866.238	29191.098	-8581.637
0.150-0.200	-23454.488	29191.098	117994.805	28803.449
0.200-0.350	-22608.464	-8581.637	28803.449	131287.372

TABLE Supp.CXXI. Systematic covariance matrix of measured cross section in T_π on lead, in units of 10^{-84} $(\text{cm}^2/\text{GeV}/\text{nucleon})^2$

Bin edges (GeV)	0.035-0.100	0.100-0.150	0.150-0.200	0.200-0.350
0.035-0.100	253210.315	191336.076	166383.958	172831.262
0.100-0.150	191336.076	174649.446	165733.149	176988.883
0.150-0.200	166383.958	165733.149	185243.795	198764.255
0.200-0.350	172831.262	176988.883	198764.255	259233.214

TABLE Supp.CXXII. Measured cross section as function of θ_π on lead, in units of 10^{-42} $\text{cm}^2/\text{degree}/\text{nucleon}$, and the absolute and fractional cross section uncertainties

Bin edges (degree)	σ	Abs. Unc.	Frac. Stat. Unc.	Frac. Sys. Unc.	Frac. Flux Unc.
0-10	2.76	1.21	0.404	0.168	0.040
10-20	5.72	1.58	0.215	0.173	0.038
20-30	6.08	1.36	0.154	0.162	0.039
30-40	8.29	1.52	0.119	0.140	0.038
40-50	8.20	1.60	0.121	0.154	0.039
50-60	7.04	1.63	0.155	0.171	0.041
60-120	6.42	1.24	0.141	0.133	0.038
120-135	4.46	0.93	0.170	0.122	0.035
135-150	3.19	0.79	0.193	0.153	0.034
150-165	1.74	0.68	0.345	0.180	0.036
165-180	0.34	0.34	0.945	0.363	0.043

TABLE Supp.CXXIII. Statistical covariance matrix of measured cross section as function of θ_π on lead, in units of 10^{-84} ($\text{cm}^2/\text{degree/nucleon}$)²

Bin edges (degree)	0-10	10-20	20-30	30-40	40-50	50-60	60-120	120-135	135-150	150-165	165-180
0-10	1.239	0.505	0.026	-0.019	-0.031	-0.034	-0.027	-0.016	-0.013	0.027	-0.003
10-20	0.505	1.513	0.471	-0.038	-0.117	-0.084	-0.043	-0.035	-0.030	-0.002	-0.004
20-30	0.026	0.471	0.873	0.417	-0.011	-0.092	-0.050	-0.030	-0.010	0.011	0.003
30-40	-0.019	-0.038	0.417	0.973	0.511	0.052	-0.092	-0.054	0.002	0.000	-0.012
40-50	-0.031	-0.117	-0.011	0.511	0.978	0.615	0.085	-0.018	-0.021	-0.012	-0.014
50-60	-0.034	-0.084	-0.092	0.052	0.615	1.199	0.446	-0.006	-0.069	-0.025	-0.013
60-120	-0.027	-0.043	-0.050	-0.092	0.085	0.446	0.814	0.157	0.007	-0.005	0.026
120-135	-0.016	-0.035	-0.030	-0.054	-0.018	-0.006	0.157	0.576	0.237	0.006	0.061
135-150	-0.013	-0.030	-0.010	0.002	-0.021	-0.069	0.007	0.237	0.381	0.185	0.011
150-165	0.027	-0.002	0.011	0.000	-0.012	-0.025	0.006	0.006	0.185	0.360	-0.003
165-180	-0.003	-0.004	0.003	-0.012	-0.014	-0.013	0.026	0.061	0.011	-0.003	0.101

K. Tables of Ratios of cross sections

TABLE Supp.CXXIV. Systematic covariance matrix of measured cross section in θ_π on lead, in units of 10^{-84} ($\text{cm}^2/\text{degree/nucleon}$)²

Bin edges (degree)	0-10	10-20	20-30	30-40	40-50	50-60	60-120	120-135	135-150	150-165	165-180
0-10	0.214	0.349	0.382	0.450	0.476	0.398	0.283	0.215	0.192	0.089	-0.001
10-20	0.349	0.981	0.884	0.904	0.855	0.675	0.447	0.387	0.329	0.152	-0.018
20-30	0.382	0.884	0.974	1.055	1.026	0.838	0.531	0.455	0.369	0.175	-0.004
30-40	0.450	0.904	1.055	1.344	1.395	1.255	0.828	0.522	0.446	0.207	0.020
40-50	0.476	0.855	1.026	1.395	1.592	1.447	0.979	0.552	0.484	0.231	0.010
50-60	0.398	0.675	0.838	1.255	1.447	1.456	0.971	0.433	0.386	0.183	0.037
60-120	0.283	0.447	0.531	0.828	0.979	0.971	0.725	0.301	0.294	0.128	0.020
120-135	0.215	0.387	0.455	0.522	0.552	0.433	0.301	0.297	0.238	0.117	-0.004
135-150	0.192	0.329	0.369	0.446	0.484	0.386	0.294	0.238	0.239	0.122	-0.008
150-165	0.089	0.152	0.175	0.207	0.231	0.183	0.128	0.117	0.122	0.098	-0.004
165-180	-0.001	-0.018	-0.004	0.020	0.010	0.037	0.020	-0.004	-0.008	-0.004	0.015

TABLE Supp.CXXVI. Statistical covariance matrix of measured cross section ratio of carbon over scintillator in p_μ

Bin edges (GeV/c)	1.5-3.0	3.0-4.0	4.0-5.0	5.0-6.0	6.0-7.0	7.0-8.5	8.5-10.0	10.0-20.0
1.5-3.0	0.1507	0.0181	0.0020	0.0012	0.0015	0.0009	0.0002	0.0014
3.0-4.0	0.0181	0.0626	0.0115	0.0023	0.0008	0.0002	0.0000	0.0000
4.0-5.0	0.0020	0.0115	0.0352	0.0103	0.0019	0.0006	0.0003	0.0000
5.0-6.0	0.0012	0.0023	0.0103	0.0265	0.0116	0.0037	0.0022	0.0010
6.0-7.0	0.0015	0.0008	0.0019	0.0116	0.0225	0.0156	0.0069	0.0088
7.0-8.5	0.0009	0.0002	0.0006	0.0037	0.0156	0.0366	0.0270	0.0089
8.5-10.0	0.0002	0.0000	0.0003	0.0022	0.0069	0.0270	0.0607	0.0427
10.0-20.0	0.0014	0.0000	0.0000	0.0010	0.0088	0.0089	0.0427	0.2838

TABLE Supp.CXXV. Measured cross section ratio of carbon over scintillator in p_μ , and the absolute and fractional cross section ratio uncertainties

Bin edges (GeV/c)	Ratio	Abs. Unc.	Frac. Stat. Unc.	Frac. Sys. Unc.	Frac. Flux Unc.
1.5-3.0	1.11	0.411	0.350	0.122	0.004
3.0-4.0	1.20	0.279	0.209	0.104	0.003
4.0-5.0	1.02	0.229	0.184	0.129	0.005
5.0-6.0	0.95	0.213	0.171	0.144	0.002
6.0-7.0	0.77	0.197	0.195	0.166	0.008
7.0-8.5	0.74	0.239	0.258	0.194	0.020
8.5-10.0	0.67	0.304	0.366	0.265	0.025
10.0-20.0	1.18	0.610	0.450	0.251	0.016

TABLE Supp.CXXVII. Systematic covariance matrix of measured cross section ratio of carbon over scintillator in p_μ

Bin edges (GeV/c)	1.5-3.0	3.0-4.0	4.0-5.0	5.0-6.0	6.0-7.0	7.0-8.5	8.5-10.0	10.0-20.0
1.5-3.0	0.018	0.013	0.012	0.013	0.012	0.008	0.014	0.032
3.0-4.0	0.013	0.015	0.012	0.014	0.013	0.010	0.014	0.030
4.0-5.0	0.012	0.012	0.017	0.016	0.015	0.013	0.013	0.028
5.0-6.0	0.013	0.014	0.016	0.019	0.016	0.014	0.016	0.032
6.0-7.0	0.012	0.013	0.015	0.016	0.016	0.015	0.017	0.030
7.0-8.5	0.008	0.010	0.013	0.014	0.015	0.021	0.022	0.026
8.5-10.0	0.014	0.014	0.013	0.016	0.017	0.022	0.032	0.038
10.0-20.0	0.032	0.030	0.028	0.032	0.030	0.026	0.038	0.089

TABLE Supp.CXXVIII. Measured cross section ratio of carbon over scintillator in θ_μ , and the absolute and fractional cross section ratio uncertainties

Bin edges (degree)	Ratio	Abs. Unc.	Frac. Stat. Unc.	Frac. Sys. Unc.	Frac. Flux Unc.
0-2	0.76	0.233	0.299	0.072	0.004
2-3	1.31	0.331	0.228	0.109	0.004
3-4	0.84	0.248	0.270	0.123	0.004
4-5	0.86	0.286	0.277	0.181	0.002
5-6	0.40	0.244	0.511	0.319	0.011
6-8	0.72	0.356	0.412	0.274	0.011
8-10	1.58	0.636	0.349	0.201	0.009
10-13	1.88	0.811	0.388	0.191	0.010

TABLE Supp.CXXIX. Statistical covariance matrix of measured cross section ratio of carbon over scintillator in θ_μ

Bin edges (degree)	0-2	2-3	3-4	4-5	5-6	6-8	8-10	10-13
0-2	0.0513	-0.0020	-0.0024	-0.0004	0.0000	0.0000	-0.0001	-0.0003
2-3	-0.0020	0.0892	0.0037	-0.0056	-0.0010	-0.0000	-0.0005	-0.0001
3-4	-0.0024	0.0037	0.0509	0.0071	-0.0037	-0.0009	-0.0001	-0.0003
4-5	-0.0004	-0.0056	0.0071	0.0574	0.0083	-0.0050	-0.0008	0.0001
5-6	0.0000	-0.0010	-0.0037	0.0083	0.0429	0.0054	-0.0041	-0.0003
6-8	0.0000	-0.0000	-0.0009	-0.0050	0.0054	0.0879	-0.0032	-0.0056
8-10	-0.0001	-0.0005	-0.0001	-0.0008	-0.0041	-0.0032	0.3035	-0.0178
10-13	-0.0003	-0.0001	-0.0003	0.0001	-0.0003	-0.0056	-0.0178	0.5289

TABLE Supp.CXXX. Systematic covariance matrix of measured cross section ratio of carbon over scintillator in θ_μ

Bin edges (degree)	0-2	2-3	3-4	4-5	5-6	6-8	8-10	10-13
0-2	0.003	0.001	0.002	0.002	0.002	0.002	0.006	0.001
2-3	0.001	0.020	0.009	0.015	0.010	0.014	0.023	0.035
3-4	0.002	0.009	0.010	0.014	0.011	0.012	0.019	0.024
4-5	0.002	0.015	0.014	0.024	0.016	0.021	0.036	0.037
5-6	0.002	0.010	0.011	0.016	0.017	0.016	0.026	0.026
6-8	0.002	0.014	0.012	0.021	0.016	0.039	0.042	0.040
8-10	0.006	0.023	0.019	0.036	0.026	0.042	0.101	0.062
10-13	0.001	0.035	0.024	0.037	0.026	0.040	0.062	0.129

TABLE Supp.CXXXI. Measured cross section ratio of carbon over scintillator in $p_{\mu,||}$, and the absolute and fractional cross section ratio uncertainties

Bin edges (GeV/c)	Ratio	Abs. Unc.	Frac. Stat. Unc.	Frac. Sys. Unc.	Frac. Flux Unc.
1.5-3.0	1.07	0.404	0.355	0.128	0.005
3.0-4.0	1.21	0.281	0.209	0.102	0.003
4.0-5.0	1.03	0.229	0.183	0.128	0.005
5.0-6.0	0.92	0.212	0.175	0.149	0.002
6.0-7.0	0.80	0.202	0.194	0.163	0.007
7.0-8.5	0.74	0.239	0.260	0.194	0.020
8.5-10.0	0.67	0.306	0.372	0.267	0.025
10.0-20.0	1.19	0.613	0.449	0.251	0.016

TABLE Supp.CXXXII. Statistical covariance matrix of measured cross section ratio of carbon over scintillator in $p_{\mu,||}$

Bin edges (GeV/c)	1.5-3.0	3.0-4.0	4.0-5.0	5.0-6.0	6.0-7.0	7.0-8.5	8.5-10.0	10.0-20.0
1.5-3.0	0.1447	0.0160	0.0019	0.0011	0.0014	0.0008	0.0002	0.0013
3.0-4.0	0.0160	0.0639	0.0111	0.0020	0.0007	0.0001	0.0000	0.0000
4.0-5.0	0.0019	0.0111	0.0353	0.0103	0.0020	0.0006	0.0003	0.0000
5.0-6.0	0.0011	0.0020	0.0103	0.0259	0.0119	0.0038	0.0021	0.0010
6.0-7.0	0.0014	0.0007	0.0020	0.0119	0.0239	0.0153	0.0065	0.0089
7.0-8.5	0.0008	0.0001	0.0006	0.0038	0.0153	0.0367	0.0271	0.0091
8.5-10.0	0.0002	0.0000	0.0003	0.0021	0.0065	0.0271	0.0620	0.0436
10.0-20.0	0.0013	0.0000	0.0000	0.0010	0.0089	0.0091	0.0436	0.2857

TABLE Supp.CXXXIII. Systematic covariance matrix of measured cross section ratio of carbon over scintillator in $p_{\mu,||}$

Bin edges (GeV/c)	1.5-3.0	3.0-4.0	4.0-5.0	5.0-6.0	6.0-7.0	7.0-8.5	8.5-10.0	10.0-20.0
1.5-3.0	0.019	0.012	0.013	0.013	0.013	0.009	0.014	0.033
3.0-4.0	0.012	0.015	0.012	0.014	0.013	0.009	0.013	0.028
4.0-5.0	0.013	0.012	0.017	0.016	0.015	0.013	0.013	0.028
5.0-6.0	0.013	0.014	0.016	0.019	0.017	0.014	0.016	0.032
6.0-7.0	0.013	0.013	0.015	0.017	0.017	0.015	0.017	0.031
7.0-8.5	0.009	0.009	0.013	0.014	0.015	0.020	0.022	0.025
8.5-10.0	0.014	0.013	0.013	0.016	0.017	0.022	0.032	0.038
10.0-20.0	0.033	0.028	0.028	0.032	0.031	0.025	0.038	0.090

TABLE Supp.CXXXIV. Measured cross section ratio of carbon over scintillator in $p_{\mu,T}$, and the absolute and fractional cross section ratio uncertainties

Bin edges (GeV/c)	Ratio	Abs. Unc.	Frac. Stat. Unc.	Frac. Sys. Unc.	Frac. Flux Unc.
0.00-0.15	1.07	0.355	0.323	0.070	0.003
0.15-0.30	0.80	0.192	0.226	0.080	0.002
0.30-0.45	0.99	0.224	0.201	0.103	0.003
0.45-0.60	0.92	0.255	0.228	0.160	0.004
0.60-0.75	0.84	0.314	0.306	0.212	0.008
0.75-0.90	0.65	0.579	0.688	0.569	0.039
0.90-1.25	1.33	0.945	0.586	0.399	0.021
1.25-2.50	1.97	3.141	1.434	0.693	0.021

TABLE Supp.CXXXV. Statistical covariance matrix of measured cross section ratio of carbon over scintillator in $p_{\mu,T}$

Bin edges (GeV/c)	0.00-0.15	0.15-0.30	0.30-0.45	0.45-0.60	0.60-0.75	0.75-0.90	0.90-1.25	1.25-2.50
0.00-0.15	0.1200	0.0004	-0.0045	-0.0005	-0.0000	0.0007	-0.0004	-0.0002
0.15-0.30	0.0004	0.0328	0.0022	-0.0032	-0.0007	-0.0007	-0.0003	-0.0006
0.30-0.45	-0.0045	0.0022	0.0396	0.0048	-0.0051	-0.0032	-0.0017	-0.0073
0.45-0.60	-0.0005	-0.0032	0.0048	0.0437	0.0083	-0.0064	-0.0115	0.0076
0.60-0.75	-0.0000	-0.0007	-0.0051	0.0083	0.0667	0.0340	-0.0028	-0.0370
0.75-0.90	0.0007	-0.0007	-0.0032	-0.0064	0.0340	0.1992	0.1252	-0.0123
0.90-1.25	-0.0004	-0.0003	-0.0017	-0.0115	-0.0028	0.1252	0.6101	-0.0227
1.25-2.50	-0.0002	-0.0006	-0.0073	0.0076	-0.0370	-0.0123	-0.0227	7.9959

TABLE Supp.CXXXVI. Systematic covariance matrix of measured cross section ratio of carbon over scintillator in $p_{\mu,T}$

Bin edges (GeV/c)	0.00-0.15	0.15-0.30	0.30-0.45	0.45-0.60	0.60-0.75	0.75-0.90	0.90-1.25	1.25-2.50
0.00-0.15	0.006	0.003	0.002	0.002	0.004	0.003	0.002	0.020
0.15-0.30	0.003	0.004	0.004	0.005	0.008	0.011	0.014	0.041
0.30-0.45	0.002	0.004	0.010	0.013	0.014	0.025	0.031	0.097
0.45-0.60	0.002	0.005	0.013	0.021	0.022	0.034	0.043	0.131
0.60-0.75	0.004	0.008	0.014	0.022	0.032	0.047	0.048	0.164
0.75-0.90	0.003	0.011	0.025	0.034	0.047	0.136	0.162	0.355
0.90-1.25	0.002	0.014	0.031	0.043	0.048	0.162	0.283	0.461
1.25-2.50	0.020	0.041	0.097	0.131	0.164	0.355	0.461	1.868

TABLE Supp.CXXXVII. Measured cross section ratio of carbon over scintillator in Q^2 , and the absolute and fractional cross section ratio uncertainties

Bin edges (GeV^2/c^2)	Ratio	Abs. Unc.	Frac. Stat. Unc.	Frac. Sys. Unc.	Frac. Flux Unc.
0.000-0.025	1.08	0.344	0.311	0.068	0.003
0.025-0.050	0.86	0.256	0.290	0.062	0.003
0.050-0.100	0.76	0.214	0.259	0.111	0.003
0.100-0.200	1.12	0.250	0.199	0.099	0.003
0.200-0.300	0.77	0.238	0.272	0.146	0.004
0.300-0.400	0.87	0.296	0.282	0.191	0.003
0.400-0.500	0.75	0.321	0.354	0.239	0.005
0.500-0.700	0.66	0.380	0.467	0.336	0.018
0.700-1.000	1.09	0.704	0.518	0.387	0.029
1.000-1.300	1.47	0.903	0.548	0.274	0.022
1.300-2.000	1.13	1.733	1.264	0.878	0.022
2.000-3.000	2.46	4.688	1.695	0.871	0.033

TABLE Supp.CXXXVIII. Statistical covariance matrix of measured cross section ratio of carbon over scintillator in Q^2

Bin edges (GeV^2/c^2)	0.000-0.025	0.025-0.050	0.050-0.100	0.100-0.200	0.200-0.300	0.300-0.400	0.400-0.500	0.500-0.700	0.700-1.000	1.000-1.300	1.300-2.000	2.000-3.000
0.000-0.025	0.1131	0.0081	-0.0065	-0.0025	-0.0000	-0.0000	-0.0001	-0.0001	0.0005	-0.0001	-0.0004	-0.0002
0.025-0.050	0.0081	0.0629	0.0155	-0.0052	-0.0020	-0.0004	-0.0002	-0.0003	-0.0007	-0.0003	-0.0006	0.0002
0.050-0.100	-0.0065	0.0155	0.0388	0.0083	-0.0038	-0.0018	-0.0007	-0.0002	0.0001	-0.0004	-0.0015	-0.0010
0.100-0.200	-0.0025	-0.0052	0.0083	0.0501	0.0080	-0.0051	-0.0045	-0.0009	-0.0012	-0.0020	-0.0013	-0.0044
0.200-0.300	-0.0000	-0.0020	-0.0038	0.0080	0.0440	0.0203	-0.0013	-0.0054	-0.0038	-0.0039	-0.0076	-0.0037
0.300-0.400	-0.0000	-0.0004	-0.0018	-0.0051	0.0203	0.0601	0.0381	0.0002	-0.0128	-0.0109	0.0098	-0.0019
0.400-0.500	-0.0001	-0.0002	-0.0007	-0.0045	-0.0013	0.0381	0.0709	0.0375	-0.0018	-0.0130	-0.0081	-0.0134
0.500-0.700	-0.0001	-0.0003	-0.0002	-0.0009	-0.0054	0.0002	0.0375	0.0953	0.0637	-0.0046	-0.0017	-0.0267
0.700-1.000	0.0005	-0.0007	0.0001	-0.0012	-0.0038	-0.0128	-0.0018	0.0637	0.3184	0.2083	0.0089	-0.0939
1.000-1.300	-0.0001	-0.0003	-0.0004	-0.0020	-0.0039	-0.0109	-0.0130	-0.0046	0.2083	0.6520	0.2704	-0.1106
1.300-2.000	-0.0004	-0.0006	-0.0015	-0.0013	-0.0076	0.0098	-0.0081	-0.0017	0.0089	0.2704	2.0261	1.2873
2.000-3.000	-0.0002	0.0002	-0.0010	-0.0044	-0.0037	-0.0019	-0.0134	-0.0267	-0.0939	-0.1106	1.2873	17.3908

TABLE Supp.CXXXIX. Systematic covariance matrix of measured cross section ratio of carbon over scintillator in Q^2

Bin edges (GeV^2/c^2)	0.000-0.025	0.025-0.050	0.050-0.100	0.100-0.200	0.200-0.300	0.300-0.400	0.400-0.500	0.500-0.700	0.700-1.000	1.000-1.300	1.300-2.000	2.000-3.000
0.000-0.025	0.005	0.001	0.003	0.002	0.002	0.002	0.004	0.002	-0.001	0.003	-0.000	0.023
0.025-0.050	0.001	0.003	0.002	0.003	0.001	0.001	0.003	0.005	0.005	0.007	0.006	0.034
0.050-0.100	0.003	0.002	0.007	0.007	0.007	0.009	0.011	0.013	0.017	0.019	0.030	0.070
0.100-0.200	0.002	0.003	0.007	0.012	0.011	0.013	0.015	0.020	0.024	0.028	0.054	0.124
0.200-0.300	0.002	0.001	0.007	0.011	0.013	0.016	0.017	0.019	0.025	0.029	0.057	0.105
0.300-0.400	0.002	0.001	0.009	0.013	0.016	0.028	0.026	0.027	0.034	0.035	0.087	0.137
0.400-0.500	0.004	0.003	0.011	0.015	0.017	0.026	0.032	0.031	0.035	0.036	0.083	0.144
0.500-0.700	0.002	0.005	0.013	0.020	0.019	0.027	0.031	0.049	0.072	0.066	0.129	0.244
0.700-1.000	-0.001	0.005	0.017	0.024	0.025	0.034	0.035	0.072	0.178	0.145	0.257	0.462
1.000-1.300	0.003	0.007	0.019	0.028	0.029	0.035	0.036	0.066	0.145	0.163	0.271	0.506
1.300-2.000	-0.000	0.006	0.030	0.054	0.057	0.087	0.083	0.129	0.257	0.271	0.979	0.596
2.000-3.000	0.023	0.034	0.070	0.124	0.105	0.137	0.144	0.244	0.462	0.506	0.596	4.588

TABLE Supp.CXL. Measured cross section ratio of carbon over scintillator in W_{exp} , and the absolute and fractional cross section ratio uncertainties

Bin edges (GeV/c ²)	Ratio	Abs. Unc.	Frac. Stat. Unc.	Frac. Sys. Unc.	Frac. Flux Unc.
0.9-1.1	1.66	1.128	0.636	0.237	0.019
1.1-1.2	1.05	0.202	0.177	0.075	0.002
1.2-1.3	0.84	0.220	0.201	0.167	0.006
1.3-1.4	0.58	0.454	0.531	0.571	0.009

TABLE Supp.CXLI. Statistical covariance matrix of measured cross section ratio of carbon over scintillator in W_{exp}

Bin edges (GeV/c ²)	0.9-1.1	1.1-1.2	1.2-1.3	1.3-1.4
0.9-1.1	1.1178	-0.0021	-0.0769	-0.0717
1.1-1.2	-0.0021	0.0348	0.0017	-0.0224
1.2-1.3	-0.0769	0.0017	0.0286	0.0188
1.3-1.4	-0.0717	-0.0224	0.0188	0.0955

TABLE Supp.CXLII. Systematic covariance matrix of measured cross section ratio of carbon over scintillator in W_{exp}

Bin edges (GeV/c ²)	0.9-1.1	1.1-1.2	1.2-1.3	1.3-1.4
0.9-1.1	0.155	0.004	0.005	0.002
1.1-1.2	0.004	0.006	0.002	0.004
1.2-1.3	0.005	0.002	0.020	0.044
1.3-1.4	0.002	0.004	0.044	0.110

TABLE Supp.CXLIII. Measured cross section ratio of carbon over scintillator in T_π , and the absolute and fractional cross section ratio uncertainties

Bin edges (GeV)	Ratio	Abs. Unc.	Frac. Stat. Unc.	Frac. Sys. Unc.	Frac. Flux Unc.
0.035-0.100	0.87	0.190	0.177	0.128	0.002
0.100-0.150	0.95	0.167	0.133	0.115	0.003
0.150-0.200	0.85	0.255	0.227	0.194	0.008
0.200-0.350	0.80	0.450	0.427	0.364	0.021

TABLE Supp.CXLIV. Statistical covariance matrix of measured cross section ratio of carbon over scintillator in T_π

Bin edges (GeV)	0.035-0.100	0.100-0.150	0.150-0.200	0.200-0.350
0.035-0.100	0.0236	0.0034	-0.0041	-0.0001
0.100-0.150	0.0034	0.0160	0.0090	0.0073
0.150-0.200	-0.0041	0.0090	0.0375	0.0362
0.200-0.350	-0.0001	0.0073	0.0362	0.1174

TABLE Supp.CXLV. Systematic covariance matrix of measured cross section ratio of carbon over scintillator in T_π

Bin edges (GeV)	0.035-0.100	0.100-0.150	0.150-0.200	0.200-0.350
0.035-0.100	0.012	0.011	0.015	0.024
0.100-0.150	0.011	0.012	0.017	0.023
0.150-0.200	0.015	0.017	0.027	0.039
0.200-0.350	0.024	0.023	0.039	0.085

TABLE Supp.CXLVI. Measured cross section ratio of carbon over scintillator in θ_π , and the absolute and fractional cross section ratio uncertainties

Bin edges (degree)	Ratio	Abs. Unc.	Frac. Stat. Unc.	Frac. Sys. Unc.	Frac. Flux Unc.
0-10	1.06	1.715	1.486	0.652	0.013
10-20	0.87	0.604	0.629	0.302	0.007
20-30	0.85	0.348	0.341	0.229	0.004
30-40	0.84	0.282	0.280	0.183	0.009
40-50	1.10	0.297	0.231	0.142	0.007
50-60	0.82	0.245	0.258	0.153	0.007
60-120	0.90	0.211	0.209	0.106	0.003
120-135	1.01	0.315	0.293	0.108	0.003
135-150	1.27	0.426	0.312	0.119	0.009
150-165	1.63	1.047	0.559	0.316	0.007
165-180	1.69	1.465	0.777	0.389	0.017

TABLE Supp.CXLVII. Statistical covariance matrix of measured cross section ratio of carbon over scintillator in θ_π

Bin edges (degree)	0-10	10-20	20-30	30-40	40-50	50-60	60-120	120-135	135-150	150-165	165-180
0-10	2.4667	0.3428	0.0833	-0.0202	0.0355	-0.0057	-0.0090	-0.0090	-0.0207	-0.0504	0.0468
10-20	0.3428	0.2965	0.0649	-0.0038	-0.0037	-0.0053	-0.0022	0.0001	-0.0020	0.0089	0.3371
20-30	0.0833	0.0649	0.0837	0.0156	-0.0059	-0.0034	-0.0025	-0.0050	-0.0053	0.0082	0.0700
30-40	-0.0202	-0.0038	0.0156	0.0558	0.0193	-0.0013	-0.0023	-0.0017	0.0011	-0.0037	-0.0167
40-50	0.0355	-0.0037	-0.0059	0.0193	0.0640	0.0146	-0.0012	-0.0035	-0.0046	-0.0178	-0.0252
50-60	-0.0057	-0.0053	-0.0034	-0.0013	0.0146	0.0445	0.0099	-0.0020	-0.0030	-0.0084	-0.0121
60-120	-0.0090	-0.0022	-0.0025	-0.0023	-0.0012	0.0099	0.0354	0.0075	-0.0009	-0.0033	-0.0018
120-135	-0.0090	0.0001	-0.0050	-0.0017	-0.0035	-0.0020	0.0075	0.0872	0.0207	0.0024	0.0100
135-150	-0.0207	-0.0020	-0.0053	0.0011	-0.0046	-0.0030	-0.0009	0.0207	0.1586	0.2220	0.0990
150-165	-0.0504	0.0089	0.0082	-0.0037	-0.0178	-0.0084	-0.0033	0.0024	0.2220	0.8311	0.0499
165-180	0.0468	0.3371	0.0700	-0.0167	-0.0252	-0.0121	-0.0018	0.0100	0.0990	0.0499	1.7155

TABLE Supp.CXLVIII. Systematic covariance matrix of measured cross section ratio of carbon over scintillator in θ_π

Bin edges (degree)	0-10	10-20	20-30	30-40	40-50	50-60	60-120	120-135	135-150	150-165	165-180
0-10	0.475	0.048	0.047	0.036	0.027	0.023	0.023	0.021	0.036	0.129	0.004
10-20	0.048	0.068	0.045	0.032	0.036	0.028	0.018	0.022	0.027	0.043	0.102
20-30	0.047	0.045	0.038	0.027	0.025	0.019	0.013	0.015	0.021	0.030	0.057
30-40	0.036	0.032	0.027	0.024	0.018	0.014	0.010	0.011	0.017	0.030	0.045
40-50	0.027	0.036	0.025	0.018	0.024	0.019	0.011	0.014	0.017	0.018	0.051
50-60	0.023	0.028	0.019	0.014	0.019	0.016	0.009	0.012	0.014	0.019	0.042
60-120	0.023	0.018	0.013	0.010	0.011	0.009	0.009	0.009	0.008	0.017	0.043
120-135	0.021	0.022	0.015	0.011	0.014	0.012	0.009	0.012	0.011	0.023	0.047
135-150	0.036	0.027	0.021	0.017	0.017	0.014	0.008	0.011	0.023	0.014	0.028
150-165	0.129	0.043	0.030	0.030	0.018	0.019	0.017	0.023	0.014	0.265	0.099
165-180	0.004	0.102	0.057	0.045	0.051	0.042	0.043	0.047	0.028	0.099	0.430

TABLE Supp.CXLIX. Measured cross section ratio of water over scintillator in p_μ , and the absolute and fractional cross section ratio uncertainties

Bin edges (GeV/c)	Ratio	Abs. Unc.	Frac. Stat. Unc.	Frac. Sys. Unc.	Frac. Flux Unc.
1.5-3.0	0.89	0.393	0.412	0.163	0.005
3.0-4.0	0.55	0.255	0.387	0.264	0.023
4.0-5.0	0.94	0.235	0.211	0.132	0.008
5.0-6.0	0.92	0.209	0.188	0.127	0.005
6.0-7.0	0.87	0.207	0.208	0.116	0.006
7.0-8.5	0.91	0.255	0.234	0.153	0.009
8.5-10.0	0.85	0.307	0.320	0.167	0.006
10.0-20.0	0.65	0.309	0.441	0.172	0.016

TABLE Supp.CL. Statistical covariance matrix of measured cross section ratio of water over scintillator in p_μ

Bin edges (GeV/c)	1.5-3.0	3.0-4.0	4.0-5.0	5.0-6.0	6.0-7.0	7.0-8.5	8.5-10.0	10.0-20.0
1.5-3.0	0.1333	0.0098	0.0011	0.0005	0.0005	0.0005	0.0012	0.0000
3.0-4.0	0.0098	0.0444	0.0126	0.0032	0.0005	0.0006	0.0002	0.0004
4.0-5.0	0.0011	0.0126	0.0397	0.0138	0.0037	0.0016	0.0012	0.0006
5.0-6.0	0.0005	0.0032	0.0138	0.0299	0.0154	0.0052	0.0020	0.0016
6.0-7.0	0.0005	0.0005	0.0037	0.0154	0.0326	0.0181	0.0040	0.0004
7.0-8.5	0.0005	0.0006	0.0016	0.0052	0.0181	0.0454	0.0225	0.0062
8.5-10.0	0.0012	0.0002	0.0012	0.0020	0.0040	0.0225	0.0739	0.0410
10.0-20.0	0.0000	0.0004	0.0006	0.0016	0.0004	0.0062	0.0410	0.0830

TABLE Supp.CLI. Systematic covariance matrix of measured cross section ratio of water over scintillator in p_μ

Bin edges (GeV/c)	1.5-3.0	3.0-4.0	4.0-5.0	5.0-6.0	6.0-7.0	7.0-8.5	8.5-10.0	10.0-20.0
1.5-3.0	0.021	0.009	0.009	0.007	0.010	0.015	0.014	0.005
3.0-4.0	0.009	0.021	0.013	0.013	0.009	0.010	0.009	0.006
4.0-5.0	0.009	0.013	0.016	0.012	0.010	0.011	0.009	0.007
5.0-6.0	0.007	0.013	0.012	0.014	0.009	0.008	0.008	0.007
6.0-7.0	0.010	0.009	0.010	0.009	0.010	0.011	0.010	0.007
7.0-8.5	0.015	0.010	0.011	0.008	0.011	0.020	0.016	0.008
8.5-10.0	0.014	0.009	0.009	0.008	0.010	0.016	0.020	0.006
10.0-20.0	0.005	0.006	0.007	0.007	0.007	0.008	0.006	0.013

TABLE Supp.CLII. Measured cross section ratio of water over scintillator in θ_μ , and the absolute and fractional cross section ratio uncertainties

Bin edges (degree)	Ratio	Abs. Unc.	Frac. Stat. Unc.	Frac. Sys. Unc.	Frac. Flux Unc.
0-2	0.69	0.193	0.261	0.108	0.009
2-3	0.96	0.274	0.272	0.086	0.007
3-4	0.90	0.263	0.269	0.116	0.005
4-5	0.74	0.304	0.383	0.150	0.004
5-6	0.52	0.309	0.537	0.258	0.014
6-8	1.03	0.441	0.367	0.221	0.008
8-10	1.78	0.686	0.343	0.178	0.007
10-13	0.13	0.512	3.400	1.891	0.150

TABLE Supp.CLIII. Statistical covariance matrix of measured cross section ratio of water over scintillator in θ_μ

Bin edges (degree)	0-2	2-3	3-4	4-5	5-6	6-8	8-10	10-13
0-2	0.0319	0.0026	-0.0040	-0.0007	-0.0000	-0.0002	-0.0000	0.0000
2-3	0.0026	0.0681	0.0080	-0.0081	-0.0013	-0.0003	-0.0003	0.0000
3-4	-0.0040	0.0080	0.0582	0.0122	-0.0055	-0.0018	0.0001	0.0000
4-5	-0.0007	-0.0081	0.0122	0.0803	0.0161	-0.0072	-0.0009	0.0000
5-6	-0.0000	-0.0013	-0.0055	0.0161	0.0776	0.0100	-0.0079	-0.0001
6-8	-0.0002	-0.0003	-0.0018	-0.0072	0.0100	0.1428	-0.0106	-0.0028
8-10	-0.0000	-0.0003	0.0001	-0.0009	-0.0079	-0.0106	0.3704	0.0322
10-13	0.0000	0.0000	0.0000	0.0000	-0.0001	-0.0028	0.0322	0.2003

TABLE Supp.CLIV. Systematic covariance matrix of measured cross section ratio of water over scintillator in θ_μ

Bin edges (degree)	0-2	2-3	3-4	4-5	5-6	6-8	8-10	10-13
0-2	0.005	0.004	0.004	0.001	0.000	0.000	0.001	-0.002
2-3	0.004	0.007	0.006	0.005	0.006	0.009	0.005	0.008
3-4	0.004	0.006	0.011	0.007	0.006	0.015	0.018	0.010
4-5	0.001	0.005	0.007	0.012	0.012	0.016	0.015	0.018
5-6	0.000	0.006	0.006	0.012	0.018	0.015	0.017	0.024
6-8	0.000	0.009	0.015	0.016	0.015	0.052	0.039	0.035
8-10	0.001	0.005	0.018	0.015	0.017	0.039	0.100	0.037
10-13	-0.002	0.008	0.010	0.018	0.024	0.035	0.037	0.062

TABLE Supp.CLV. Measured cross section ratio of water over scintillator in $p_{\mu,||}$, and the absolute and fractional cross section ratio uncertainties

Bin edges (GeV/c)	Ratio	Abs. Unc.	Frac. Stat. Unc.	Frac. Sys. Unc.	Frac. Flux Unc.
1.5-3.0	0.99	0.431	0.390	0.193	0.005
3.0-4.0	0.60	0.260	0.358	0.241	0.020
4.0-5.0	0.96	0.240	0.212	0.133	0.008
5.0-6.0	0.88	0.204	0.193	0.128	0.005
6.0-7.0	0.86	0.208	0.211	0.116	0.007
7.0-8.5	0.87	0.251	0.240	0.162	0.010
8.5-10.0	0.83	0.303	0.321	0.171	0.006
10.0-20.0	0.66	0.312	0.439	0.171	0.016

TABLE Supp.CLVI. Statistical covariance matrix of measured cross section ratio of water over scintillator in $p_{\mu,||}$

Bin edges (GeV/c)	1.5-3.0	3.0-4.0	4.0-5.0	5.0-6.0	6.0-7.0	7.0-8.5	8.5-10.0	10.0-20.0
1.5-3.0	0.1490	0.0105	0.0011	0.0005	0.0006	0.0004	0.0013	0.0000
3.0-4.0	0.0105	0.0463	0.0129	0.0029	0.0004	0.0006	0.0002	0.0004
4.0-5.0	0.0011	0.0129	0.0413	0.0136	0.0036	0.0016	0.0012	0.0006
5.0-6.0	0.0005	0.0029	0.0136	0.0291	0.0148	0.0050	0.0020	0.0016
6.0-7.0	0.0006	0.0004	0.0036	0.0148	0.0332	0.0178	0.0040	0.0004
7.0-8.5	0.0004	0.0006	0.0016	0.0050	0.0178	0.0434	0.0225	0.0061
8.5-10.0	0.0013	0.0002	0.0012	0.0020	0.0040	0.0225	0.0715	0.0414
10.0-20.0	0.0000	0.0004	0.0006	0.0016	0.0004	0.0061	0.0414	0.0843

TABLE Supp.CLVII. Systematic covariance matrix of measured cross section ratio of water over scintillator in $p_{\mu,||}$

Bin edges (GeV/c)	1.5-3.0	3.0-4.0	4.0-5.0	5.0-6.0	6.0-7.0	7.0-8.5	8.5-10.0	10.0-20.0
1.5-3.0	0.037	0.006	0.010	0.007	0.010	0.018	0.016	0.006
3.0-4.0	0.006	0.021	0.013	0.013	0.009	0.010	0.009	0.006
4.0-5.0	0.010	0.013	0.016	0.012	0.010	0.010	0.009	0.007
5.0-6.0	0.007	0.013	0.012	0.013	0.009	0.008	0.008	0.007
6.0-7.0	0.010	0.009	0.010	0.009	0.010	0.011	0.009	0.007
7.0-8.5	0.018	0.010	0.010	0.008	0.011	0.020	0.016	0.008
8.5-10.0	0.016	0.009	0.009	0.008	0.009	0.016	0.020	0.006
10.0-20.0	0.006	0.006	0.007	0.007	0.007	0.008	0.006	0.013

TABLE Supp.CLVIII. Measured cross section ratio of water over scintillator in $p_{\mu,T}$, and the absolute and fractional cross section ratio uncertainties

Bin edges (GeV/c)	Ratio	Abs. Unc.	Frac. Stat. Unc.	Frac. Sys. Unc.	Frac. Flux Unc.
0.00-0.15	0.66	0.239	0.352	0.096	0.011
0.15-0.30	0.71	0.196	0.253	0.110	0.005
0.30-0.45	1.08	0.256	0.213	0.103	0.005
0.45-0.60	0.88	0.294	0.289	0.172	0.004
0.60-0.75	0.28	0.276	0.740	0.641	0.016
0.75-0.90	1.40	0.670	0.421	0.228	0.010
0.90-1.25	1.88	1.082	0.545	0.187	0.014
1.25-2.50	2.94	4.698	0.959	1.279	0.055

TABLE Supp.CLIX. Statistical covariance matrix of measured cross section ratio of water over scintillator in $p_{\mu,T}$

Bin edges (GeV/c)	0.00-0.15	0.15-0.30	0.30-0.45	0.45-0.60	0.60-0.75	0.75-0.90	0.90-1.25	1.25-2.50
0.00-0.15	0.0533	0.0002	-0.0033	-0.0005	-0.0001	-0.0001	-0.0000	0.0001
0.15-0.30	0.0002	0.0321	0.0019	-0.0039	-0.0011	-0.0006	-0.0026	-0.0007
0.30-0.45	-0.0033	0.0019	0.0531	0.0075	-0.0023	-0.0068	-0.0021	-0.0149
0.45-0.60	-0.0005	-0.0039	0.0075	0.0640	0.0179	-0.0075	-0.0038	0.0104
0.60-0.75	-0.0001	-0.0011	-0.0023	0.0179	0.0436	0.0540	0.0031	-0.0223
0.75-0.90	-0.0001	-0.0006	-0.0068	-0.0075	0.0540	0.3466	0.0398	-0.0432
0.90-1.25	-0.0000	-0.0026	-0.0021	-0.0038	0.0031	0.0398	1.0485	0.0088
1.25-2.50	0.0001	-0.0007	-0.0149	0.0104	-0.0223	-0.0432	0.0088	7.9464

TABLE Supp.CLX. Systematic covariance matrix of measured cross section ratio of water over scintillator in $p_{\mu,T}$

Bin edges (GeV/c)	0.00-0.15	0.15-0.30	0.30-0.45	0.45-0.60	0.60-0.75	0.75-0.90	0.90-1.25	1.25-2.50
0.00-0.15	0.004	0.004	0.001	0.000	-0.001	-0.001	0.000	-0.015
0.15-0.30	0.004	0.006	0.004	0.004	0.004	0.008	0.008	0.006
0.30-0.45	0.001	0.004	0.012	0.011	0.009	0.019	0.021	0.059
0.45-0.60	0.000	0.004	0.011	0.023	0.020	0.029	0.008	0.206
0.60-0.75	-0.001	0.004	0.009	0.020	0.033	0.043	0.014	0.205
0.75-0.90	-0.001	0.008	0.019	0.029	0.043	0.102	0.050	0.192
0.90-1.25	0.000	0.008	0.021	0.008	0.014	0.050	0.123	-0.226
1.25-2.50	-0.015	0.006	0.059	0.206	0.205	0.192	-0.226	14.125

TABLE Supp.CLXI. Measured cross section ratio of water over scintillator in Q^2 , and the absolute and fractional cross section ratio uncertainties

Bin edges (GeV^2/c^2)	Ratio	Abs. Unc.	Frac. Stat. Unc.	Frac. Sys. Unc.	Frac. Flux Unc.
0.000-0.025	0.65	0.232	0.348	0.091	0.010
0.025-0.050	0.61	0.225	0.331	0.163	0.005
0.050-0.100	0.79	0.225	0.269	0.093	0.008
0.100-0.200	1.12	0.285	0.225	0.117	0.005
0.200-0.300	1.03	0.295	0.254	0.133	0.003
0.300-1.300	0.60	0.291	0.376	0.309	0.007
1.300-2.000	6.21	4.215	0.628	0.257	0.028
2.000-3.000	2.11	3.800	0.967	1.520	0.077

TABLE Supp. CLXII. Statistical covariance matrix of measured cross section ratio of water over scintillator in Q^2

Bin edges (GeV^2/c^2)	0.000-0.025	0.025-0.050	0.050-0.100	0.100-0.200	0.200-0.300	0.300-1.300	1.300-2.000	2.000-3.000
0.000-0.025	0.0505	0.0079	-0.0051	-0.0020	-0.0002	-0.0001	-0.0000	-0.0000
0.025-0.050	0.0079	0.0409	0.0165	-0.0050	-0.0029	-0.0002	-0.0012	-0.0000
0.050-0.100	-0.0051	0.0165	0.0452	0.0068	-0.0055	-0.0014	-0.0070	-0.0007
0.100-0.200	-0.0020	-0.0050	0.0068	0.0641	0.0219	-0.0057	-0.0184	-0.0060
0.200-0.300	-0.0002	-0.0029	-0.0055	0.0219	0.0683	0.0069	-0.0417	0.0018
0.300-1.300	-0.0001	-0.0002	-0.0014	-0.0057	0.0069	0.0505	0.0168	-0.0113
1.300-2.000	-0.0000	-0.0012	-0.0070	-0.0184	-0.0417	0.0168	15.2090	0.0360
2.000-3.000	-0.0000	-0.0000	-0.0007	-0.0060	0.0018	-0.0113	0.0360	4.1625

TABLE Supp. CLXIII. Systematic covariance matrix of measured cross section ratio of water over scintillator in Q^2

Bin edges (GeV^2/c^2)	0.000-0.025	0.025-0.050	0.050-0.100	0.100-0.200	0.200-0.300	0.300-1.300	1.300-2.000	2.000-3.000
0.000-0.025	0.003	0.005	0.003	0.002	0.001	-0.001	0.009	-0.009
0.025-0.050	0.005	0.010	0.005	0.007	0.004	0.003	0.017	-0.002
0.050-0.100	0.003	0.005	0.005	0.004	0.004	0.007	0.016	0.014
0.100-0.200	0.002	0.007	0.004	0.017	0.012	0.011	0.031	0.059
0.200-0.300	0.001	0.004	0.004	0.012	0.019	0.016	0.019	0.082
0.300-1.300	-0.001	0.003	0.007	0.011	0.016	0.034	0.075	0.147
1.300-2.000	0.009	0.017	0.016	0.031	0.019	0.075	2.555	0.282
2.000-3.000	-0.009	-0.002	0.014	0.059	0.082	0.147	0.282	10.275

TABLE Supp.CLXIV. Measured cross section ratio of water over scintillator in W_{exp} , and the absolute and fractional cross section ratio uncertainties

Bin edges (GeV/c ²)	Ratio	Abs. Unc.	Frac. Stat. Unc.	Frac. Sys. Unc.	Frac. Flux Unc.
0.9-1.1	2.88	2.560	0.852	0.250	0.023
1.1-1.2	1.54	0.367	0.208	0.115	0.007
1.2-1.3	0.51	0.239	0.369	0.296	0.008
1.3-1.4	0.20	0.184	0.666	0.613	0.015

TABLE Supp.CLXV. Statistical covariance matrix of measured cross section ratio of water over scintillator in W_{exp}

Bin edges (GeV/c ²)	0.9-1.1	1.1-1.2	1.2-1.3	1.3-1.4
0.9-1.1	6.0348	-0.2345	-0.0974	-0.0478
1.1-1.2	-0.2345	0.1030	-0.0183	-0.0113
1.2-1.3	-0.0974	-0.0183	0.0347	0.0201
1.3-1.4	-0.0478	-0.0113	0.0201	0.0183

TABLE Supp.CLXVI. Systematic covariance matrix of measured cross section ratio of water over scintillator in W_{exp}

Bin edges (GeV/c ²)	0.9-1.1	1.1-1.2	1.2-1.3	1.3-1.4
0.9-1.1	0.521	0.012	0.008	0.002
1.1-1.2	0.012	0.032	0.000	-0.001
1.2-1.3	0.008	0.000	0.022	0.018
1.3-1.4	0.002	-0.001	0.018	0.015

TABLE Supp.CLXVII. Measured cross section ratio of water over scintillator in T_π , and the absolute and fractional cross section ratio uncertainties

Bin edges (GeV)	Ratio	Abs. Unc.	Frac. Stat. Unc.	Frac. Sys. Unc.	Frac. Flux Unc.
0.035-0.100	1.14	0.282	0.227	0.096	0.007
0.100-0.150	0.84	0.189	0.195	0.113	0.002
0.150-0.200	0.91	0.278	0.265	0.154	0.003
0.200-0.350	0.85	0.365	0.350	0.250	0.010

TABLE Supp.CLXVIII. Statistical covariance matrix of measured cross section ratio of water over scintillator in T_π

Bin edges (GeV)	0.035-0.100	0.100-0.150	0.150-0.200	0.200-0.350
0.035-0.100	0.0676	0.0068	-0.0075	-0.0044
0.100-0.150	0.0068	0.0268	0.0048	-0.0031
0.150-0.200	-0.0075	0.0048	0.0576	0.0103
0.200-0.350	-0.0044	-0.0031	0.0103	0.0880

TABLE Supp.CLXIX. Systematic covariance matrix of measured cross section ratio of water over scintillator in T_π

Bin edges (GeV)	0.035-0.100	0.100-0.150	0.150-0.200	0.200-0.350
0.035-0.100	0.012	0.007	0.007	0.011
0.100-0.150	0.007	0.009	0.009	0.014
0.150-0.200	0.007	0.009	0.020	0.023
0.200-0.350	0.011	0.014	0.023	0.045

TABLE Supp.CLXX. Measured cross section ratio of water over scintillator in θ_π , and the absolute and fractional cross section ratio uncertainties

Bin edges (degree)	Ratio	Abs. Unc.	Frac. Stat. Unc.	Frac. Sys. Unc.	Frac. Flux Unc.
0-10	1.01	0.940	0.901	0.251	0.010
10-20	0.59	0.312	0.482	0.211	0.013
20-30	0.73	0.255	0.308	0.170	0.007
30-40	0.68	0.266	0.325	0.219	0.005
40-50	0.87	0.254	0.260	0.131	0.008
50-60	1.34	0.345	0.243	0.085	0.006
60-120	1.08	0.318	0.279	0.090	0.003
120-135	1.11	0.585	0.503	0.165	0.007
135-150	1.30	0.582	0.429	0.132	0.009
150-165	0.94	0.860	0.853	0.336	0.008
165-180	0.50	0.752	1.423	0.487	0.014

TABLE Supp.CLXXI. Statistical covariance matrix of measured cross section ratio of water over scintillator in θ_π

Bin edges (degree)	0-10	10-20	20-30	30-40	40-50	50-60	60-120	120-135	135-150	150-165	165-180
0-10	0.8207	0.0635	-0.0173	0.0020	-0.0045	-0.0046	-0.0045	-0.0042	-0.0049	-0.0030	0.0294
10-20	0.0635	0.0816	0.0165	-0.0030	-0.0030	0.0012	-0.0052	-0.0040	0.0028	-0.0020	0.1282
20-30	-0.0173	0.0165	0.0498	0.0082	-0.0017	-0.0052	-0.0011	-0.0008	-0.0035	-0.0044	-0.0028
30-40	0.0020	-0.0030	0.0082	0.0487	0.0103	-0.0038	0.0029	-0.0065	-0.0036	-0.0024	-0.0074
40-50	-0.0045	-0.0030	-0.0017	0.0103	0.0514	0.0145	0.0001	-0.0021	0.0033	-0.0130	-0.0017
50-60	-0.0046	0.0012	-0.0052	-0.0038	0.0145	0.1063	0.0286	-0.0060	-0.0166	-0.0156	0.0068
60-120	-0.0045	-0.0052	-0.0011	0.0029	0.0001	0.0286	0.0914	0.0155	0.0009	0.0090	-0.0075
120-135	-0.0042	-0.0040	-0.0008	-0.0065	-0.0021	-0.0060	0.0155	0.3089	0.0888	0.0063	-0.0054
135-150	-0.0049	0.0028	-0.0035	-0.0036	0.0033	-0.0166	0.0009	0.0888	0.3099	0.2742	0.0028
150-165	-0.0030	-0.0020	-0.0044	-0.0024	-0.0130	-0.0156	0.0090	0.0063	0.2742	0.6408	-0.0054
165-180	0.0294	0.1282	-0.0028	-0.0074	-0.0017	0.0068	-0.0075	-0.0054	0.0028	-0.0054	0.5064

TABLE Supp.CLXXII. Systematic covariance matrix of measured cross section ratio of water over scintillator in θ_π

Bin edges (degree)	0-10	10-20	20-30	30-40	40-50	50-60	60-120	120-135	135-150	150-165	165-180
0-10	0.064	0.006	0.011	0.021	0.013	0.009	0.006	0.021	0.005	-0.007	0.017
10-20	0.006	0.016	0.012	0.008	0.007	0.004	0.006	0.009	0.006	0.012	0.014
20-30	0.011	0.012	0.015	0.013	0.010	0.007	0.006	0.010	0.008	0.014	0.010
30-40	0.021	0.008	0.013	0.022	0.014	0.009	0.008	0.007	0.013	0.009	0.006
40-50	0.013	0.007	0.010	0.014	0.013	0.009	0.008	0.009	0.012	0.013	0.005
50-60	0.009	0.004	0.007	0.009	0.009	0.013	0.007	0.010	0.009	0.014	-0.000
60-120	0.006	0.006	0.006	0.008	0.008	0.007	0.009	0.006	0.009	0.003	0.000
120-135	0.021	0.009	0.010	0.007	0.009	0.010	0.006	0.033	0.003	0.016	0.016
135-150	0.005	0.006	0.008	0.013	0.012	0.009	0.009	0.003	0.029	0.032	-0.013
150-165	-0.007	0.012	0.014	0.009	0.013	0.014	0.003	0.016	0.032	0.100	-0.008
165-180	0.017	0.014	0.010	0.006	0.005	-0.000	0.000	0.016	-0.013	-0.008	0.059

TABLE Supp.CLXXIII. Measured cross section ratio of iron over scintillator in p_μ , and the absolute and fractional cross section ratio uncertainties

Bin edges (GeV/c)	Ratio	Abs. Unc.	Frac. Stat. Unc.	Frac. Sys. Unc.	Frac. Flux Unc.
1.5-3.0	0.86	0.163	0.157	0.105	0.004
3.0-4.0	0.78	0.125	0.110	0.116	0.007
4.0-5.0	0.62	0.102	0.099	0.132	0.009
5.0-6.0	0.62	0.098	0.090	0.130	0.006
6.0-7.0	0.60	0.100	0.095	0.136	0.005
7.0-8.5	0.59	0.114	0.120	0.152	0.015
8.5-10.0	0.66	0.139	0.147	0.150	0.012
10.0-20.0	0.94	0.218	0.174	0.154	0.005

TABLE Supp.CLXXIV. Statistical covariance matrix of measured cross section ratio of iron over scintillator in p_μ

Bin edges (GeV/c)	1.5-3.0	3.0-4.0	4.0-5.0	5.0-6.0	6.0-7.0	7.0-8.5	8.5-10.0	10.0-20.0
1.5-3.0	0.0184	0.0023	0.0003	0.0002	0.0001	0.0000	0.0002	0.0002
3.0-4.0	0.0023	0.0074	0.0013	0.0003	0.0001	0.0001	0.0001	0.0002
4.0-5.0	0.0003	0.0013	0.0038	0.0013	0.0004	0.0001	0.0001	0.0001
5.0-6.0	0.0002	0.0003	0.0013	0.0031	0.0014	0.0004	0.0002	0.0002
6.0-7.0	0.0001	0.0001	0.0004	0.0014	0.0033	0.0018	0.0007	0.0004
7.0-8.5	0.0000	0.0001	0.0001	0.0004	0.0018	0.0050	0.0035	0.0014
8.5-10.0	0.0002	0.0001	0.0001	0.0002	0.0007	0.0035	0.0095	0.0060
10.0-20.0	0.0002	0.0002	0.0001	0.0002	0.0004	0.0014	0.0060	0.0266

TABLE Supp.CLXXV. Systematic covariance matrix of measured cross section ratio of iron over scintillator in p_μ

Bin edges (GeV/c)	1.5-3.0	3.0-4.0	4.0-5.0	5.0-6.0	6.0-7.0	7.0-8.5	8.5-10.0	10.0-20.0
1.5-3.0	0.008	0.006	0.005	0.005	0.005	0.004	0.005	0.008
3.0-4.0	0.006	0.008	0.007	0.007	0.007	0.007	0.008	0.011
4.0-5.0	0.005	0.007	0.007	0.006	0.006	0.006	0.007	0.009
5.0-6.0	0.005	0.007	0.006	0.007	0.006	0.007	0.007	0.010
6.0-7.0	0.005	0.007	0.006	0.006	0.007	0.007	0.007	0.010
7.0-8.5	0.004	0.007	0.006	0.007	0.007	0.008	0.008	0.011
8.5-10.0	0.005	0.008	0.007	0.007	0.007	0.008	0.010	0.012
10.0-20.0	0.008	0.011	0.009	0.010	0.010	0.011	0.012	0.021

TABLE Supp.CLXXVI. Measured cross section ratio of iron over scintillator in θ_μ , and the absolute and fractional cross section ratio uncertainties

Bin edges (degree)	Ratio	Abs. Unc.	Frac. Stat. Unc.	Frac. Sys. Unc.	Frac. Flux Unc.
0-2	0.62	0.093	0.130	0.076	0.002
2-3	0.59	0.090	0.132	0.078	0.002
3-4	0.62	0.102	0.133	0.096	0.001
4-5	0.53	0.113	0.161	0.138	0.004
5-6	0.48	0.143	0.207	0.212	0.003
6-8	0.71	0.159	0.143	0.173	0.002
8-10	0.94	0.241	0.182	0.181	0.003
10-13	0.89	0.321	0.275	0.234	0.006

TABLE Supp.CLXXVII. Statistical covariance matrix of measured cross section ratio of iron over scintillator in θ_μ

Bin edges (degree)	0-2	2-3	3-4	4-5	5-6	6-8	8-10	10-13
0-2	0.0065	0.0001	-0.0005	-0.0001	0.0000	0.0000	-0.0000	-0.0001
2-3	0.0001	0.0060	0.0008	-0.0006	-0.0002	-0.0000	-0.0000	-0.0000
3-4	-0.0005	0.0008	0.0069	0.0010	-0.0007	-0.0001	-0.0000	-0.0001
4-5	-0.0001	-0.0006	0.0010	0.0074	0.0016	-0.0005	-0.0001	0.0000
5-6	0.0000	-0.0002	-0.0007	0.0016	0.0100	0.0006	-0.0007	-0.0001
6-8	0.0000	-0.0000	-0.0001	-0.0005	0.0006	0.0104	-0.0002	-0.0009
8-10	-0.0000	-0.0000	-0.0000	-0.0001	-0.0007	-0.0002	0.0291	-0.0009
10-13	-0.0001	-0.0000	-0.0001	0.0000	-0.0001	-0.0009	-0.0009	0.0599

TABLE Supp.CLXXVIII. Systematic covariance matrix of measured cross section ratio of iron over scintillator in θ_μ

Bin edges (degree)	0-2	2-3	3-4	4-5	5-6	6-8	8-10	10-13
0-2	0.002	0.001	0.001	0.001	0.002	0.002	0.003	0.004
2-3	0.001	0.002	0.002	0.003	0.004	0.004	0.006	0.007
3-4	0.001	0.002	0.004	0.004	0.005	0.006	0.009	0.011
4-5	0.001	0.003	0.004	0.005	0.007	0.008	0.011	0.013
5-6	0.002	0.004	0.005	0.007	0.010	0.011	0.016	0.018
6-8	0.002	0.004	0.006	0.008	0.011	0.015	0.019	0.023
8-10	0.003	0.006	0.009	0.011	0.016	0.019	0.029	0.032
10-13	0.004	0.007	0.011	0.013	0.018	0.023	0.032	0.043

TABLE Supp.CLXXIX. Measured cross section ratio of iron over scintillator in $p_{\mu,||}$, and the absolute and fractional cross section ratio uncertainties

Bin edges (GeV/c)	Ratio	Abs. Unc.	Frac. Stat. Unc.	Frac. Sys. Unc.	Frac. Flux Unc.
1.5-3.0	0.82	0.164	0.164	0.114	0.005
3.0-4.0	0.81	0.126	0.107	0.113	0.006
4.0-5.0	0.61	0.102	0.100	0.133	0.009
5.0-6.0	0.61	0.098	0.091	0.132	0.006
6.0-7.0	0.61	0.101	0.095	0.137	0.005
7.0-8.5	0.60	0.115	0.120	0.152	0.015
8.5-10.0	0.65	0.134	0.150	0.144	0.013
10.0-20.0	0.95	0.219	0.174	0.150	0.004

TABLE Supp.CLXXX. Statistical covariance matrix of measured cross section ratio of iron over scintillator in $p_{\mu,||}$

Bin edges (GeV/c)	1.5-3.0	3.0-4.0	4.0-5.0	5.0-6.0	6.0-7.0	7.0-8.5	8.5-10.0	10.0-20.0
1.5-3.0	0.0181	0.0021	0.0003	0.0002	0.0001	0.0000	0.0002	0.0002
3.0-4.0	0.0021	0.0075	0.0013	0.0003	0.0001	0.0001	0.0001	0.0002
4.0-5.0	0.0003	0.0013	0.0037	0.0013	0.0004	0.0001	0.0001	0.0001
5.0-6.0	0.0002	0.0003	0.0013	0.0031	0.0014	0.0004	0.0002	0.0002
6.0-7.0	0.0001	0.0001	0.0004	0.0014	0.0033	0.0018	0.0007	0.0004
7.0-8.5	0.0000	0.0001	0.0001	0.0004	0.0018	0.0051	0.0034	0.0013
8.5-10.0	0.0002	0.0001	0.0001	0.0002	0.0007	0.0034	0.0093	0.0060
10.0-20.0	0.0002	0.0002	0.0001	0.0002	0.0004	0.0013	0.0060	0.0275

TABLE Supp.CLXXXI. Systematic covariance matrix of measured cross section ratio of iron over scintillator in $p_{\mu,||}$

Bin edges (GeV/c)	1.5-3.0	3.0-4.0	4.0-5.0	5.0-6.0	6.0-7.0	7.0-8.5	8.5-10.0	10.0-20.0
1.5-3.0	0.009	0.006	0.006	0.005	0.005	0.005	0.006	0.009
3.0-4.0	0.006	0.008	0.007	0.007	0.007	0.008	0.008	0.012
4.0-5.0	0.006	0.007	0.007	0.006	0.006	0.006	0.006	0.009
5.0-6.0	0.005	0.007	0.006	0.006	0.006	0.007	0.007	0.009
6.0-7.0	0.005	0.007	0.006	0.006	0.007	0.007	0.007	0.010
7.0-8.5	0.005	0.008	0.006	0.007	0.007	0.008	0.008	0.011
8.5-10.0	0.006	0.008	0.006	0.007	0.007	0.008	0.009	0.011
10.0-20.0	0.009	0.012	0.009	0.009	0.010	0.011	0.011	0.021

TABLE Supp.CLXXXII. Measured cross section ratio of iron over scintillator in $p_{\mu,T}$, and the absolute and fractional cross section ratio uncertainties

Bin edges (GeV/c)	Ratio	Abs. Unc.	Frac. Stat. Unc.	Frac. Sys. Unc.	Frac. Flux Unc.
0.00-0.15	0.58	0.115	0.179	0.084	0.003
0.15-0.30	0.59	0.078	0.110	0.074	0.001
0.30-0.45	0.59	0.089	0.111	0.100	0.001
0.45-0.60	0.70	0.121	0.111	0.132	0.001
0.60-0.75	0.62	0.168	0.161	0.217	0.003
0.75-0.90	0.70	0.263	0.215	0.306	0.008
0.90-1.25	1.01	0.395	0.293	0.260	0.008
1.25-2.50	1.50	1.483	0.912	0.390	0.014

TABLE Supp.CLXXXIII. Statistical covariance matrix of measured cross section ratio of iron over scintillator in $p_{\mu,T}$

Bin edges (GeV/c)	0.00-0.15	0.15-0.30	0.30-0.45	0.45-0.60	0.60-0.75	0.75-0.90	0.90-1.25	1.25-2.50
0.00-0.15	0.0109	0.0001	-0.0005	-0.0001	-0.0000	-0.0000	-0.0000	-0.0000
0.15-0.30	0.0001	0.0042	0.0003	-0.0004	-0.0001	-0.0000	-0.0001	-0.0004
0.30-0.45	-0.0005	0.0003	0.0043	0.0005	-0.0004	-0.0003	-0.0003	-0.0001
0.45-0.60	-0.0001	-0.0004	0.0005	0.0061	0.0012	-0.0009	-0.0010	-0.0005
0.60-0.75	-0.0000	-0.0001	-0.0004	0.0012	0.0100	0.0037	-0.0022	-0.0006
0.75-0.90	-0.0000	-0.0000	-0.0003	-0.0009	0.0037	0.0229	0.0145	-0.0136
0.90-1.25	-0.0000	-0.0001	-0.0003	-0.0010	-0.0022	0.0145	0.0872	0.0567
1.25-2.50	-0.0000	-0.0004	-0.0001	-0.0005	-0.0006	-0.0136	0.0567	1.8586

TABLE Supp.CLXXXIV. Systematic covariance matrix of measured cross section ratio of iron over scintillator in $p_{\mu,T}$

Bin edges (GeV/c)	0.00-0.15	0.15-0.30	0.30-0.45	0.45-0.60	0.60-0.75	0.75-0.90	0.90-1.25	1.25-2.50
0.00-0.15	0.002	0.001	0.000	0.000	0.001	-0.000	0.002	0.001
0.15-0.30	0.001	0.002	0.002	0.003	0.004	0.006	0.008	0.011
0.30-0.45	0.000	0.002	0.004	0.005	0.007	0.011	0.013	0.018
0.45-0.60	0.000	0.003	0.005	0.009	0.011	0.019	0.021	0.032
0.60-0.75	0.001	0.004	0.007	0.011	0.018	0.027	0.032	0.043
0.75-0.90	-0.000	0.006	0.011	0.019	0.027	0.046	0.051	0.078
0.90-1.25	0.002	0.008	0.013	0.021	0.032	0.051	0.069	0.100
1.25-2.50	0.001	0.011	0.018	0.032	0.043	0.078	0.100	0.340

TABLE Supp.CLXXXV. Measured cross section ratio of iron over scintillator in Q^2 , and the absolute and fractional cross section ratio uncertainties

Bin edges (GeV^2/c^2)	Ratio	Abs. Unc.	Frac. Stat. Unc.	Frac. Sys. Unc.	Frac. Flux Unc.
0.000-0.025	0.56	0.108	0.172	0.084	0.003
0.025-0.050	0.54	0.088	0.147	0.071	0.003
0.050-0.100	0.57	0.086	0.127	0.082	0.002
0.100-0.200	0.62	0.090	0.109	0.096	0.001
0.200-0.300	0.72	0.115	0.124	0.099	0.002
0.300-0.400	0.67	0.138	0.141	0.149	0.002
0.400-0.500	0.58	0.159	0.174	0.211	0.002
0.500-0.700	0.62	0.211	0.203	0.275	0.005
0.700-1.000	0.81	0.298	0.230	0.286	0.007
1.000-1.300	1.05	0.438	0.339	0.244	0.006
1.300-2.000	0.82	0.721	0.704	0.524	0.033
2.000-3.000	0.80	0.898	1.010	0.489	0.021

TABLE Supp.CLXXXVI. Statistical covariance matrix of measured cross section ratio of iron over scintillator in Q^2

Bin edges (GeV ² /c ²)	0.000-0.025	0.025-0.050	0.050-0.100	0.100-0.200	0.200-0.300	0.300-0.400	0.400-0.500	0.500-0.700	0.700-1.000	1.000-1.300	1.300-2.000	2.000-3.000
0.000-0.025	0.0094	0.0017	-0.0007	-0.0003	-0.0000	-0.0000	-0.0000	-0.0000	-0.0000	-0.0000	-0.0000	0.0000
0.025-0.050	0.0017	0.0063	0.0018	-0.0004	-0.0003	-0.0000	-0.0000	-0.0000	-0.0000	-0.0000	-0.0001	-0.0001
0.050-0.100	-0.0007	0.0018	0.0053	0.0009	-0.0006	-0.0003	-0.0001	-0.0000	-0.0000	-0.0000	-0.0002	-0.0003
0.100-0.200	-0.0003	-0.0004	0.0009	0.0046	0.0011	-0.0004	-0.0005	-0.0002	-0.0002	-0.0004	0.0001	0.0003
0.200-0.300	-0.0000	-0.0003	-0.0006	0.0011	0.0081	0.0026	0.0000	-0.0007	-0.0006	-0.0007	-0.0011	-0.0020
0.300-0.400	-0.0000	-0.0000	-0.0003	-0.0004	0.0026	0.0090	0.0041	-0.0004	-0.0011	-0.0008	-0.0003	0.0026
0.400-0.500	-0.0000	-0.0000	-0.0001	-0.0005	0.0000	0.0041	0.0102	0.0049	-0.0008	-0.0031	-0.0009	0.0014
0.500-0.700	-0.0000	-0.0000	-0.0000	-0.0002	-0.0007	-0.0004	0.0049	0.0157	0.0068	-0.0015	-0.0015	-0.0020
0.700-1.000	-0.0000	-0.0000	-0.0000	-0.0002	-0.0006	-0.0011	-0.0008	0.0068	0.0348	0.0295	0.0017	-0.0016
1.000-1.300	-0.0000	-0.0000	-0.0000	-0.0004	-0.0007	-0.0008	-0.0031	-0.0015	0.0295	0.1264	0.0751	-0.0011
1.300-2.000	-0.0000	-0.0001	-0.0002	0.0001	-0.0011	-0.0003	-0.0009	-0.0015	0.0017	0.0751	0.3339	0.1520
2.000-3.000	0.0000	-0.0001	-0.0003	0.0003	-0.0020	0.0026	0.0014	-0.0020	-0.0016	-0.0011	0.1520	0.6530

TABLE Supp.CLXXXVII. Systematic covariance matrix of measured cross section ratio of iron over scintillator in Q^2

Bin edges (GeV^2/c^2)	0.000-0.025	0.025-0.050	0.050-0.100	0.100-0.200	0.200-0.300	0.300-0.400	0.400-0.500	0.500-0.700	0.700-1.000	1.000-1.300	1.300-2.000	2.000-3.000
0.000-0.025	0.002	0.001	0.001	0.000	0.000	-0.000	0.000	0.000	-0.000	0.002	0.002	-0.002
0.025-0.050	0.001	0.001	0.001	0.001	0.001	0.002	0.002	0.003	0.004	0.005	0.007	0.004
0.050-0.100	0.001	0.001	0.002	0.002	0.003	0.004	0.004	0.006	0.008	0.009	0.012	0.010
0.100-0.200	0.000	0.001	0.002	0.004	0.004	0.005	0.006	0.009	0.012	0.014	0.019	0.015
0.200-0.300	0.000	0.001	0.003	0.004	0.005	0.007	0.008	0.011	0.015	0.015	0.021	0.020
0.300-0.400	-0.000	0.002	0.004	0.005	0.007	0.010	0.011	0.015	0.020	0.021	0.028	0.030
0.400-0.500	0.000	0.002	0.004	0.006	0.008	0.011	0.015	0.019	0.026	0.027	0.042	0.037
0.500-0.700	0.000	0.003	0.006	0.009	0.011	0.015	0.019	0.029	0.037	0.038	0.060	0.049
0.700-1.000	-0.000	0.004	0.008	0.012	0.015	0.020	0.026	0.037	0.054	0.051	0.077	0.069
1.000-1.300	0.002	0.005	0.009	0.014	0.015	0.021	0.027	0.038	0.051	0.066	0.091	0.066
1.300-2.000	0.002	0.007	0.012	0.019	0.021	0.028	0.042	0.060	0.077	0.091	0.185	0.122
2.000-3.000	-0.002	0.004	0.010	0.015	0.020	0.030	0.037	0.049	0.069	0.066	0.122	0.153

TABLE Supp.CLXXXVIII. Measured cross section ratio of iron over scintillator in W_{exp} , and the absolute and fractional cross section ratio uncertainties

Bin edges (GeV/c ²)	Ratio	Abs. Unc.	Frac. Stat. Unc.	Frac. Sys. Unc.	Frac. Flux Unc.
0.9-1.1	0.56	0.291	0.488	0.170	0.013
1.1-1.2	0.70	0.113	0.136	0.086	0.002
1.2-1.3	0.65	0.123	0.098	0.162	0.002
1.3-1.4	0.60	0.220	0.182	0.319	0.003

TABLE Supp.CLXXXIX. Statistical covariance matrix of measured cross section ratio of iron over scintillator in W_{exp}

Bin edges (GeV/c ²)	0.9-1.1	1.1-1.2	1.2-1.3	1.3-1.4
0.9-1.1	0.0757	0.0031	-0.0058	-0.0026
1.1-1.2	0.0031	0.0090	-0.0022	-0.0059
1.2-1.3	-0.0058	-0.0022	0.0040	0.0037
1.3-1.4	-0.0026	-0.0059	0.0037	0.0118

TABLE Supp.CXC. Systematic covariance matrix of measured cross section ratio of iron over scintillator in W_{exp}

Bin edges (GeV/c ²)	0.9-1.1	1.1-1.2	1.2-1.3	1.3-1.4
0.9-1.1	0.009	0.002	0.004	0.006
1.1-1.2	0.002	0.004	-0.001	-0.004
1.2-1.3	0.004	-0.001	0.011	0.019
1.3-1.4	0.006	-0.004	0.019	0.036

TABLE Supp.CXCI. Measured cross section ratio of iron over scintillator in T_π , and the absolute and fractional cross section ratio uncertainties

Bin edges (GeV)	Ratio	Abs. Unc.	Frac. Stat. Unc.	Frac. Sys. Unc.	Frac. Flux Unc.
0.035-0.100	0.74	0.101	0.083	0.110	0.001
0.100-0.150	0.67	0.083	0.070	0.102	0.002
0.150-0.200	0.69	0.121	0.102	0.142	0.001
0.200-0.350	0.55	0.217	0.210	0.332	0.003

TABLE Supp.CXCII. Statistical covariance matrix of measured cross section ratio of iron over scintillator in T_π

Bin edges (GeV)	0.035-0.100	0.100-0.150	0.150-0.200	0.200-0.350
0.035-0.100	0.0037	0.0011	-0.0006	-0.0006
0.100-0.150	0.0011	0.0022	0.0009	-0.0003
0.150-0.200	-0.0006	0.0009	0.0050	0.0024
0.200-0.350	-0.0006	-0.0003	0.0024	0.0134

TABLE Supp.CXCIII. Systematic covariance matrix of measured cross section ratio of iron over scintillator in T_π

Bin edges (GeV)	0.035-0.100	0.100-0.150	0.150-0.200	0.200-0.350
0.035-0.100	0.007	0.004	0.005	0.008
0.100-0.150	0.004	0.005	0.006	0.010
0.150-0.200	0.005	0.006	0.010	0.017
0.200-0.350	0.008	0.010	0.017	0.034

TABLE Supp.CXCIV. Measured cross section ratio of iron over scintillator in θ_π , and the absolute and fractional cross section ratio uncertainties

Bin edges (degree)	Ratio	Abs. Unc.	Frac. Stat. Unc.	Frac. Sys. Unc.	Frac. Flux Unc.
0-10	1.12	0.484	0.403	0.153	0.002
10-20	0.71	0.190	0.218	0.153	0.006
20-30	0.65	0.130	0.137	0.147	0.001
30-40	0.62	0.116	0.121	0.141	0.001
40-50	0.61	0.106	0.111	0.134	0.003
50-60	0.73	0.115	0.109	0.114	0.001
60-120	0.73	0.111	0.109	0.106	0.002
120-135	0.74	0.178	0.189	0.149	0.002
135-150	0.63	0.193	0.256	0.171	0.006
150-165	0.62	0.341	0.496	0.242	0.006
165-180	1.64	1.981	1.107	0.482	0.017

TABLE Supp.CXCV. Statistical covariance matrix of measured cross section ratio of iron over scintillator in θ_π

Bin edges (degree)	0-10	10-20	20-30	30-40	40-50	50-60	60-120	120-135	135-150	150-165	165-180
0-10	0.2045	0.0238	-0.0016	-0.0003	0.0001	-0.0006	-0.0006	-0.0007	0.0009	0.0022	-0.0007
10-20	0.0238	0.0242	0.0039	-0.0006	-0.0008	-0.0004	-0.0002	-0.0005	-0.0005	-0.0005	-0.0012
20-30	-0.0016	0.0039	0.0079	0.0020	-0.0003	-0.0005	-0.0003	-0.0005	-0.0001	0.0003	-0.0016
30-40	-0.0003	-0.0006	0.0020	0.0057	0.0019	-0.0004	-0.0004	-0.0005	0.0002	0.0004	-0.0022
40-50	0.0001	-0.0008	-0.0003	0.0019	0.0046	0.0019	-0.0003	-0.0003	-0.0000	-0.0004	-0.0016
50-60	-0.0006	-0.0004	-0.0005	-0.0004	0.0019	0.0063	0.0020	-0.0006	-0.0009	-0.0011	0.0002
60-120	-0.0006	-0.0002	-0.0003	-0.0004	-0.0003	0.0020	0.0063	0.0017	-0.0003	-0.0002	0.0039
120-135	-0.0007	-0.0005	-0.0005	-0.0005	-0.0003	-0.0006	0.0017	0.0196	0.0083	0.0014	-0.0208
135-150	0.0009	-0.0005	-0.0001	0.0002	-0.0000	-0.0009	-0.0003	0.0083	0.0259	0.0242	0.0300
150-165	0.0022	-0.0005	0.0003	0.0004	-0.0004	-0.0011	-0.0002	0.0014	0.0242	0.0940	0.3147
165-180	-0.0007	-0.0012	-0.0016	-0.0022	-0.0016	0.0002	0.0039	-0.0208	0.0300	0.3147	3.3000

TABLE Supp.CXCVI. Systematic covariance matrix of measured cross section ratio of iron over scintillator in θ_π

Bin edges (degree)	0-10	10-20	20-30	30-40	40-50	50-60	60-120	120-135	135-150	150-165	165-180
0-10	0.030	0.014	0.012	0.011	0.010	0.011	0.011	0.014	0.010	0.012	-0.043
10-20	0.014	0.012	0.009	0.008	0.008	0.007	0.006	0.009	0.007	0.011	-0.015
20-30	0.012	0.009	0.009	0.008	0.007	0.006	0.006	0.009	0.008	0.010	-0.007
30-40	0.011	0.008	0.008	0.008	0.007	0.006	0.006	0.008	0.006	0.009	0.000
40-50	0.010	0.008	0.007	0.007	0.007	0.006	0.005	0.008	0.007	0.008	-0.003
50-60	0.011	0.007	0.006	0.006	0.006	0.007	0.006	0.008	0.007	0.006	0.001
60-120	0.011	0.006	0.006	0.006	0.005	0.006	0.006	0.007	0.005	0.006	0.005
120-135	0.014	0.009	0.009	0.008	0.008	0.008	0.007	0.012	0.010	0.011	-0.009
135-150	0.010	0.007	0.008	0.006	0.007	0.007	0.005	0.010	0.011	0.011	-0.011
150-165	0.012	0.011	0.010	0.009	0.008	0.006	0.006	0.011	0.011	0.022	-0.003
165-180	-0.043	-0.015	-0.007	0.000	-0.003	0.001	0.005	-0.009	-0.011	-0.003	0.626

TABLE Supp.CXC VII. Measured cross section ratio of lead over scintillator in p_μ , and the absolute and fractional cross section ratio uncertainties

Bin edges (GeV/c)	Ratio	Abs. Unc.	Frac. Stat. Unc.	Frac. Sys. Unc.	Frac. Flux Unc.
1.5-3.0	0.43	0.108	0.225	0.109	0.007
3.0-4.0	0.50	0.088	0.140	0.106	0.008
4.0-5.0	0.43	0.069	0.108	0.120	0.008
5.0-6.0	0.40	0.066	0.102	0.129	0.004
6.0-7.0	0.35	0.060	0.117	0.130	0.006
7.0-8.5	0.34	0.062	0.134	0.117	0.017
8.5-10.0	0.38	0.083	0.182	0.120	0.023
10.0-20.0	0.38	0.133	0.310	0.166	0.035

TABLE Supp.CXC VIII. Statistical covariance matrix of measured cross section ratio of lead over scintillator in p_μ

Bin edges (GeV/c)	1.5-3.0	3.0-4.0	4.0-5.0	5.0-6.0	6.0-7.0	7.0-8.5	8.5-10.0	10.0-20.0
1.5-3.0	0.0094	0.0012	0.0002	0.0000	0.0001	0.0000	0.0000	0.0000
3.0-4.0	0.0012	0.0049	0.0010	0.0002	0.0001	0.0000	0.0000	0.0000
4.0-5.0	0.0002	0.0010	0.0022	0.0007	0.0002	0.0001	0.0001	0.0000
5.0-6.0	0.0000	0.0002	0.0007	0.0017	0.0009	0.0003	0.0001	0.0001
6.0-7.0	0.0001	0.0001	0.0002	0.0009	0.0016	0.0010	0.0004	0.0002
7.0-8.5	0.0000	0.0000	0.0001	0.0003	0.0010	0.0021	0.0017	0.0007
8.5-10.0	0.0000	0.0000	0.0001	0.0001	0.0004	0.0017	0.0048	0.0038
10.0-20.0	0.0000	0.0000	0.0000	0.0001	0.0002	0.0007	0.0038	0.0139

TABLE Supp.CXCIX. Systematic covariance matrix of measured cross section ratio of lead over scintillator in p_μ

Bin edges (GeV/c)	1.5-3.0	3.0-4.0	4.0-5.0	5.0-6.0	6.0-7.0	7.0-8.5	8.5-10.0	10.0-20.0
1.5-3.0	0.002	0.002	0.002	0.002	0.002	0.001	0.001	0.002
3.0-4.0	0.002	0.003	0.002	0.002	0.002	0.001	0.002	0.002
4.0-5.0	0.002	0.002	0.003	0.003	0.002	0.002	0.001	0.002
5.0-6.0	0.002	0.002	0.003	0.003	0.002	0.002	0.002	0.002
6.0-7.0	0.002	0.002	0.002	0.002	0.002	0.002	0.002	0.002
7.0-8.5	0.001	0.001	0.002	0.002	0.002	0.002	0.002	0.002
8.5-10.0	0.001	0.002	0.001	0.002	0.002	0.002	0.002	0.002
10.0-20.0	0.002	0.002	0.002	0.002	0.002	0.002	0.002	0.004

TABLE Supp.CC. Measured cross section ratio of lead over scintillator in θ_μ , and the absolute and fractional cross section ratio uncertainties

Bin edges (degree)	Ratio	Abs. Unc.	Frac. Stat. Unc.	Frac. Sys. Unc.	Frac. Flux Unc.
0-2	0.35	0.070	0.180	0.084	0.006
2-3	0.37	0.069	0.168	0.081	0.003
3-4	0.30	0.063	0.178	0.109	0.003
4-5	0.34	0.072	0.179	0.113	0.006
5-6	0.31	0.084	0.220	0.154	0.006
6-8	0.36	0.090	0.192	0.159	0.003
8-10	0.59	0.156	0.205	0.165	0.002
10-13	0.78	0.237	0.255	0.162	0.005

TABLE Supp.CCI. Statistical covariance matrix of measured cross section ratio of lead over scintillator in θ_μ

Bin edges (degree)	0-2	2-3	3-4	4-5	5-6	6-8	8-10	10-13
0-2	0.0040	0.0001	-0.0003	-0.0000	0.0000	-0.0000	-0.0000	-0.0000
2-3	0.0001	0.0038	0.0005	-0.0003	-0.0001	-0.0000	-0.0000	-0.0000
3-4	-0.0003	0.0005	0.0029	0.0005	-0.0003	-0.0001	-0.0000	-0.0000
4-5	-0.0000	-0.0003	0.0005	0.0037	0.0008	-0.0003	-0.0001	0.0000
5-6	0.0000	-0.0001	-0.0003	0.0008	0.0047	0.0003	-0.0004	-0.0000
6-8	-0.0000	-0.0000	-0.0001	-0.0003	0.0003	0.0048	-0.0000	-0.0006
8-10	-0.0000	-0.0000	-0.0000	-0.0001	-0.0004	-0.0000	0.0148	-0.0005
10-13	-0.0000	-0.0000	-0.0000	0.0000	-0.0000	-0.0006	-0.0005	0.0400

TABLE Supp.CCII. Systematic covariance matrix of measured cross section ratio of lead over scintillator in θ_μ

Bin edges (degree)	0-2	2-3	3-4	4-5	5-6	6-8	8-10	10-13
0-2	0.001	0.001	0.001	0.001	0.001	0.001	0.001	0.002
2-3	0.001	0.001	0.001	0.001	0.001	0.001	0.002	0.002
3-4	0.001	0.001	0.001	0.001	0.001	0.002	0.002	0.003
4-5	0.001	0.001	0.001	0.001	0.002	0.002	0.003	0.004
5-6	0.001	0.001	0.001	0.002	0.002	0.003	0.004	0.005
6-8	0.001	0.001	0.002	0.002	0.003	0.003	0.005	0.006
8-10	0.001	0.002	0.002	0.003	0.004	0.005	0.010	0.010
10-13	0.002	0.002	0.003	0.004	0.005	0.006	0.010	0.016

TABLE Supp.CCIII. Measured cross section ratio of lead over scintillator in $p_{\mu,||}$, and the absolute and fractional cross section ratio uncertainties

Bin edges (GeV/c)	Ratio	Abs. Unc.	Frac. Stat. Unc.	Frac. Sys. Unc.	Frac. Flux Unc.
1.5-3.0	0.46	0.110	0.216	0.107	0.007
3.0-4.0	0.49	0.088	0.140	0.111	0.009
4.0-5.0	0.42	0.069	0.111	0.122	0.009
5.0-6.0	0.40	0.065	0.102	0.128	0.004
6.0-7.0	0.34	0.060	0.117	0.128	0.007
7.0-8.5	0.35	0.061	0.134	0.116	0.017
8.5-10.0	0.39	0.083	0.179	0.116	0.021
10.0-20.0	0.38	0.134	0.308	0.164	0.034

TABLE Supp.CCIV. Statistical covariance matrix of measured cross section ratio of lead over scintillator in $p_{\mu,||}$

Bin edges (GeV/c)	1.5-3.0	3.0-4.0	4.0-5.0	5.0-6.0	6.0-7.0	7.0-8.5	8.5-10.0	10.0-20.0
1.5-3.0	0.0098	0.0011	0.0002	0.0000	0.0001	0.0000	0.0000	0.0000
3.0-4.0	0.0011	0.0047	0.0009	0.0002	0.0001	0.0001	0.0000	0.0000
4.0-5.0	0.0002	0.0009	0.0022	0.0007	0.0002	0.0001	0.0001	0.0000
5.0-6.0	0.0000	0.0002	0.0007	0.0017	0.0008	0.0003	0.0001	0.0001
6.0-7.0	0.0001	0.0001	0.0002	0.0008	0.0016	0.0010	0.0004	0.0001
7.0-8.5	0.0000	0.0001	0.0001	0.0003	0.0010	0.0021	0.0017	0.0008
8.5-10.0	0.0000	0.0000	0.0001	0.0001	0.0004	0.0017	0.0048	0.0038
10.0-20.0	0.0000	0.0000	0.0000	0.0001	0.0001	0.0008	0.0038	0.0139

TABLE Supp.CCV. Systematic covariance matrix of measured cross section ratio of lead over scintillator in $p_{\mu,||}$

Bin edges (GeV/c)	1.5-3.0	3.0-4.0	4.0-5.0	5.0-6.0	6.0-7.0	7.0-8.5	8.5-10.0	10.0-20.0
1.5-3.0	0.002	0.002	0.002	0.002	0.002	0.001	0.001	0.002
3.0-4.0	0.002	0.003	0.003	0.002	0.002	0.002	0.002	0.002
4.0-5.0	0.002	0.003	0.003	0.002	0.002	0.002	0.001	0.002
5.0-6.0	0.002	0.002	0.002	0.003	0.002	0.002	0.002	0.002
6.0-7.0	0.002	0.002	0.002	0.002	0.002	0.002	0.002	0.002
7.0-8.5	0.001	0.002	0.002	0.002	0.002	0.002	0.001	0.002
8.5-10.0	0.001	0.002	0.001	0.002	0.002	0.001	0.002	0.002
10.0-20.0	0.002	0.002	0.002	0.002	0.002	0.002	0.002	0.004

TABLE Supp.CCVI. Measured cross section ratio of lead over scintillator in $p_{\mu,T}$, and the absolute and fractional cross section ratio uncertainties

Bin edges (GeV/c)	Ratio	Abs. Unc.	Frac. Stat. Unc.	Frac. Sys. Unc.	Frac. Flux Unc.
0.00-0.15	0.36	0.093	0.240	0.093	0.004
0.15-0.30	0.33	0.057	0.152	0.086	0.001
0.30-0.45	0.38	0.056	0.116	0.089	0.001
0.45-0.60	0.33	0.067	0.148	0.134	0.002
0.60-0.75	0.35	0.103	0.207	0.215	0.010
0.75-0.90	0.40	0.141	0.258	0.239	0.009
0.90-1.25	0.98	0.274	0.234	0.151	0.006
1.25-2.50	2.14	1.439	0.601	0.306	0.030

TABLE Supp.CCVII. Statistical covariance matrix of measured cross section ratio of lead over scintillator in $p_{\mu,T}$

Bin edges (GeV/c)	0.00-0.15	0.15-0.30	0.30-0.45	0.45-0.60	0.60-0.75	0.75-0.90	0.90-1.25	1.25-2.50
0.00-0.15	0.0076	0.0003	-0.0003	-0.0001	-0.0000	-0.0000	-0.0000	-0.0002
0.15-0.30	0.0003	0.0025	0.0002	-0.0002	-0.0001	-0.0000	-0.0000	-0.0001
0.30-0.45	-0.0003	0.0002	0.0019	0.0003	-0.0003	-0.0002	-0.0001	-0.0001
0.45-0.60	-0.0001	-0.0002	0.0003	0.0024	0.0008	-0.0003	-0.0006	-0.0006
0.60-0.75	-0.0000	-0.0001	-0.0003	0.0008	0.0051	0.0018	-0.0007	-0.0016
0.75-0.90	-0.0000	-0.0000	-0.0002	-0.0003	0.0018	0.0107	0.0059	-0.0108
0.90-1.25	-0.0000	-0.0000	-0.0001	-0.0006	-0.0007	0.0059	0.0530	0.0383
1.25-2.50	-0.0002	-0.0001	-0.0001	-0.0006	-0.0016	-0.0108	0.0383	1.6442

TABLE Supp.CCVIII. Systematic covariance matrix of measured cross section ratio of lead over scintillator in $p_{\mu,T}$

Bin edges (GeV/c)	0.00-0.15	0.15-0.30	0.30-0.45	0.45-0.60	0.60-0.75	0.75-0.90	0.90-1.25	1.25-2.50
0.00-0.15	0.001	0.001	0.000	0.000	0.000	0.001	0.003	0.004
0.15-0.30	0.001	0.001	0.001	0.001	0.001	0.002	0.003	0.002
0.30-0.45	0.000	0.001	0.001	0.001	0.002	0.003	0.004	0.006
0.45-0.60	0.000	0.001	0.001	0.002	0.003	0.004	0.005	0.006
0.60-0.75	0.000	0.001	0.002	0.003	0.006	0.007	0.007	0.005
0.75-0.90	0.001	0.002	0.003	0.004	0.007	0.009	0.011	0.008
0.90-1.25	0.003	0.003	0.004	0.005	0.007	0.011	0.022	0.029
1.25-2.50	0.004	0.002	0.006	0.006	0.005	0.008	0.029	0.427

TABLE Supp.CCIX. Measured cross section ratio of lead over scintillator in Q^2 , and the absolute and fractional cross section ratio uncertainties

Bin edges (GeV^2/c^2)	Ratio	Abs. Unc.	Frac. Stat. Unc.	Frac. Sys. Unc.	Frac. Flux Unc.
0.000-0.025	0.36	0.089	0.234	0.089	0.003
0.025-0.050	0.35	0.069	0.183	0.073	0.001
0.050-0.100	0.30	0.060	0.175	0.096	0.002
0.100-0.200	0.38	0.058	0.122	0.091	0.001
0.200-0.300	0.35	0.068	0.148	0.125	0.002
0.300-0.400	0.30	0.075	0.198	0.150	0.003
0.400-0.500	0.36	0.094	0.201	0.166	0.005
0.500-0.700	0.36	0.121	0.233	0.238	0.010
0.700-1.000	0.51	0.171	0.251	0.226	0.007
1.000-1.300	1.03	0.318	0.271	0.148	0.009
1.300-2.000	0.95	0.531	0.508	0.231	0.017
2.000-3.000	3.01	3.221	0.989	0.412	0.050

TABLE Supp.CCX. Statistical covariance matrix of measured cross section ratio of lead over scintillator in Q^2

Bin edges (GeV ² /c ²)	0.000-0.025	0.025-0.050	0.050-0.100	0.100-0.200	0.200-0.300	0.300-0.400	0.400-0.500	0.500-0.700	0.700-1.000	1.000-1.300	1.300-2.000	2.000-3.000
0.000-0.025	0.0069	0.0014	-0.0005	-0.0002	-0.0000	-0.0000	-0.0000	0.0000	-0.0000	0.0000	-0.0000	-0.0002
0.025-0.050	0.0014	0.0042	0.0012	-0.0003	-0.0002	-0.0000	-0.0000	-0.0000	-0.0000	-0.0000	-0.0000	-0.0000
0.050-0.100	-0.0005	0.0012	0.0027	0.0005	-0.0003	-0.0001	-0.0001	-0.0000	-0.0000	-0.0001	-0.0001	0.0000
0.100-0.200	-0.0002	-0.0003	0.0005	0.0022	0.0006	-0.0002	-0.0003	-0.0001	-0.0001	-0.0001	-0.0000	-0.0002
0.200-0.300	-0.0000	-0.0002	-0.0003	0.0006	0.0027	0.0013	0.0001	-0.0003	-0.0002	-0.0000	-0.0001	-0.0002
0.300-0.400	-0.0000	-0.0000	-0.0001	-0.0002	0.0013	0.0036	0.0026	-0.0000	-0.0006	-0.0007	-0.0009	-0.0001
0.400-0.500	-0.0000	-0.0000	-0.0001	-0.0003	0.0001	0.0026	0.0052	0.0028	-0.0003	-0.0013	-0.0009	-0.0013
0.500-0.700	0.0000	-0.0000	-0.0000	-0.0001	-0.0003	-0.0000	0.0028	0.0072	0.0038	-0.0014	-0.0001	-0.0029
0.700-1.000	-0.0000	-0.0000	-0.0000	-0.0001	-0.0002	-0.0006	-0.0003	0.0038	0.0161	0.0115	-0.0010	-0.0170
1.000-1.300	0.0000	-0.0000	-0.0001	-0.0001	-0.0000	-0.0007	-0.0013	-0.0014	0.0115	0.0777	0.0194	-0.0262
1.300-2.000	-0.0000	-0.0000	-0.0001	-0.0000	-0.0001	-0.0009	-0.0009	-0.0001	-0.0010	0.0194	0.2330	0.1241
2.000-3.000	-0.0002	-0.0000	0.0000	-0.0002	-0.0002	-0.0001	-0.0013	-0.0029	-0.0170	-0.0262	0.1241	8.8446

TABLE Supp.CCXI. Systematic covariance matrix of measured cross section ratio of lead over scintillator in Q^2

Bin edges (GeV ² /c ²)	0.000-0.025	0.025-0.050	0.050-0.100	0.100-0.200	0.200-0.300	0.300-0.400	0.400-0.500	0.500-0.700	0.700-1.000	1.000-1.300	1.300-2.000	2.000-3.000
0.000-0.025	0.001	0.001	0.001	0.001	0.000	0.000	0.001	0.001	0.001	0.002	0.001	0.008
0.025-0.050	0.001	0.001	0.001	0.001	0.001	0.001	0.001	0.001	0.001	0.002	0.002	0.005
0.050-0.100	0.001	0.001	0.001	0.001	0.001	0.001	0.001	0.002	0.002	0.004	0.002	0.005
0.100-0.200	0.001	0.001	0.001	0.001	0.001	0.001	0.002	0.002	0.003	0.005	0.004	0.012
0.200-0.300	0.000	0.001	0.001	0.001	0.002	0.002	0.002	0.003	0.004	0.004	0.004	0.002
0.300-0.400	0.000	0.001	0.001	0.001	0.002	0.002	0.003	0.003	0.004	0.005	0.006	0.008
0.400-0.500	0.001	0.001	0.001	0.002	0.002	0.003	0.004	0.005	0.006	0.007	0.009	0.012
0.500-0.700	0.001	0.001	0.002	0.002	0.003	0.003	0.005	0.007	0.009	0.008	0.014	0.005
0.700-1.000	0.001	0.001	0.002	0.003	0.004	0.004	0.006	0.009	0.013	0.011	0.019	0.011
1.000-1.300	0.002	0.002	0.004	0.005	0.004	0.005	0.007	0.008	0.011	0.023	0.013	0.061
1.300-2.000	0.001	0.002	0.002	0.004	0.004	0.006	0.009	0.014	0.019	0.013	0.048	0.000
2.000-3.000	0.008	0.005	0.005	0.012	0.002	0.008	0.012	0.005	0.011	0.061	0.000	1.531

TABLE Supp.CCXII. Measured cross section ratio of lead over scintillator in W_{exp} , and the absolute and fractional cross section ratio uncertainties

Bin edges (GeV/c ²)	Ratio	Abs. Unc.	Frac. Stat. Unc.	Frac. Sys. Unc.	Frac. Flux Unc.
0.9-1.1	0.58	0.267	0.432	0.148	0.013
1.1-1.2	0.20	0.051	0.239	0.088	0.011
1.2-1.3	0.38	0.056	0.092	0.113	0.003
1.3-1.4	0.63	0.165	0.164	0.204	0.005

TABLE Supp.CCXIII. Statistical covariance matrix of measured cross section ratio of lead over scintillator in W_{exp}

Bin edges (GeV/c ²)	0.9-1.1	1.1-1.2	1.2-1.3	1.3-1.4
0.9-1.1	0.0636	0.0039	-0.0033	-0.0063
1.1-1.2	0.0039	0.0023	0.0005	-0.0031
1.2-1.3	-0.0033	0.0005	0.0012	0.0007
1.3-1.4	-0.0063	-0.0031	0.0007	0.0107

TABLE Supp.CCXIV. Systematic covariance matrix of measured cross section ratio of lead over scintillator in W_{exp}

Bin edges (GeV/c ²)	0.9-1.1	1.1-1.2	1.2-1.3	1.3-1.4
0.9-1.1	0.007	0.001	-0.000	-0.001
1.1-1.2	0.001	0.000	-0.000	-0.001
1.2-1.3	-0.000	-0.000	0.002	0.005
1.3-1.4	-0.001	-0.001	0.005	0.016

TABLE Supp.CCXV. Measured cross section ratio of lead over scintillator in T_π , and the absolute and fractional cross section ratio uncertainties

Bin edges (GeV)	Ratio	Abs. Unc.	Frac. Stat. Unc.	Frac. Sys. Unc.	Frac. Flux Unc.
0.035-0.100	0.39	0.055	0.114	0.084	0.002
0.100-0.150	0.36	0.048	0.092	0.094	0.003
0.150-0.200	0.40	0.074	0.128	0.132	0.004
0.200-0.350	0.62	0.168	0.172	0.210	0.003

TABLE Supp.CCXVI. Statistical covariance matrix of measured cross section ratio of lead over scintillator in T_π

Bin edges (GeV)	0.035-0.100	0.100-0.150	0.150-0.200	0.200-0.350
0.035-0.100	0.0020	0.0006	-0.0003	-0.0005
0.100-0.150	0.0006	0.0011	0.0004	-0.0003
0.150-0.200	-0.0003	0.0004	0.0026	0.0012
0.200-0.350	-0.0005	-0.0003	0.0012	0.0114

TABLE Supp.CCXVII. Systematic covariance matrix of measured cross section ratio of lead over scintillator in T_π

Bin edges (GeV)	0.035-0.100	0.100-0.150	0.150-0.200	0.200-0.350
0.035-0.100	0.001	0.001	0.001	0.003
0.100-0.150	0.001	0.001	0.002	0.004
0.150-0.200	0.001	0.002	0.003	0.006
0.200-0.350	0.003	0.004	0.006	0.017

TABLE Supp.CCXVIII. Measured cross section ratio of lead over scintillator in θ_π , and the absolute and fractional cross section ratio uncertainties

Bin edges (degree)	Ratio	Abs. Unc.	Frac. Stat. Unc.	Frac. Sys. Unc.	Frac. Flux Unc.
0-10	0.75	0.329	0.412	0.159	0.004
10-20	0.54	0.141	0.219	0.141	0.002
20-30	0.38	0.079	0.157	0.135	0.001
30-40	0.43	0.071	0.122	0.113	0.004
40-50	0.38	0.067	0.124	0.127	0.004
50-60	0.31	0.066	0.158	0.145	0.005
60-120	0.34	0.062	0.142	0.112	0.004
120-135	0.49	0.097	0.172	0.098	0.001
135-150	0.53	0.124	0.196	0.126	0.003
150-165	0.58	0.222	0.349	0.148	0.003
165-180	0.50	0.514	0.953	0.365	0.025

TABLE Supp. CCXIX. Statistical covariance matrix of measured cross section ratio of lead over scintillator in θ_π

Bin edges (degree)	0-10	10-20	20-30	30-40	40-50	50-60	60-120	120-135	135-150	150-165	165-180
0-10	0.0945	0.0129	0.0004	-0.0003	-0.0004	-0.0004	-0.0004	-0.0005	-0.0006	0.0025	-0.0011
10-20	0.0129	0.0140	0.0028	-0.0002	-0.0005	-0.0003	-0.0002	-0.0004	-0.0005	-0.0000	-0.0006
20-30	0.0004	0.0028	0.0036	0.0014	-0.0000	-0.0003	-0.0002	-0.0002	-0.0001	0.0002	0.0003
30-40	-0.0003	-0.0002	0.0014	0.0027	0.0012	0.0001	-0.0003	-0.0003	0.0000	0.0000	-0.0009
40-50	-0.0004	-0.0005	-0.0000	0.0012	0.0022	0.0012	0.0002	-0.0001	-0.0002	-0.0002	-0.0010
50-60	-0.0004	-0.0003	-0.0003	0.0001	0.0012	0.0024	0.0010	-0.0000	-0.0005	-0.0004	-0.0009
60-120	-0.0004	-0.0002	-0.0002	-0.0003	0.0002	0.0010	0.0023	0.0009	0.0001	-0.0001	0.0021
120-135	-0.0005	-0.0004	-0.0002	-0.0003	-0.0001	-0.0000	0.0009	0.0071	0.0043	0.0002	0.0100
135-150	-0.0006	-0.0005	-0.0001	0.0000	-0.0002	-0.0005	0.0001	0.0043	0.0109	0.0104	0.0028
150-165	0.0025	-0.0000	0.0002	0.0000	-0.0002	-0.0004	-0.0001	0.0002	0.0104	0.0416	-0.0017
165-180	-0.0011	-0.0006	0.0003	-0.0009	-0.0010	-0.0009	0.0021	0.0100	0.0028	-0.0017	0.2299

TABLE Supp.CCXX. Systematic covariance matrix of measured cross section ratio of lead over scintillator in θ_π

Bin edges (degree)	0-10	10-20	20-30	30-40	40-50	50-60	60-120	120-135	135-150	150-165	165-180
0-10	0.014	0.007	0.005	0.005	0.004	0.003	0.003	0.004	0.006	0.004	-0.001
10-20	0.007	0.006	0.003	0.003	0.003	0.002	0.002	0.002	0.003	0.003	-0.003
20-30	0.005	0.003	0.003	0.002	0.002	0.002	0.001	0.002	0.003	0.002	-0.001
30-40	0.005	0.003	0.002	0.002	0.002	0.002	0.002	0.002	0.003	0.002	0.000
40-50	0.004	0.003	0.002	0.002	0.002	0.002	0.002	0.002	0.003	0.002	-0.001
50-60	0.003	0.002	0.002	0.002	0.002	0.002	0.001	0.001	0.002	0.001	0.002
60-120	0.003	0.002	0.001	0.002	0.002	0.001	0.001	0.001	0.002	0.001	-0.000
120-135	0.004	0.002	0.002	0.002	0.002	0.001	0.001	0.002	0.003	0.003	-0.000
135-150	0.006	0.003	0.003	0.003	0.003	0.002	0.002	0.003	0.005	0.004	-0.003
150-165	0.004	0.003	0.002	0.002	0.002	0.001	0.001	0.003	0.004	0.007	-0.005
165-180	-0.001	-0.003	-0.001	0.000	-0.001	0.002	-0.000	-0.000	-0.003	-0.005	0.034